UC Santa Barbara
UC Santa Barbara Electronic Theses and Dissertations

Title
Explainable Models of Performance on Networks

Permalink
https://escholarship.org/uc/item/27v6k0d4

Author
Askarisichani, Omid

Publication Date
2020

Peer reviewed|Thesis/dissertation

University of California
Santa Barbara

Explainable Models of Performance on Networks

A dissertation submitted in partial satisfaction
of the requirements for the degree

Doctor of Philosophy
in
Computer Science

by

Omid Askarisichani

Committee in charge:

Professor Ambuj K. Singh, Chair
Professor Noah E. Friedkin
Professor Francesco Bullo
Professor Xifeng Yan

December 2020

The Dissertation of Omid Askarisichani is approved.

_____

Professor Noah E. Friedkin

_____

Professor Francesco Bullo

_____

Professor Xifeng Yan

_____

Professor Ambuj K. Singh, Committee Chair

November 2020

Explainable Models of Performance on Networks

Copyright © 2020

by

Omid Askarisichani

To my self-sacrificing parents

Acknowledgements

Throughout the journey of my Ph.D., I have had the pleasure of interacting with, learning from, and being influenced by many special people who I hope one day I can reciprocate their pure kindness. The least I can do is to acknowledge them here.

Foremost, I would like to express my gratitude to my research advisor, Prof. Ambuj K. Singh for being the best supporter, the greatest mentor I have ever had, and an absolute role model for academic excellence. I have tremendously benefited from Ambuj's depth of vision, technical knowledge, and his perspective regarding how to do successful scientific research. Since the beginning of my Ph.D., Ambuj trusted me with choosing and leading open problems in our funded project on network science of teams. He generously helped me at many different times and always led by example in productivity and academic success. Ambuj has made me a wiser researcher and a better person. I truly could not have asked for a better advisor.

I am extremely grateful to Prof. Noah E. Friedkin. I have known Noah since I started my Masters back in Iran due to his highly acclaimed Friedkin-Johnson model. Since I joined, I was thrilled to work with him. I cannot begin to describe how much I benefited from working with Noah. His unquestionable kindness, his care for my academic success, and his excitement about research have made me forever in debt to him. At many times, he supported me through his funding, his soul generosity, and diligence. I want to thank Noah for allowing me to design a protocol and run human subject studies. As a result, I have acquired a unique skill in the department of Computer Science. His level of attention to detail, his integrity in research, and his unconditional support for me throughout my entire Ph.D. has shown me how an ideal professor and human being can be. I am proud to learn from him in my Ph.D.

I am profusely grateful to Prof. Francesco Bullo. Since I joined the Ph.D. program,

always supported me as the Junior student in the projects and I am beyond thankful for how much they helped me throughout my Ph.D. My gratitude further extends to all the members of the Network Science of Teams MURI for their collegiality. I wanted to specifically thank Haraldur for his kindness and generous help throughout my Ph.D. He had been always the senior lab-mate that I looked up to.

I had the pleasure to spent time with some awesome colleagues in the Dyanmo lab: Wei, Sourav, Arlei, Xuan-Hong, Victor, Hongyuan, Haraldur, Alex, Zexi, Mert, Rachel, Yuning, Furkan, Sikun, Minh, Richika, Ashwini, Chandana, Nikhil, Aneesha, and Koa.

I am grateful to Prof. Yu-Xiang Wang for countless extremely helpful machine learning discussions. Almost every single time I met with him I learned something new and helped me to improve my modeling or mathematical proof. I am also grateful to Prof. Amr El Abbadi who I had the pleasure to work with as a teaching assistant and truly enjoyed working with. I am thankful to Prof. Linda Petzold who responded to my email when applying for Ph.D. and was the reason I joined UCSB.

I am grateful to my loving family. Thanks to my mother Ozra, my father Abbasali, and my two brothers Mohammad Reza and Amir for their immense belief in me. Without them, I will not be able to make this far. I would like to thank my girlfriend Jessamyn for her unconditional love. She has been very supportive through my Ph.D. She believed in me and constantly encouraged me in my journey. I consider myself extremely lucky to have her in my life.

Curriculum Vitæ
Omid Askarisichani

Education

2015-2020	Ph.D. in Computer Science (GPA: 3.95/4.0), University of California, Santa Barbara, USA.
2011-2014	M.Sc. in Artificial Intelligence (GPA: 4.0/4.0), Sharif University of Technology, Tehran, Iran.
2007-2011	B.Sc. in Software Engineering (GPA: 3.86/4.0), University of Isfahan, Isfahan, Iran.

Publications

1. **O. Askarisichani**, Elizabeth Y. Huang, Koa K. Sato, Noah E. Friedkin, Francesco Bullo, and Ambuj K. Singh. "Expertise and confidence explain how social influence evolves along intellective tasks", *submitted* (2020). **Git**

2. **O. Askarisichani**, AK Singh, F. Bullo, and NE Friedkin. "The 1995-2018 Global Evolution of the Network of Amicable and Hostile Relations Among Nation-States.", *Communications Physics*, vol. 3, p. 215, Nov (2020). **Git**

3. Ye, Wei, **O. Askarisichani**, AT Jone, AK Singh. "DeepMap: Learning Deep Graph Representations.", *IEEE Transactions on Knowledge and Data Engineering (TKDE)*(2019). **Arxiv**

4. **O. Askarisichani**, JN Lane, F Bullo, NE Friedkin, AK Singh, B Uzzi, **"Structural balance emerges and explains performance in risky decision-making,"** *Journal of Nature Communications* 10, 2019. **Link News Media Git**

5. Dang, X-H, **O. Askarisichani**, Singh. AK., " **Discovery of Varying Predictive Features in Multitask Learning with Smooth SVM,**" *Big Data IEEE Conference*, Seattle, US, 2018.

6. V Amelkin, **O Askarisichani**, YJ Kim, TW Malone, AK Singh, **"Dynamics of Collective Performance in Collaboration Networks,"** *Journal of PLOS ONE*, 13(10): e0204547, 2018. **Link News**

7. **O. Askarisichani**, M. Jalili, " **Inference of Hidden Social Power through Opinion Formation in Complex Networks,**" *Journal of IEEE Transactions on Network Science and Engineering*, (TNSE), Vol. 4, No. 3, Pages 154-164, DOI:10.1109/TNSE.2017.2691405, ISSN:2327-4697, http://ieeexplore.ieee.org/document/7892936/#full-text-section, 2017. **Link Git**

8. **O. Askarisichani**, M. Jalili, " **Influence Maximization of Informed Agents in Social Networks,**" *Journal of Applied Mathematics and Computation*, (AMC), Vol. 254, Pages 229-239, 3/1/2015, *Elsevier*, http://www.sciencedirect.com/science/article/pii/S0096300314018001, 2015. **Link Git**

9. **O. Askarisichani**, M. Jalili, " **Large-scale Global Optimization through Consensus of Opinions Over Networks,**" *Journal of the Complex Adaptive Systems Modeling, Springer*, 1(1):11, 2013.   **Link**   **Git**

10. M. Jalili, **O. Askarisichani**, Xinghuo Yu " **Optimal pinning controllability of complex networks: Dependence on network structure,**" *Journal of Physical Review E*, (PRE), Vol. 91, No. 1, Page 012803, *American Physical Society*, DOI:10.1103/PhysRevE.91.012803, 2015.   **Link**   **Git**

11. SM Hill, LM Heiser, T Cokelear, M Unger, D Carlin, Y Zhang, A Sokolov, E Paull, CK Wong, K Graim, A Bivol, H Wang, F Zhu, B Afsari, LV Danilova, AV Favorov, W Lee, D Taylor, HPN-DREAM Consortium (**O. Askarisichani**), GB Mills, JW Gray, M Kellen, T Norman, S Friend, EJ Fertig, Y Guan, M Song, J Stuart, H Koeppl, PT Spellman, G Stolovitzky, J Saez-Rodriguez, and S Mukherjee " **Inferring causal molecular networks: empirical assessment through a community-based effort, *Nature Methods***, Feb 2016.   **Link**   **Git**

12. M. Shahriari, **O. Askarisichani**, J. Gharibshah, M. Jalili, " **Sign prediction in social networks based on users reputation and optimism,** *Journal of Social Network Analysis and Mining*, Vol. 6, No. 1, DOI:10.1007/s13278-016-0401-6, 6:91, *Springer*, 2016.   **link**

13. V. Amelkin, **O. Askarisichani**, Y. J. Kim, A. K. Singh, T. W. Malone, " **Dynamics of Collective Performance in Collaboration Networks,**" *XXXVI Sunbelt Conference*, page 6, April 2016.   **Link**

14. A. Fatemi, K. Zamanifar, N. Nematbakhsh, **O. Askarisichani**, " **A Team-Based Organizational Model for Adaptive Multi Agent Systems,**" in *3rd International Conference on Agents and Artificial Intelligence*, *ICAART* 2011, *Rome, Italy*, Volume 2, No. 297, session 10:30-11:00, 2011.   **Link**   **Git**

15. A. Gharipour, A. Yousefian, **O. Askarisichani**, "**Clustering Based on Fuzzy Rules and Genetic Algorithm for alpha-Reliability Decision of Asset Classification and Portfolio Selection,**" *Journal of the Asian Economic Review*, Volume 55, No. 1, Pages 47-60, 2013.   **Link**

Awards

- Awarded $2000 **Computer Science Fellowship** in UC Santa Barbara, Sept 2015.

- Awarded $6000 **Computer Science Endowment Fellowship** in UC Santa Barbara, Sept 2015.

- Ranked 1_{st} in Bioinformatics HPN-DREAM Consortium Breast Cancer Network Inference Challenge, Feb 2014.

- Ranked 1_{st} in B.Sc. within a class of 47, Department of Computer Engineering, July 2011.

- Ranked $\mathbf{4}_{th}$ in M.Sc. within a class of 56, Department of Computer Engineering, Feb 2013.
- Awarded **Fellowship of Exceptional Talents** for M.Sc. program in Sharif University of Technology, Sept 2011.

Teaching

- Lead Teaching Assistant, UC Santa Barbara, CA (Sept 2016 – June 2017)
- Project Mentor: IGERT Bootcamp, UC Santa Barbara, CA (Sept 2017 - Oct 2017)
- Teaching Assistant: Data Structure and Algorithms, UC Santa Barbara, CA (Jan 2016 – Mar 2017)
- Teaching Assistant: Machine Learning, Sharif University of Technology, Tehran, Iran (Sept 2012 – Dec 2012)
- Teaching Assistant: Neural networks and fuzzy systems, Sharif University of Technology, Tehran, Iran (Feb 2013 – May 2013)
- Teaching Assistant: Data Structure and Algorithms, University of Isfahan, Isfahan, Iran (Sept 2009 – Dec 2010)

Research Mentorship

- Koa K. Sato, M.Sc. student, Department of Computer Science, University of California Santa Barbara (2019 - 2020)
  Machine learning-based interpersonal influence estimation
- Aneesha Mathur, M.Sc. student, Department of Computer Science, University of California Santa Barbara (2019 - 2020)
  Impact of work/life balance on risky decision-making

Professional Service

- External Reviewer for KDD - ACM SIGKDD Conference on Knowledge Discovery and Data Mining (2017, 2018, 2020)
- External Reviewer for ICDM - IEEE International Conference on Data Mining (2020)
- External Reviewer for WebConf - International World Wide Web Conference (2020)
- External Reviewer for AAAI - Association for the Advancement of Artificial Intelligence (2019)
- External Reviewer for WWW - International World Wide Web Conference (2018, 2019)
- External Reviewer for SDM - SIAM International Conference on Data Mining (2018)
- Reviewer for TKDD - ACM Transactions on Knowledge Discovery from Data (2018)
- Reviewer for Journal of Complex Networks (2017)

Published Content, Contributions, and Permissions

Some of the materials presented in this thesis have either been published by the thesis' author or are currently in submission. The author has made principal contributions to all stages of the conception and production of the published, under publication and submitted works mentioned below.

A major part of the content of Chapter 2 has been published as

O. Askarisichani, J.N. Lane, F Bullo, NE Friedkin, AK Singh, and B Uzzi. "Structural balance emerges and explains performance in risky decision-making." *Nature Communications* volume 10, page 2648, (2019). DOI: https://doi.org/10.1038/s41467-019-10548-8

A large part of Chapter 3's content is accepted and currently under publication as

O. Askarisichani, A.K. Singh, F. Bullo, and N.E. Friedkin. "The 1995-2018 Global Evolution of the Network of Amicable and Hostile Relations Among Nation-States." *Communications Physics*, vol. 3, p. 215, Nov (2020).

Finally a major part of Chapter 4's content is currently in submission and its arXiv version is also available. This study can be referred as

O. Askarisichani, Elizabeth Y. Huang, Koa K. Sato, Noah E. Friedkin, Francesco Bullo, and Ambuj K. Singh. "Expertise and confidence explain how social influence evolves along intellective tasks." *submitted* (2020).

Both Nature Communications and Communications Physics are under Nature publications, are open access and do not require obtaining explicit permission for the reuse of the above mentioned content in this dissertation.

Three other related papers to this dissertation, which due to limit on pages, are briefly described in the introduction are published and can be referred as

Ye, Wei, O. Askarisichani, AT Jone, AK Singh. "DeepMap: Learning Deep Graph Representations." *IEEE Transactions on Knowledge and Data Engineering (TKDE)* (2019). DOI: https://doi.org/10.1109/TKDE.2020.3014089

Dang, X-H, O. Askarisichani, and AK. Singh. "Learning Multiclassifiers with Predictive Features that Vary with Data Distribution." In 2018 *IEEE International Conference on Big Data (Big Data)*, pp. 673-682. IEEE, (2018). DOI: https://doi.org/10.1109/BigData.2018.8622407

V Amelkin, O Askarisichani, YJ Kim, TW Malone, AK Singh, "Dynamics of Collective Performance in Collaboration Networks." *Journal of PLOS ONE*, 13(10): e0204547 (2018).
DOI: https://doi.org/10.1371/journal.pone.0204547

Abstract

Explainable Models of Performance on Networks

by

Omid Askarisichani

Networks model complex systems in myriad applications, including social media, finance, and political systems. In such settings, nodes often represent people, artificial agents, or political parties while edges portray their relationships. Interpersonal relationships change due to a person's cognitive biases, societal roles, and what their in-group perceptions are. These relationships impact one's task performance. Often times, there is a need to estimate the underlying relationships and forecast their changes. This dissertation is at the intersection of machine learning, network science, and social science. In our studies, we use graph theory, natural language processing, and convex optimization to extract information on how to improve the performance of individuals in financial and social systems.

First, by leveraging data, we study how the patterns of change in positive and negative relationships may impact the performance of stock traders. We build upon theories from sociology, namely structural balance theory—which describes the dynamics that govern the sentiment of interpersonal relationships—and assess the impact on stock traders' profitability. Our studies show traders trade best when their social network at their workplace is structurally balanced.

Second, we show a generalization of structural balance theory that describes the dynamics of relationships among countries over more than two decades. We capture their dynamics using a time-varying Markov model, pinpoint the international shocks, and international conflicts. We also present rigorous proof for the convergence rate of

the proposed model.

Third, we collect data from human subjects answering trivia questions in teams of four. After individually answering a question, subjects collaborate on a final answer through a chat system. The participants are periodically asked to assess their appraisals of each other. We seek to find underlying factors that contribute to the awarded appraisals. We report that expertise and social confidence are the two most salient factors in determining the amount of influence one may receive. Furthermore, we build a model using message content, message times, and individual task performance to estimate the interpersonal influence matrix. Our experimental results demonstrate that the proposed neural network model surpasses baseline algorithms.

Contents

List of Figures

xix

List of Tables

Chapter 1

Introduction

In the current world, objects and individuals rarely function in isolation. Most objects are connected to each other and most individuals interact with one another. Scientists represent theses connections and interactions as graphs or as so-called, networks. Such networks are comprised of interactive components that dynamically modify their connections. Nowadays, networks are everywhere. From computers on the world wide web to the neural networks of brain cells, complex networks among entities are ubiquitous. It is incontrovertibly axiomatic that networks play pivotal roles in both society and the natural world. Social networks such as Facebook and Twitter connect people from all around the globe, protein-protein interaction networks aid with cancer treatment, and interconnected home appliances help our lives to be more enjoyable and efficient. Therefore, the network analysis and modeling has attracted much attention in recent years and has welcomed researchers from a incredible range of disciplines.

Abundant researches focus on networks among humans. Us humans are a social species. Every day, we tend to work together, consult with each other, and achieve more by building efficient and multi-dimensional teams. Teams are now a basic unit of knowledge work. Organizations increasingly rely on teams, as work has become complex

enough to require a wide variety of skills and expertise from a group of individuals [19]. Scientific knowledge is increasingly produced by teams of researchers instead of an individual author [20]. Research shows that teams produce better outcomes than individuals alone for complex knowledge work. It is also found that science research by teams has been more impactful and novel than solo work [21, 22].

There are many practical and challenging problems regarding network science of teams and performance: How the group dynamics, sentiment, and their appraisals can determine the group's success? How does work/life balance impact success? How do individuals become influential within a team and to what extend is influence affected by cognitive biases and heuristics? How do interpersonal networks evolve along sequences of tasks? Can we estimate these dynamics and determine the right intervention? Our goal is to compose a set of explainable models to understand and eventually increase the chance of individual's and organization's success, estimate the dynamics of relationships, and help managers intervene in the teams they manage.

Luckily, the current era is rife with conversation data available for analysis. The number of social and communication platforms have skyrocketed and softwares such as Facebook Messenger, Instagram, and WhatsApp to name but a few have attracted million of users in the past decade. People exchange emails and Instant Messages (IM) everyday. Aside from personal usage, many companies and businesses use private platforms for their work chat such as Instant Bloomberg and Slack. Hence, there exist an immense amount of communication data available. Globally, as of 2019, a staggering 293.6 billion emails were sent each day and there exists currently now over 4 billion email users worldwide [23]. The average office worker receives around 121 emails every workday [23]. Today's business culture truly is in emails, with 86% of professionals naming email as their preferred means of business communication and email ranked as the third most influential source of information for business to business audiences [23]. Moreover,

statistics show Americans send roughly 26 billion text messages every day [24]. Aside from the data, research in Natural Language Processing (NLP) has offered an unprecedented opportunity for analyzing conversation data. Word embedding models [25, 26], self-attention mechanism [27, 28] and pre-trained deep neural network models for text understanding [18] have paved the way for data-driven research in conversation mining. In this dissertation, we rely on numerous communication data to tackle research questions.

Despite the availability of field data that has made the research on team networks plausible, the complexity of these data sometimes impede scientists to draw meaningful conclusion. To overcome this challenge, one needs to be able to conduct human subject experiment studies and collect data using specifically designed protocols. There exists a software called Platform for Online Group Studies (POGS) designed for such purposes to gather written responses to questions, and collect the chat logs of team discussions. It also has the ability to constrain group discussions to a prespecified network topologies to test and validate different hypothesis by composing groups of different sizes. Chapter 4 is the compendium of a specifically designed and implemented protocol using POGS to collect logs from teams of four individuals answering trivia questions over multiple rounds. Thanks to POGS, this experimental data presents an unprecedented opportunity to measure how the interpersonal influence system of teammates changes over time and how the dynamics are related to individual performance and communication.

Research in the field of networks can be split into studies on static networks, and studies on dynamic networks. Time is the key difference as static networks do not change over time, while dynamic networks do. In what follows, we introduce impactful and pertinent studies in the two subfields.

1.1 Static Networks

Static networks are the most common type of networks. They are simple yet powerful tools for many problems. The research in static networks goes back to the renowned Euler's Seven Bridges problem [29]. A network G is represented by $G(V, E)$ where V stands for a set of nodes and E for a set of edges. Nodes can represent nonliving entities such as buildings, cities, or countries as well as living entities such as individuals, group of individuals or parties. Edges represent the connection and relation among nodes and can be directed or undirected. For instance, a flight from city A to city B would be represented as a directed edge; however, the proximity of two city would be represented as an undirected edge. Edges, so-called ties, can be weighted, for instance an edge weight could be the distance between two cities in the scale of miles. In a network, when edge weights are only signs (positive or negative), that is called a signed network.

Analysis of static networks is usually involved with node or edge centrality metrics [30, 31, 32, 33]. Degree, the easiest centrality metric, is the number of edges connecting to a node. Betweenness centrality measures the extent to which a vertex lies on paths among nodes. High amount of betweenness for a node depicts that node is involved with a large proportion of shortest paths in the network. Closeness centrality of a node is calculated as the reciprocal of the sum of the length of the shortest paths between the node and all other nodes in the graph. Nodes with a high closeness metric have the shortest distances to all nodes and in a way lie in the center of the network. Eigenvector centrality or so-called prestige score is computed based on the idea of connection to high-scoring nodes contribute higher than connection to low-scoring ones. This metric for a node is large when that node is connected to many nodes which themselves have high scores. This centrality metric is extremely popular and pragmatic. PageRank algorithm [34] that is used in Google Search is one of the variants of eigenvector centralities.

Real networks often are very large. For example, at the time of this dissertation, Facebook social network has 2.7 billion nodes. To make qualitative and quantitative conclusion about networks it is common to consider a subset of nodes in the network. The network only inducing that subset of nodes is called a subgraph. Subgraphs are not only easier to interpret compared to the entire network, but also they can reveal nontrivial information about the underlying network.

To analyze and model the dynamics of networks, a common approach is to study the subgraphs. In this dissertation, we track subgraphs in network snapshots, model the dynamics, and predict the network states. This is a general problem on static networks that is called subgraph mining. Scientists often search for specific structural pattern that satisfies a desirable properties such as structural anomaly [35]. Another pattern could be based on the frequency of subgraphs. For instance, Yan *et al.* [36] introduced an efficient model to search for the most frequent subgraph [37]. On the other hand, those subgraphs which are far less frequent than usual may include prominent information. It has been shown there exists a set of subgraphs in several real networks that their frequency differ statistically from randomized networks with the same number of nodes and edges, in-degree and out-degree distribution. These subgraphs are called motifs and they are found to be the distinctive in classification of different types of networks, solely based on their connectivity information [38]. Similarly, in another study, we also use the subgraph structure for graph classification purposes [39].

1.2 Dynamic Networks

Many systems are represented as networks comprised of interactive components that dynamically modify their connections. Dynamic network science encompasses early works on random graphs such as Erdős Rényi networks to complex models of physics, socio-

economic, and deep neural networks. In this literate, many studies introduce mathematical models that generate realistic dynamic network formation. Notable network formation models are Erdős Rényi networks [40], Watts-Strogatz [41], and Barabási-Albert [42]. A more recent network generating model, so-called Forest Fire [43] was introduced to mimic the phenomenon of network densification and shrinking diameters from real network structures. Aside from network formation, many studies focus on estimating the evolution of network structures from empirical data. One specific type of dynamic networks, which is the focal attention of this dissertation, are dynamic signed networks. In this dissertation, we intend to study signed relational networks such as friendship among finance traders, trust among Bitcoin traders, and allyship among world nations which evolve over time. Dynamic signed networks provide a suitable framework for such studies. We briefly describe this subfield in network science and focus on the theories related to the context of this dissertation in the following.

1.2.1 Dynamic signed networks

Edges in signed networks usually represent like/dislike, trust/distrust, or friendship/enmity. Depending on the network, they may also reflect praise/blame or influence/negative influence. Connections and signs in these networks can naturally change over time. There is a rich body of work on analysis, modeling, and control on dynamic signed networks.

There exist many examples of dynamic signed networks, especially in social networks. Recent world events have rekindled interest in social networks of positive and negative relations. Examples prevail across geopolitics, national elections, social media, and religious groups where polarization is frequent. The local topologies of positive and negative relations in these networks can have profound implications on individual performance.

Evidence strongly indicates that people experience mental discomfort or cognitive dissonance when they hold contradictory beliefs, and when it is present, individuals are motivated to reduce it to restore cognitive consistency [44]. If unresolved, cognitive dissonance in one's interpersonal sentiment network can lead to biased, suboptimal and undesirable behaviors [45, 46]. Yet despite the potential negative consequences of cognitive dissonance on one's performance, little is known about the patterns that characterize the formation, change, and dissolution of relationships over time, and what changes in personal affective relationships are associated with improved performance. For example, people tend to prefer others who are similar to them, but dissimilar individuals are more likely to hold non-overlapping knowledge that can lead to informational advantages and more successful outcomes [21]. Consequently, it is not surprising that collaboration networks are often homophilous and based on prior relationships, rather than diverse in composition [47, 48] [49].

In such networks, positive and negative interpretations of links between people have been modeled as scientists see these links through social science lens. Hence, researchers introduced their mathematical models inspired from multiple social psychological theories. In this regard, one of the extensively studied theories is Structural Balance Theory [50]. Since, this dissertation heavily focuses on Structural Balance Theory, in the following subsection, we delineate a comprehensive literature review on this subject.

1.2.2   Structural Balance Theory

The theory of social balance, so-called structural balance theory, is first proposed by Heider in 1940s [50]. This theory has been utilized to describe the social dynamics processes in networks and has been advocated by countless scholars from different disciplines such as sociology, computer science, and psychology [51]. Heider originally defined

structural balance theory as the theory of attitude change [50, 52]. Heider's study was the cornerstone for a flock of upcoming publications in this subject. Cartwright and Harary [53] published an impactful study that provided empirical support for balance theory as well as macro-structure analysis which has been relevant up to this date. Since then, numerous researchers have studied, generalized, and designed empirical experiments on structural balance theory [54, 55, 56]. The theory is usually addressed to the activity of individuals in appraising positively or negatively other individuals in their social networks. This activity automatically locates individuals in a network environment of people who they see as allies (friends, advisors, supporters) or competitors (detractors, foes, combatants). The theory of structural balance posits that individuals alter their sentiments on the basis of a bipolar attraction toward some configurations of sentiments and repulsion from other configurations. The theory has deep roots in social sciences [57] and social psychology [52]. It has been applied in variety of disciplines, including psychology [58], consumer-branding [59], and sports [60]. Other applications include international relationships [61, 62], virtual worlds [63], and even social relationships among animals [64]. The common theme in all these publications is studying the subgraph structure in networks.

Similar to study of motifs [38], scientists ascertained that subgraphs of three nodes are sufficient and descriptive building blocks for signed networks. In the literature, a subgraph of three is called a triad. Triads not only provide a local viewpoint to the ties in the network; but also they enjoy a sufficient complexity that multiple theories have been needed to be developed to describe their behavior. Structural balance theory is one of impactful theories that focuses on the study of triads in networks. The theory proposes a systematic dynamic on triads with four simple rules. It claims that these rules orchestrate most of the dynamics that happen in signed networks over time. The four rules, also known as Heider's axioms, are:

1. A friend of a friend is a friend

2. A friend of a foe is a foe

3. A foe of a friend is a foe

4. A foe of a foe is a friend

where friendship depicts a positive and foeship depicts a negative tie. For every triad, if all of above axioms hold, that triad is considered *structurally balanced*. Expanding these rules to networks, a network is considered structurally balanced where every triad in that network is *structurally balanced*. It is widely known that violation of these axioms leads to cognitive dissonance and eventually creates an effort to resolve contradiction and reduce discomfort in the social network. That is the reason that structural balance theory describes dynamics of the networks. This theory posits networks change toward more balanced states over time. The major development of structural balance theory was set in motion with Cartwright and Harary's [53] formal definition of attractive and repulsive sentiment configurations. Cartwright and Harary extended the fundamental study by Heider with allowing network to be undirected. Their approach, which has become the standard model of structural balance, assumes a complete sentiment network in which all individuals have either a positive or negative sentiment of any other individual in the network.

Cartwright and Harary's model is defined on fully connected networks; therefore, any triad of three individuals in the network must entail six positive or negative signed inter-personal sentiments. We know the configuration of these six sentiments must be one of 16 types. The classical structural balance theory model, which satisfies Cartwright and Harary's criterion of structural balance, permits only two of the 16 feasible types, known as *balanced* triads. On this basis, a network topology must converge to be either a com-

plete network of all-positive sentiments or a network partitioned into two subgraphs with no negative within-subgraphs sentiments and all negative between-subgraphs sentiments. These converging structures are called a network's Macro-structure [65]. More precisely, macro-structure of a signed network is the the structure that the network moves toward when time goes to infinity. Extensions of balance theory posit different macro-structures. Table 1.1 shows the details about classical models and Table 1.2 the details about generalized models. Both tables include the corresponding citation, macro-structure, and criteria for each model.

Model name	Classical Heider [52, 66]	Classical Cartwright & Harary [53]
Criteria	Axioms 1, 2, 3, 4	All cycles should have even number of negative edges
Edges	Complete	Incomplete
Network	Undirected	Undirected and directed
Macro-structure	One or two all positive clique(s) and all negative edges in between	One or two all positive subgraph(s) and all negative edges in between

Table 1.1: Classical structural balance theory models from literature, their rules, and the corresponding macro-structures.

The macro-structures for these models are determined via theoretical studies using either simulation, i.e. Kulakowski *et al.* [15] or rigorous mathematical proofs, i.e. Marvel *et al.* [70]. In a relevant study, Altafini *et al.* [71] used structural balance theory to model opinion dynamics in signed networks and arrived at the same macro-structures. Moreover, Johnson *et al.* [65] and the survey article by Zheng *et al.* [51] provide a comprehensive image including a set of pertinent references and corresponding macro-structures for the models mentioned in Table 1.2 and Table 1.1. All these models of balance theory have been frequently applied in the area of network science.

One of the common applications for structural balance theory is sign prediction.

Model name	Clustering [67]	Ranked clustering [68]	Transitivity [69]
Criteria	Axioms 1, 2, 3	Axiom 1 but forbidding the triad with one singly positive edge	Axiom 1
Edges	Complete	Complete	Complete
Network	Undirected	Directed	Directed
Macro-structure	One or multiple cliques of all positive insides and all negative edges in between	All subgraphs become multiple pointed subgraphs of positive and negative	All subgraphs become transitive

Table 1.2: Generalized structural balance theory models from literature, their rules, and the corresponding macro-structures.

Using this theory, Leskovec *et al.* [72] published a computer science targeted article in which predict sign of unknown edges in three large scale social networks. Additionally, another application is to offer reasonable explanations for various social phenomena, e.g. the cascade effect of feeling, opinion and belief diffusion in teams [73], and the political conflicts among international nations [74].

1.3   Markov Models

Markov models are one of the most versatile and powerful tools in network science. Their simplicity paves the way for facilitated mathematical derivation and eventually solving problems from different fields. Markov property claims that the state of the system at time t only depends on the state at time $t-1$. In other words, knowledge of only one step prior is sufficient in Markov chains. This means in order to determine the state at time t, we do not need any information about the system from time 1 to $t-2$. Due to Markov property, in signed networks, one can study the transition of triads from subsequent time stamps and compute the Markov probability matrix for triads [75]. A Markov transition matrix for triads would shed light on the systematic dynamics that

governs the network structure over time.

Another prominent feature of Markov models is stationary distribution. When time goes to infinity, the system reaches to a state, which is so-called stationary distribution. This state can be computed using the left eigenvector of corresponding to eigenvalue equals to 1 for the row-stochastic Markov transition matrix. Note also that it has been proved an ergodic, aperiodic and irreducible Markov chain has a unique and absorbing stationary distribution [76]. In other words, stationary distribution of Markov model provides the convergence point of the system. This feature lays out an important view of the system especially for forecasting and for intervention if needed. Another related concept is the mixing time of a Markov chain. Mixing time quantifies how far a Markov chain is from its stationary distribution. More precisely, a fundamental feature about Markov chains is that a finite-state, irreducible and aperiodic chain has a unique stationary distribution, and regardless of the initial state, the distribution of states in the chain converges to the corresponding stationary distribution as time tends to infinity [77].

1.4   Network science of teams

This dissertation focuses on analysis of task performance in multiple datasets of networked teams. Team performance is commonly considered an output of the input-process-output (I-P-O) model [78], the widely known conceptual framework for studying groups. Research based on the I-P-O model tends to assume that inputs such as group composition, lead to processes, which in turn lead to outcomes such as performance [79]. One apparent input factor of team performance is the task-related proficiency of the team members, and has been studied in various disciplines. In computer science and engineering, a large number of studies focus on optimal team design, with team optimality typically being defined in terms of the skill coverage of team members [80, 81, 82] or team

members' skill diversity [83]. Similarly, much of social scientific research focuses on the impact of cognitive abilities of team members upon the team's performance [84, 85]. However, the team members' proficiencies define the potential for good team performance, constraining rather than defining the actual performance.

The empirical studies as early as the 1949 work of Deutsch [86] have shown that collaboration and cooperation are important contributors to team performance. More recently, Barron has shown in her study [87] of the performance of small teams of students on solving mathematical problems that equally competent teams can perform very differently depending on how these teams' members work together. Similarly, Devine and Philips [88] have shown the lack of connection between the variance of team members' cognitive abilities and the team performance; an analogous result has been reported by Shim and Srivastava [89] in their study of massively multiplayer online role-playing games. The discrepancy between team members' individual abilities and the team's performance is attributed to team processes, which mediate the translation of inputs to outputs [84]. The critical dependence of team performance outcomes upon the team process is also assumed in existing works on transactive memory systems [90], where team performance depends on team members' efficiently learning each other's capabilities, and has also been recently studied by Grand et al. [91] in the context of tasks the success on which heavily depends on efficient knowledge sharing. Thus, in studying team performance, it is essential to investigate the team process, defined as the actions and interactions team members engage in while working on tasks.

In an empirical study [92] related to this field, we have focused on the analysis of the dynamics of the team process for the purposes of understanding and predicting team performance. Using an experimental study of teams of individuals performing a battery of tasks, we addressed questions such as: What are the factors defining team performance? And how can we best predict the performance of a given team on a specific task? While

the team members' task-related capabilities constrain the potential for the team's success, the key to understanding team performance is in the analysis of the team process, encompassing the behaviors of the team members during task completion. We extend the existing body of research on team process and prediction models of team performance. Specifically, we analyze the dynamics of historical team performance over a series of tasks as well as the fine-grained patterns of collaboration between team members, and formally connect these dynamics to the team performance in the predictive models. Our major qualitative finding is that higher performing teams have well-connected collaboration networks—as indicated by the topological and spectral properties of the latter—which are more robust to perturbations, and where network processes spread more efficiently. Our major quantitative finding is that our predictive models deliver accurate team performance predictions—with a prediction error of 15-25%—on a variety of simple tasks, outperforming baseline models that do not capture the micro-level dynamics of team member behaviors. We also show how to use our models in an application, for optimal online planning of workload distribution in an organization. Our findings emphasize the importance of studying the dynamics of team collaboration as the major driver of high performance in teams.

In another study [93] for modeling the performance of teams, we used the data from groups of five individuals playing the online multiplayer battle arena video game, League of Legends. The game has five tiers of difficulty for players to join based on their skills and experience. we investigated the novel problem of training multiple classifiers and discovering succinct sets of features that vary smoothly across clusters of teams within these tiers. We presented a novel learning framework by training multiple classifiers and imposing smoothness constraints among them. We developed two algorithms formulated in the dual and primal forms of Support Vector Machines (SVM), and showed that our solution in the dual form is straightforward, while the solution in the primal form requires

a relaxation of the hinge loss function. This relaxation is technically involved; however, the final solution can be effectively optimized and achieved through the approach of gradient descent. We demonstrated the performance of our novel learning framework on two important real-world applications of online team-task performance, and of the highway road traffic network. The empirical results demonstrate that our framework not only outperforms existing methods in term of prediction accuracy, but more importantly it can effectively discover succinct sets of smoothly varying features that truly capture and reflect the variation in the underlying data distribution. Such patterns considerably enhance our understanding regarding the mechanism behind the observed data.

1.5   Overview of the Present Work

This dissertation consists of three major parts contributing to dynamic networks study in longitudinal or experimental settings: we study structural balance theory in risky decision-making, generalize structural balance theory in international networks, and estimate interpersonal influence in groups.

In Chapter 2, we study a longitudinal dataset of day traders in a firm existed in New York City. In this chapter, we analyze a financial institutional over a two-year period that employed 66 day traders, focusing on links between changes in affective relations and trading performance. Traders' affective relations were inferred from their IMs ($>$ 2 million messages) and trading performance was measured from profit and loss statements ($>$ 1 million trades). We find that triads of relationships, the building blocks of larger social structures, have a propensity towards affective balance, but one unbalanced configuration resists change. Further, balance is positively related to performance. Traders with balanced networks have the "hot hand," showing streaks of high performance. Research implications focus on how changes in polarization relate to performance and polarized

states can depolarize.

In Chapter 3, we extend previous study from Chapter 2 by allowing null ties in a much larger longitudinal dataset of countries using over two decades curated data. In Chapter 3, we construct the networks of international amicable and hostile relations occurring in specific time-periods in order to study the global evolution of the network of such international appraisals using Integrated Crisis Early Warning System (ICEWS). We present an empirical evidence on the alignment of Structural Balance Theory with the evolution of the structure of this network, and a model of the probabilistic micro-dynamics of the alterations of international appraisals during the period 1995-2018. Also remarkably, we find that the trajectory of the Frobenius norm of sequential transition probabilities, which govern the evolution of international appraisals among nations, dramatically stabilizes. We buttress our study by replicating above findings with an analysis of two additional smaller-scale finance datasets. These datasets are two Bitcoin trust networks collected over five years with thousands of users.

In Chapter 4, we study interpersonal influence in small groups of individuals who collectively execute a sequence of intellective tasks. We observe that along an issue sequence with feedback, individuals with higher expertise and social confidence are accorded higher interpersonal influence. We also observe well-performing individuals are to better recognize experts in their team. Based on these observations, we introduce three hypotheses which we provide empirical and theoretical support for. In this chapter, we report empirical evidence for longstanding theories of Transactive Memory Systems, Social comparison, and Confidence heuristic regarding the origins of social influence and team efficiency. Moreover, we propose a cognitive dynamical model inspired by these hypotheses to describe the process by which individuals adjust interpersonal influences in intellective tasks. We provide rigorous analytical results on its asymptotic behavior and demonstrate its accuracy in predicting the influence on the empirical data. Lastly,

we propose a novel approach using deep neural networks on a pre-trained text embedding model for predicting the influence of individuals. Using message contents, message times and individual correctness collected from teams during tasks, we are able to accurately predict the self-reported influence in every round. Extensive experiments verify the effectiveness of the proposed dynamical and machine learning models in comparison with the baseline methods such as structural balance, and reflected appraisal model.

In Chapter 5, we conclude by summarizing the studies from previous chapters and introduce open problems that are pertinent to the studies in this dissertation.

Chapter 2

Classical Structural Balance in Finance Networks

In this chapter, we design methods for data-driven analysis of social network dynamics in risky decision-making. For such analysis, it is particularly important to be able to analyze the dynamics over a long period of time. The overall goals of this chapter is to find a simple yet powerful model that describes the changes that govern social networks in risky environments and to identify a generalized coordination process that leads an individual to perform intelligently in these situations.

For this purpose, we use a unique dataset collected from a day trading firm in New York. This dataset encompasses both trading and communication logs for over two years. For every single day, we know all trading timestamps, quantity and price as well all instant messages exchanged among the employees. In this company, we know there exists a complete social network of financial day traders that collaborate with others in ad hoc teams. They all know each other as the firm only has 66 employees. The individual's trading performance in this dataset is particularly straightforward as day traders do not hold stocks over days. They start and end everyday with cash which

makes their performance, which here is their daily profit, distinctly easy to track. Due to their risky and stressful work environment, positive and negative attitudes are formed quite easily and naturally.

To study the underlying dynamics among friends and enemies in this firm, we use structural balance theory, which is rooted in several theories of sociology and social psychology. Structural balance is a theory that examines how networks of positive or negative interpersonal sentiments evolve toward stable topologies. Contrary to the vast popularity of this theory, its theoretical advancements and dynamic predictions of network state changes have rarely been tested with empirical investigations of longitudinal data. Moreover, the implications of these network changes on task-performance metrics have not been examined.

The key result of this chapter, that enables answering the above stated questions, is using Markov transition matrix to track the probability transition of subgraphs with three nodes in subsequent social networks among traders. To this end, our statistical analyses reveal that a network of interpersonal sentiments does indeed move toward structural balance and that these movements are associated with task performances in competitive risky decision-making environments. Further, we find positive empirical relationship between balanced network structure and individual performance. As high balanced is associated with lower cognitive dissonance, this data shows that this company reaps the benefits when conflict among its employees is reduced. The findings of this study apply to individuals who engage in extensive high-risk decision making, particularly in situations where polarization is common, such as politics or in the military.

The chapter is organized as follows. In Section 2.1, we motivate and informally define the problem, provide a review of existing works in network dynamics modeling of structural balance theory, and briefly introduce this chapter's three contributions. Section 2.2 provides the necessary preliminaries. Section 2.3 is dedicated to the design of

the core concept of this chapter—Extracting the dynamical social network among traders
and computing the Markov transition probability matrix on triads. The experimental
results are illustrated in Section 2.4. We conclude in Section 2.5 with a discussion and
a summary of the results of this chapter, and point out potential directions for future
research.

2.1   Introduction

Recent world events have rekindled interest in social networks of positive and neg-
ative relations. Examples prevail across geopolitics, settings where firms compete on
new standards of innovation, national elections, social media, religious groups, and
many other situations where polarization is frequent. Despite the many real-world
settings where interpersonal riffs among collaborators can arise and potentially under-
mine performance [94, 95, 96, 97], research on how positive and negative relationships
among collaborators change and how those changes relate to performance is relatively
nascent [98, 99, 100]. Newly available data on the electronic communications among
networks of individuals enables an opportunity to measure changes in interpersonal sen-
timents and their relationship with changes in performance of the system [101, 102].

Polarization is common when positive and negative relations persist in a social net-
work. Polarization is frequently associated with cognitive dissonance in people's interper-
sonal sentiment networks [103, 104]. When cognitive dissonance exists, individuals are
motivated to restore cognitive consistency due to the mental comfort that unresolved ten-
sions create [44]. If left unresolved, cognitive dissonance can lead to biased, suboptimal
and undesirable behaviors [45, 46] that negative impact performance. Yet despite the im-
petus to restore balance in one's interpersonal sentiment networks, little is known about
the patterns that characterize the formation, change and dissolution of relationships over

time and how these micro-level reconfigurations are related to performance.

2.1.1 Related Work

Social networks have profound implications on people ranging from happiness to health [105, 106], access to information and resources [107, 108], advice [109], decision-making [110], socioeconomic status [111], and task performance [112]. Social balance is a theory that is addressed to the activity of individuals in appraising positively or negatively other individuals in their social networks. This activity automatically locates individuals in a network environment of people who they see as allies (friends, advisors, supporters) or competitors (detractors, foes, combatants), and people who see them as allies or competitors. The theory of structural balance posits that individuals alter their sentiments on the basis of a bipolar attraction toward some configurations of sentiments and repulsion from other configurations. The theory has deep roots in sociology [57] and social psychology [52]. It has been applied in variety of disciplines, including psychology [58], consumer-branding [59], sports [60], virtual worlds [63], and social animals [64].

Structural balance theory (SBT) provides an analytical framework for measuring and predicting how polarized sentiments among collaborators change and relate to performance. SBT characterizes every individual relationship as being either positive or negative in sentiment and is classically defined on directed networks [52, 53, 65, 75]. Positive sentiments include ally, friend, or supporter relationships and negative sentiments include competitor, foes, or detractor relationships. On the basis of four rules of interaction, SBT posits whether relationships will remain polarized (unbalanced) or will reconfigure, i.e., become "balanced." The four rules are: a friend of a friend is a friend, a friend of an enemy is an enemy, an enemy of an enemy is a friend, and an enemy of a friend is an enemy. These four rules disaggregate a network of ties into 16 different types

of triads of relationships. Triads can be characterized as balanced or polarized. Two of the 16 feasible triads are considered structurally balanced and balanced configurations have a propensity for stability. Polarized configurations are prone to dissolution and reorganization. Aggregating local triads provides non-intuitive implications for a group's macrostructure. A group's network topology moves towards either a complete network of all-positive sentiments or a network partitioned into two subgroups with no negative within-group sentiments and all negative between-group sentiments. Implicit in SBT is that stable configurations should support higher performance than polarized, unstable configurations. Thus, by examining micro patterns of sentiment changes, SBT enables understanding of how interpersonal relationships evolve and how these configurations either enable or hinder performance.

A sequence of generalizations followed, reviewed in [65], toward a SBT model in which 9 of 16 triad types are permissible and the remainder set of 7 are forbidden based on one or more violations of transitivity (if A likes B, and B likes C, then A likes C) in a triad's configuration of sentiments. This line of advancement was associated with empirical investigations of networks in field-settings as in [113], which evaluated whether the distribution of observed triads over the 16 feasible types indicated a bias toward a set of SBT model-specific permitted triads. The current frontier of work on SBT is focused on modeling advancements of the temporal evolution of sentiment networks [103, 104, 73, 114, 70, 74, 115]. These temporal models are motivated by the idea that field-setting networks are undergoing transformations in which positive sentiments are being converted to negative sentiments, and vice versa, toward the attractor state of structural balance. Investigations of longitudinal data on sentiment networks in field-settings, relevant to these dynamical models, are rare [104, 63, 72]. Moreover, despite evidence that social networks affect performance in task-oriented groups [112], there have been limited opportunities to examine the effects of structural changes on performance

over time. This chapter reports findings from the most extensive set of longitudinal data yet assembled to evaluate the theory's prediction of an evolution toward structural balance, and to investigate whether sentiment network states are linked with changing task performance metrics. Our investigation draws on a unique dataset from a financial trading firm to test dynamic predictions and to evaluate whether sentiment network states are linked with task performances in a competitive risky decision-making environment.

2.1.2   Contributions

Our contributions in this chapter are threefold.

1. We find a tendency for the sentiment network to steadily transition into states of greater balance over time, that is, with toward fewer violations of SBT predictions than expected in a suitability randomized network.

2. Using Markov Chain analysis, we find that only certain types of triads tend to transition from states that violate SBT predictions to states with no violations.

3. We find that an individual trader's degree of structural balance is positively associated with the trader's performance. There is temporal evidence that structural balance and performance are mutually reinforcing. Trader performance increases as the degree of a trader's embedding in classical balanced triads increases, after accounting for individual trader differences and market uncertainty.

2.2   Preliminary

2.2.1   Structural Balance Triads

Table 2.2.1 describes the 16 triad types. We use the classical SBT model definition of structural balance and operationalizations of positive and negative edges (see 2.3 for details). Its four axioms are: (A1) A friend of a friend is a friend, (A2) A friend of an enemy is an enemy, (A3) An enemy of a friend is an enemy, and (A4) An enemy of an enemy is a friend. The more general terms "positive" and "negative" relationships (sentiments) are often substituted for the metaphorical terms "friend" and "enemy" in practice. Thus, each triad entails six positive or negative sentiments. Only positive sentiments are displayed. A triad type with at least one violation of these axioms is a "forbidden" triad. It can be shown that in a sentiment network with no violations of any of these four axioms, only two types of triads may exist: 300 and 102. We refer to these two types as "permitted" triads.

Fig. 2.2 conceptualizes how Markov Chain analysis is used to compute the state transition probabilities for the 16 triad types in Table 2.2.1. Here we show the steps involved in computing the transition probability from the unbalanced or polarized triad state 210 to the balanced triad state 300 over time period $(t, t + 1)$.

2.3   Methods and Materials

2.3.1   Trade Data and Trader Performance

We observed all of the dynamic sentiment network of day traders at an anonymous trading firm from October 1, 2007 to March 31, 2009. Day traders keep short-term positions and do not hold inventories of stocks; they enter and exit positions each day,

24
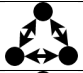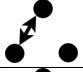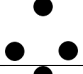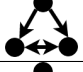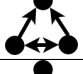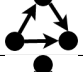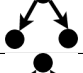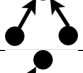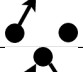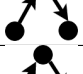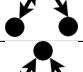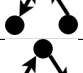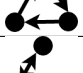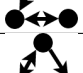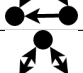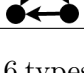
Triad Type	Triad Label	A1	A2	A3	A4
	300				
	102				
	003				X
	120D		X		
	120U			X	
	030T		X	X	X
	021D			X	X
	021U		X		X
	012				X
	021C	X			X
	111U	X		X	
	111D	X	X		
	030C	X		X	
	201	X	X	X	
	120C	X	X	X	
	210	X	X	X	

Table 2.1: SBT's 16 types of triads. Triads have 6 positive or negative sentiments (only positive sentiments are displayed) and are characterized by three numbers: the number of mutual (M), asymmetric (A), and null (N) ties, and symbols that discriminate triads with identical MAN numbers – transitive (T), up (U), down (D), and cyclic (C).

normally between 9:30 AM and 4:00 PM. We observed these traders trading ∼4,500 different stocks over various exchanges, which suggests that they sample a large part of the market. As in most trading firms, traders do not trade every day of every week for various reasons. We analyzed all of the > 1 million intra-day stock trades of these day traders and their > 2 million instant messages exchanged across their networks. The performance data were calculated using standard industry metrics.

2.3.2   Instant Messaging Communication Networks

To identify IM's containing social information, we used a dictionary-based approach, comprised of terms from the NASDAQ stock exchange and IG trading glossary to differentiate between IM's containing financial and personal information. To classify information exchanges, we tagged all IM exchanges that contained at least one word from the financial dictionary. The average IM is ∼6 words in length, consequently each one represents important information about the likely instrumental or social intent of the IM. A sample of 1,000 IM's were selected at random to validate the classification method. In the validation method, an IM tagged as having at least one word from the dictionary were read by a research assistant who agreed or disagreed that the IM represented an financial rather than a social IM.

After extracting the content of all messages to isolate social communications from instrumental communications, we used [1]'s method of estimating the strength of a social relationship from digital communication data. The method identifies positive edges between traders by comparing pairwise communication intensity levels in the observed social network vs. a statistical null-model of IM communication, where the observed pairwise level of IM exchange was randomized 10,000 times. For every period, an edge was defined as positive if the total number of IM's exchanged between two traders ex-

ceeded the random intensity scores at the $p < 0.01$ level of significance. Following prior research, edges between traders that are below the threshold are defined as non-positive or negative ties [1, 116].

Albeit balance theory research has defined non-positive edges as negative, we conducted a robustness test within our setting. To check the validity of our measurement to misclassifying ties as negative when they should be positive, we purposefully converted multiple (10,000 replicas) 5% samples at random in the observed data from negative to positive edges. The reported results were robust to these measurement tests suggesting that the definition of an edge's polarity is robust to significant measurement. Changing the polarity of edges at random in the preceding way up to 20% did not change the statistical significance or pattern of reported results.

The data setting meets the requirements of mutually acquainted individuals, for which traders develop positive and negative sentiments towards each other, not neutral attitudes [52, 53, 75, 103]. This assumption is consistent with the cognitive science literature on the automaticity of attitudes [117, 118, 119, 120] and instantaneous formation of impressions [121], as well as the communication literature examining ease of relationship formation over electronic communication [122, 123], for which use of computer screens is essential to day traders' work activities. Prior research examining negative ties as avoidance behaviors has also measured the absence of an edge as a negative tie [124, 125]; we use this approach to be consistent with the prior work.

In addition to the volume method, we used a simple threshold cutoff to define an interpersonal relationship, where the presence of an edge corresponded to a trader sending at least 1, 5, or 10 messages to another trader, respectively. Our findings are robust to methods and thresholds (Fig. 2.2(**a**)).

2.3.3 Measure of Classic Structural Balance

To quantify structural balance of the firm over time, we divided the entire observation period into six quarterly intervals, t, and defined a measure to capture the degree of balance at each quarter. For each period, we computed the ratio of balanced triads to the total number of possible triads with the measure, b_t. We used the "classic" model of structural balance, for which balanced triads were defined as the count of 300 and 102 triad types because both configurations satisfy all of Balance Theory's four rules (Table 2.2.1). To verify our selection of quarterly time intervals, we also analyzed the data using monthly, bi-monthly, biweekly and weekly time intervals and the results were robust to period interval (Fig. 2.1). The distribution of triads, transition matrices, and stationary distributions were similar in these results except that in biweekly and weekly periods, there were more 003 triads, and the probability transition to the 003 triad is higher, which is expected given the the smaller time interval (i.e., 5 or 10 business days), during which traders can IM each other. On average, traders exchange messages with two to three other contacts each week.

To ensure that our observed triadic network configurations could not be explained by chance, we constructed null models to compare the observed likelihoods of the balanced triads in the network, $\hat{b}_t$, to randomized networks, b_t, using [38], with dyadic and triadic configurations.

2.3.4 State Transition Probabilities

For each consecutive observation period, $(t, t+1)$, we compute $T_{ij}(t)$, which is the number of triads of type i that moved to type j from period t to $t+1$. Thus, row i sums to $T_{i\cdot}(t)$, which is the number of triads of type i at time t, while $T_{\cdot j}(t+1)$ is the number of triads that have transitioned to type j at time $t+1$. Using $T_{ij}(t+1)$, the transition
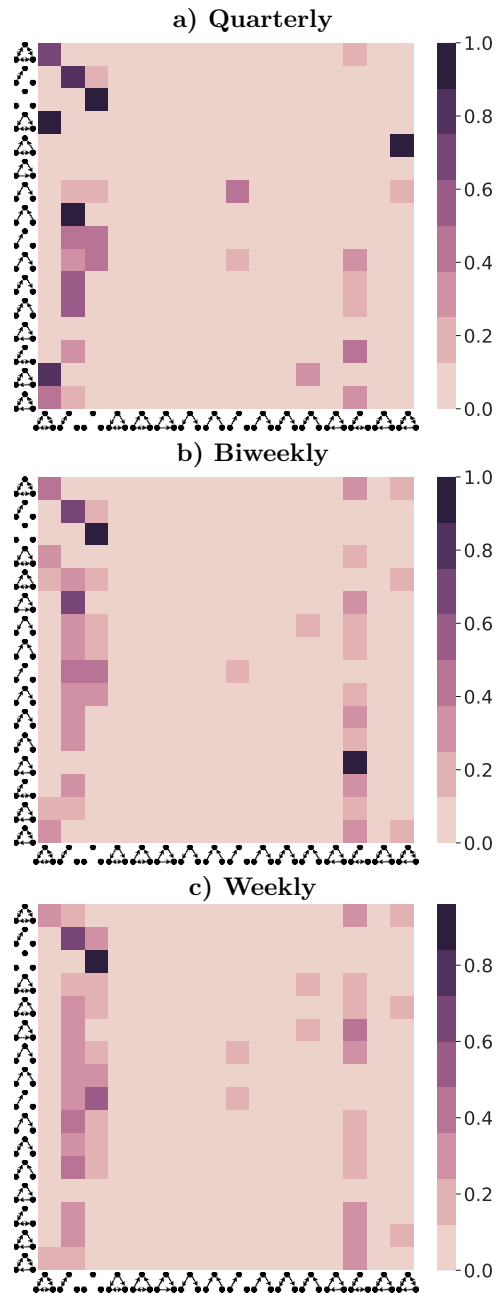
Figure 2.1: The aggregated stochastic Markov transition matrix of all periods together, with (a) quarterly, (b) biweekly and (c) weekly periods (i.e. the quarterly matrix shows the average of all matrices given in Fig. 2.3). Other designations are as Fig. 2.3). The transition probabilities are robust regardless of the choice of the period interval.

probabilities, $p_{ij}(t)$ can be estimated to obtain the transition probability matrix. These quantities can be arranged in a matrix and normalized by the sum of every row. Therefore, we have row-stochastic transition matrix P where each $p_{ij}(t)$ is conditional on i only, and not on prior states occupied by the triad. By the Markov property, they are identical for all triads, and they converge to a stationary distribution. The stationary distribution of a Markov chain is the probability distribution that a system remains unchanged as time progresses. Mathematically, it is computed as the normalized left eigenvector corresponding to the eigenvalue of 1 of the row-stochastic transition matrix [76, 126]. We compute it for every transition between two subsequent periods (Fig. 2.2(**b, c**)). The stability ratio examines the the likelihood for every transition in the observed transition matrix to happen by chance. It compares every element of the observed matrix (16×16 elements) to the corresponding element of 10,000 transition matrices computed on randomized networks [38] to determine the ratio of transitions in the observed matrix that are statistically significant for each transition period (Table 2.4.2).

Furthermore, we derive a triad count ratio, c_{xt}, for each triad configuration, x, in each period, t, to examine the distance between the current state and the stationary probability distribution for each triadic configuration and each period. Specifically, for each of the 16 triadic configurations, x, the triad count ratio is computed as the number of triads with configuration x over the total number of triads for the given period. For each transition period, we compute the triad count ratio, c_{xt} for each of the 16 triad types and compare it to the corresponding triad count ratio in the stationary probability distribution. A high degree of similarity between the two ratios indicates that ties are being reconfigured in a consistent manner that moves the system towards the stationary probability distribution.

Although the sentiment networks are fundamentally dynamic, our state transition analysis is insensitive to traders' entrances and exits. To extract communication networks

in each period, we only take into consideration those traders who have traded in the respected time. Then for every two subsequent period, we compute transitions of triads for traders who exist in both communication networks.

2.3.5   Network Triads Comparing from Observed to Randomized Networks

We compare the structural patterns of interconnections in our observed networks to randomized networks [38]. For a stringent comparison, we use randomized networks that had the same single-node in- and out-degree characteristics as the corresponding node in the real network, as well as the same dyadic subgraphs as the real network [38]. This is attained through repeatedly swapping randomly chosen pairs of connections ($S1 \leftrightarrow T1$, $S2 \leftrightarrow T2$ is replaced by $S1 \leftrightarrow T2$, $S2 \leftrightarrow T1$). Swapping is prohibited if either of the connections $S1 \leftrightarrow T2$ or $S2 \leftrightarrow T1$ already exist or these edges share nodes. The same procedure is applied for mutually connected pairs of nodes. Unlike the Milo & colleagues' work[38], in this chapter, [52], the network is fully connected, and we focus specifically on 16 directed and signed triad configurations with exactly 3 nodes. Also networks are not static but dynamic and we focus on the transition of triads over time. Results show that the triad probabilities in the randomized network are significantly different than the observed network ($p < 0.01$).

2.3.6   Structural Balance and Performance

We define a trader with a hot hand as a trader that made better than average profits over the quarterly observation period where high and low profit was split at the mean profit. To examine the robustness of the association between balance and individual relative performance (i.e., hot hand) to other potential influences, we perform the same

analysis with controls, as stated in the text.

2.4 Experimental Results

2.4.1 Trading Firm Network

We analyzed the starting, developmental, and ending states of the sentiment network of a medium-sized trading firm over a two-year period. A trading firm employs stock traders who invest the firm's money in the stock market with the expectation of maximizing the firm's return on invested capital. Day traders typically open new positions each day, trade those positions during the day, and then sell off all holdings by the end of the day. Consequently, a day trader's performance is measured on a day-to-day basis. Relationships in the firm are flat and non-hierarchical. All traders are at the same administrative level/rank and have relative autonomy in choosing the stocks they trade within the constraints of making money for the firm. Traders voluntarily form attachments with other traders to gain information relevant to their trading performance [127, 128, 129, 130, 131, 132, 133]. Typically, because relationships affect a trader's performance and create opportunities to celebrate victories and commiserate losses, traders with ongoing attachments trust and like one another [134, 127, 135, 136].

To measure relationships among traders, we analyzed $128,323$ instant messages, including content, as well as $14,259$ trades of the dynamic sentiment network of stock traders in the firm from October 2007 to March 2009 [1]. We extracted all social messages from the instant messages using content analysis because they are indicators of individuals' interpersonal, rather than instrumental relationships. On average, traders sent 228.82 ± 40.22 IM's per quarter to 5.98 ± 0.48 contacts, with a closeness centrality score of 0.15 ± 0.04. The network had an average clustering coefficient of 0.35 ± 0.04.

The complete record of IM exchanges and trades provides empirical advantages over prior work, including (i) a novel application of SBT to utilitarian relationships, in contrast to pure friendships [137, 104, 63], (ii) a minimization of self-report and mono-method biases [138], and (iii) extensive high resolution longitudinal data. All data are taken directly from the firm's servers, which archive all communication and trading data per SEC regulations. The Institutional Review Board of Northwestern University approved the study (See 2.3 for data and measurement details).

2.4.2   Markov Transitions

Fig. 2.3 shows the Markov transition probability matrix for each quarterly period of the likelihood of transition between any two triadic configurations states. Each row represents a transition out of a state i and each column represents a transition into a state j; stability of a state is represented by the diagonal (see 2.3 for details). For example, the propensity for the non-balanced triad number 210 in the last row to transition to the triad number 300 in the first row of all matrices is ~ 0.3. The transition probabilities highlight three important insights and demonstrate support for the tenets of SBT in dynamically measured settings.

First, the Markov transition probabilities are relatively stable across transition periods, as indicated by the high degree of similarity between the triad count ratios, c_{xt}, for each state and their corresponding stationary distributions. This is supported by the low L2-Norm distances of stationary probability distribution from the average distribution and steady stability ratios in the subsequent periods (Table 2.4.2), where the stability ratio denotes the proportion of transitions in the observed transition matrix that were statistically significant compared to the randomized transition matrices for each period. The stability ratios for each transition period indicate that traders reconfigure attach-

33
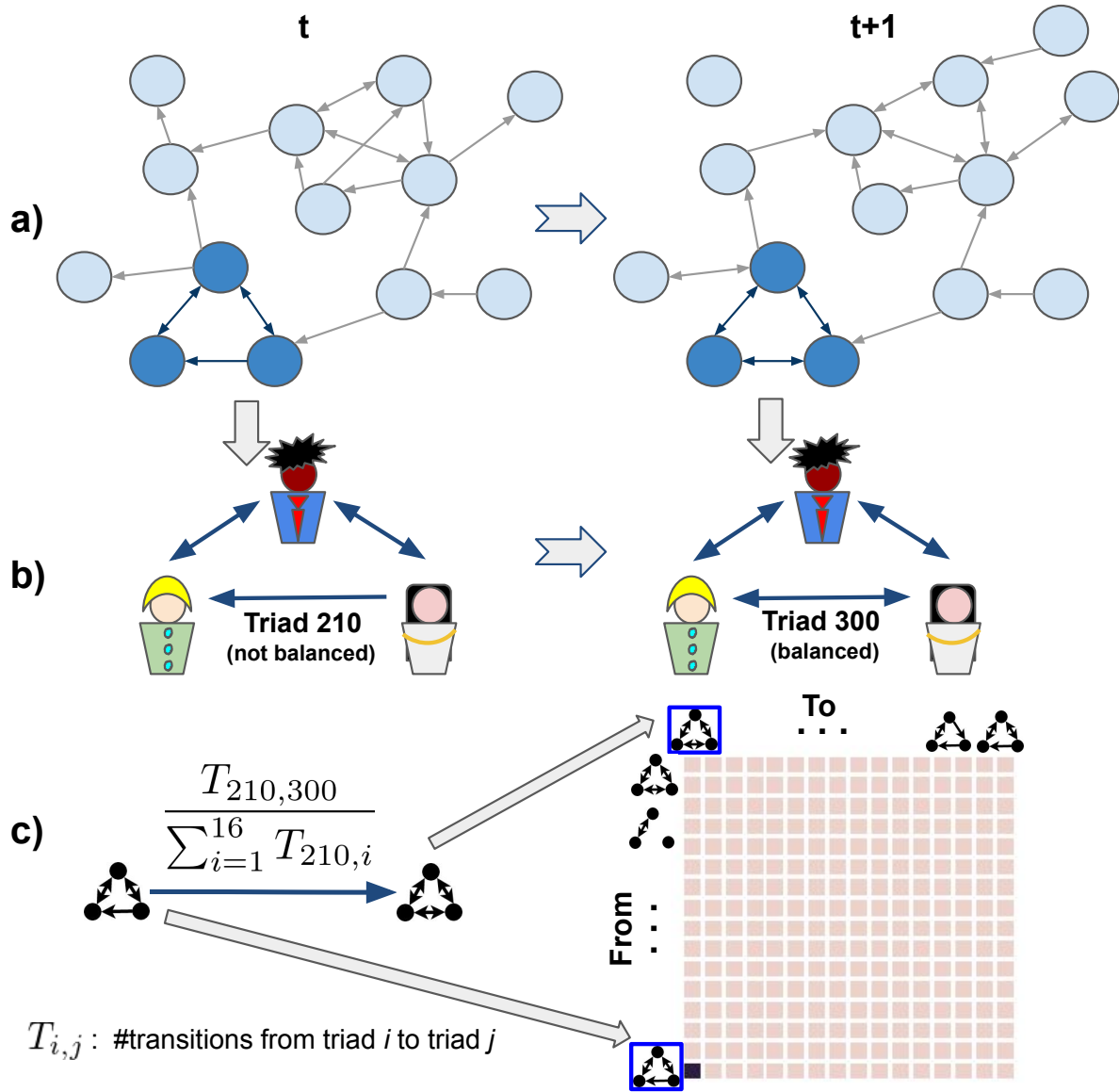
Figure 2.2: Illustrative figure showing state transition probabilities from unbalanced or polarized triad state (210) to balanced triad 300. **a)** For each period, we extract a directed graph of social IM's among traders, and identify interpersonal relations by comparing the observed relations against a statistical null-model based on Wuchty et al. 2011 [1]. **b)** We compute transition probabilities between periods for each observed triad. In this example, we demonstrate the configuration of sentiments for three illustrative nodes and compute the corresponding Markov transition probability from triad 210 to 300. **c)** We repeat for each triad in each period, resulting in a 16 state (triad) Markov Chain capturing the complete transition probabilities between states and periods (See 2.3).

ments in a consistent manner over time such that the overall system maintains a stable transition probability distribution and that the observed transitions are not likely to be explained by chance (Table 2.4.2). See 2.3 for methodological details and measurement robustness checks.

Second, examining the final stationary probability distributions associated with each triad configuration (Table 2.4.2), we find that the probability associated with being in one of the remaining 13 unbalanced states, excluding the null triad (Table 2.2.1), is just 0.03. This compares to a 0.22 probability of being in one of the two classical balanced states (and a $\sim$0.97 probability of being in balanced states allowed based on Davis et al. [67]). In this chapter, we only use Davis' theoretical deductions from his formal model. Also, we find the distributions of triads are consistently a close match to the stationary distribution over periods. Therefore, the system has very low occurrences of unbalanced states (i.e., near zero) at each period of analysis and is consistent with SBT's predictions by Heider et al. and Davis et al. [139, 67].

Third, we observe a strong propensity for stability in the "classic" balanced states, 300 and 102, as well as the null triad state, 003 (Table 2.2.1), indicating that the trader network has a tendency towards clustering into two or more subgroups [67]. Heider predicted this finding in his seminal work [139]. In particular, Heider writes "if two negative relations are given, balance can be obtained either when the triad relationship is positive or when it is negative, though there appears to be a preference for the positive alternative." [139, 67]. Davis subsequently introduced the formal theoretical model, which he called "clustering" [67] that allows for the triad 003. Finally, the overlooked prediction by Heider and Davis in balance theory [139, 67], turns out to have empirical support in a longitudinal field setting. Further, it suggests that once a triad enters the states of 300 or 102, it has a low probability of transitioning out of its current state. Thus, once traders have reconfigured their ties to a state of structural balance, they remain in these

Transition Period	L2-Norm Distance	Stability Ratio of Randomized Networks
1-2	0.07	0.84
2-3	0.08	0.92
3-4	0.06	0.94
4-5	0.05	0.91
5-6	0.20	0.83

Table 2.2: Stability of transition probabilities. L2-Norm distance of the stationary probability distribution from their average is relatively stable. Each state is defined as a vector of 16 probabilities. Stability test shows that at least 83% of transitions in each observed Markov chains are statistically significant compared to the ones computed from randomized networks.

Triad Type	300	102	003	120D	120U	030T	021D	021U	012	021C	111U	111D	030C	201	120C	210
Stationary Probability	0.02	0.20	0.75	0.00	0.00	0.00	0.00	0.00	0.02	0.00	0.00	0.00	0.00	0.01	0.00	0.00

Table 2.3: Stationary distribution of the average Markov chain over all periods. The stationarity of the null triad state suggests that forbidden triads remain in the network.

balanced configurations. Similarly, the stationarity of the null triad state suggests that the network of positive attachments remains relatively sparse over time.

2.4.3   Balance in Randomized Networks

To test whether the observed triad states can be explained by chance interactions among the traders, we compare the likelihood of observing each triad relative to the corresponding triad in 10,000 suitably randomized networks (See 2.3), for each of the 6 time periods, shown in Fig. 2.4. Informed by the stationary probability distributions (Table 2.4.2), of particular interest is the likelihood of observing the classical balanced (i.e., 102 and 300) and null (i.e., 003) triads in the actual network compared to the randomized networks. Examining Fig. 2.4, we find that while both balanced triad states are significantly more likely to occur in the actual network compared to the randomized network, our actual network has a lower occurrence of null triads than a randomized
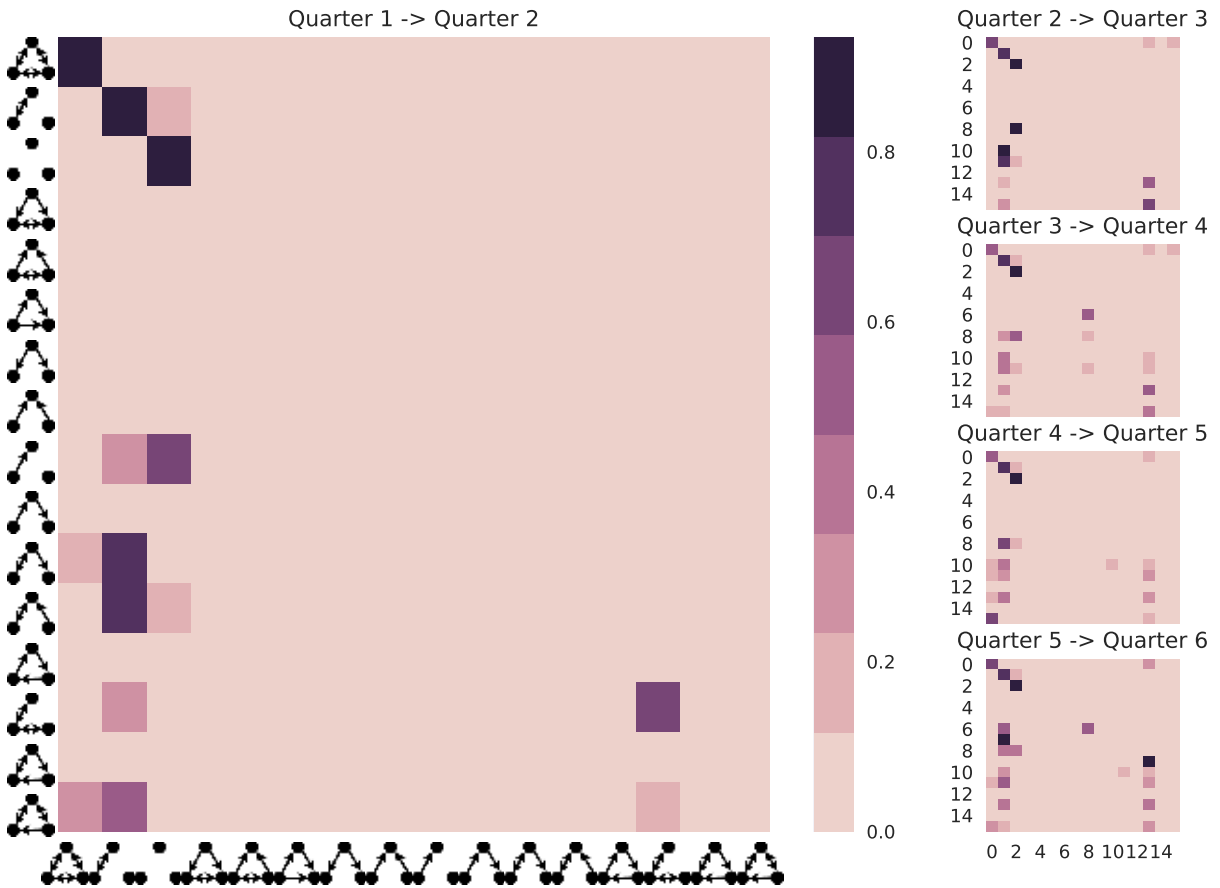
Figure 2.3: Stochastic Markov transition matrices of observing a given transition, $p_{ij}(t)$ over the period $(t, t+1)$ for all traders. Row values correspond to transitions out of a triad, column values correspond to transitions into a triad, and diagonals correspond to triad stability probabilities. Probabilities are stable across different periods and different threshold-based methodologies. Transitions occur from unbalanced to balanced triads but not vice versa. The presence of such transitions suggests once traders have reconfigured their ties to a state of structural balance, they remain in these balanced configurations.
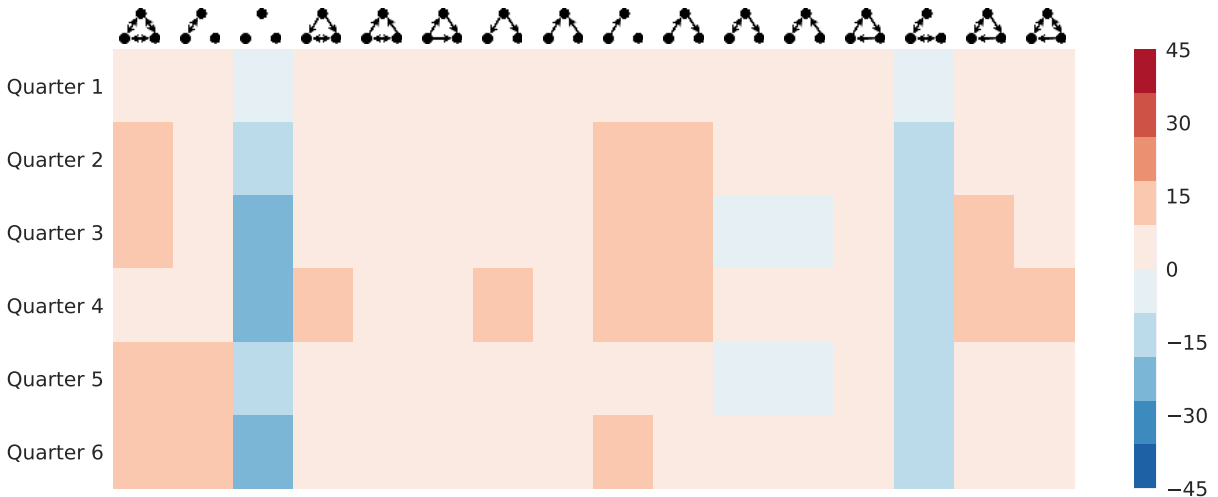
Figure 2.4: The difference in the number of standard deviations of the observed network from 10,000 suitably randomized networks. Warm colors mean more probable than random, while cold colors mean less probable. The observed networks are statistically and significantly more balanced than randomized networks.

network would suggest. The figure is computed unrelated to transition probabilities, yet shows the high significance of balanced triads. Accordingly, Fig. 2.4 confirms that the underlying assembly rules of balance theory influence the reconfiguration of interpersonal sentiments in the network towards increased balance, beyond what a random network would imply.

Further, Fig. 2.5 compares the observed degree of classic balance over time b_t to the expected $\hat{b}_t$ of the randomized network and validates that the observed, b_t is significantly higher than the expected $\hat{b}_t$ derived from the randomized network, for all observed time periods. Actual networks consistently showed significantly higher balance than the randomized networks. This finding shows that the observed triad states are not explained by chance interactions. That said, we find that the overall ratio of classically balanced triads decreases over time. This decline corresponds to the 2008-09 financial crash and aligns with prior work suggesting that a communication network tends to "turtle up" during periods of uncertainty [136].
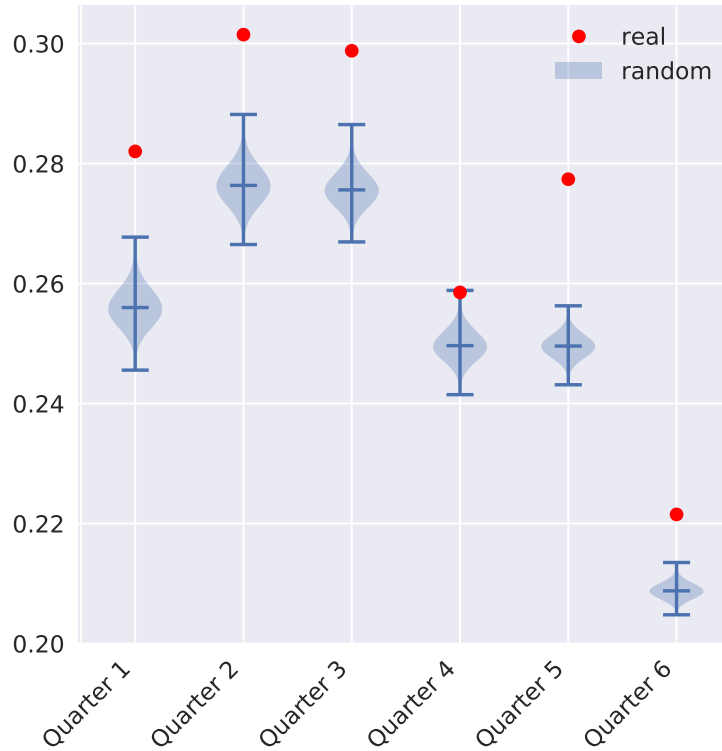
Figure 2.5: Comparison of the observed balance in the system, b_t to the expected $\hat{b}_t$ (CI is shown) in each time period indicates that the observed system is in a greater state of balance than would be expected in a comparable randomized network.

Thus, the relative likelihood of occurrence of the remaining unbalanced states in our observed network, while small, display significant differences between the structures in the network and those of a randomized network. These structural differences reflect the underlying dynamics of our particular context, as well as the social norms associated with instant messaging communication. However, despite these noted discrepancies, the stationary probability distributions (Table 2.4.2) confirm that the unbalanced configurations occur with very low probabilities and do not detract from the overall trend towards structural balance in the system. Notably, although unbalanced triads are moving towards greater balance, these transitions occur slowly; hence, few forbidden triads (201 and 021) remain within our observation period (Table 2.4.2).

An untested premise of SBT is that balance positively relates to performance [140].

Existing research indicates that ceteris paribus persons choose professional attachments they like and trust ("lovable fools") over more skillful attachments ("competent jerks") because ongoing attachments create lock-ins that lead persons to value the good relationships over performance [47, 134, 48].

2.4.4   Balance and Performance

We investigated the untested link between structural balance and trader performance by regressing an individual's trading performance on their balance b_{it}. Balance of trader i at period t is trader i's ratio of classically balanced triads (i.e., configuration 102 or 300 in Table 2.2.1) to total triad configurations in period t. Individual monthly performance, $profit_{it}$ was assessed by measuring whether trader i does better or worse than their mean individual-level performance across all time periods, i.e., whether a trader's structural balance is related to getting a "hot hand" in the market [141]. We use monthly performance because unlike the first set of analyses examining structural balance, where our focus was the long-term reconfigurations of interpersonal relationships, our focus here is on the near-term implications of balance on day traders' performance. Formally, our outcome variable is whether trader i performs better ($profit_{it} > \frac{1}{N} \sum_{t'=1}^{N} profit_{it'}$) or worse than their individual-level mean profit across all periods, where N is the number of periods. This variable is coded as $p_{it} = 1$ or $p_{it} = 0$, respectively. In our regression models we control for other factors influencing trading success, including market volatility (1=high, using the standard measure of the VIX), trader fixed effects, period fixed effects, average trade value (\$), active trading days, trader's degree centrality and IM's sent. Trader balance is measured as the log of balance. A $Logit(p_{it}) = \beta_0 + \beta_1(b_{it})$ regression was used to test the relationship and further validated with a non-parametric regression. The non-parametric regression imposes no distributional assumptions on the
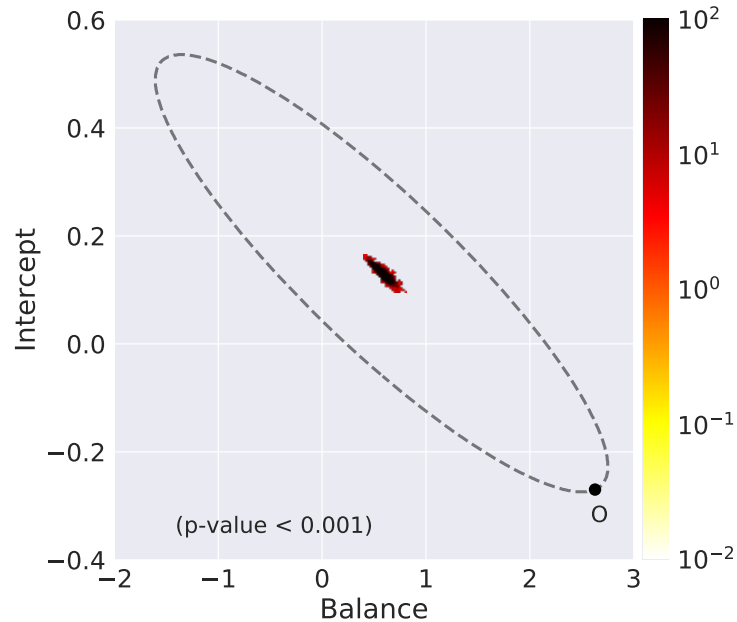
Figure 2.6: Hot hand Logit regression social balance significance, $P < 0.001$. This figure shows the results of 10,000 null models randomizing the networks, point O represents coefficient from the observed networks, dots in the middle of oval represent those of randomized networks and the color shows their distribution. The coefficients for the observed model are significantly different from randomized networks with the same in and out degree distribution. It depicts the observed balance-hot hand relationship cannot be explained by chance.

data or misspecification errors and provides a stringent test of the hypothesis by using 10-fold cross validation and bootstrapped standard errors [142, 143]. To ensure that the regression results are not due to chance, we compared the reported coefficients to those expected by chance. The results indicate the observed regressions coefficient cannot be explained by chance (Fig 2.6).

Balance is significantly and positively associated with a trader's performance for both the Logit and non-parametric regression ($p < 0.001$) (Fig 2.7). The relationship is robust to controls for market uncertainty, time period fixed effects, and individual trader effects (average trade value, number of active trading days, degree centrality), for each period (Fig 2.7a). This result demonstrates that traders typically perform best, i.e. benefit from a "hot hand", when they have relatively high balanced relationships. In fact, balance

41

presents a superlinear effect. This strong positive relationship holds for over 75% of the data. The change from medium to high balance is associated with an almost 30% increase in profits. For the bottom 25% of the data, a change in a trader's level of balance has no association with their trading performance (Fig 2.7b). This suggests that low levels of balance are unrelated to trading success but from medium to high levels of balance, any increase in balance is positively and significantly associated with increases in performance. Our result is consistent with synergy theory [144] and the classic Morrissette et al. study [145]; however, to the best of our knowledge, this is the first time the relationship has been tested on a longitudinal dataset.

2.5   Conclusion and Future Works

Balance theory provides an explanation for why interpersonal sentiment networks shift towards states of structural balance. Little quantitative work has tested the theory's underlying premise in dynamic networks or the presumed link between balance and performance. We analyzed a social network of day traders at a hedge fund using the full corpus of instant message exchanges to infer positive and negative interpersonal attachments over a two year time period. Our conclusion is that sentiment networks tend toward attractor states in which violations of the SBT theory's four axioms are removed more frequently in the observed network than expected by chance. However, there are novel findings about the temporal process of balance. We find that already balanced triads tend to be highly stable. Thus, once a triad transitions to a balanced state, it tends to remain in balance due to high probability of self-transition for balanced triads [67] (see Fig. 2.3). For unstable triads, different triads have different transition propensities and certain forbidden triads persist in the system, i.e., the null triad, which had been predicted by Heider [139], and introduced in a subsequent balance theory model by Davis

a) Fixed effects Logistic Regression
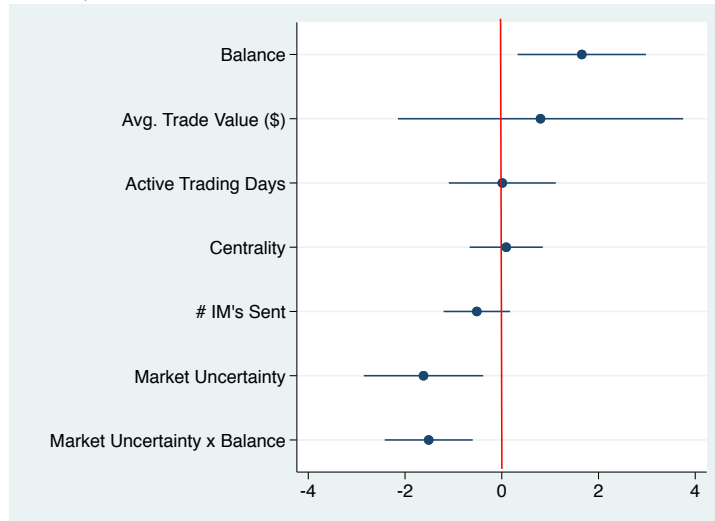
b) Predict Pr(Hot hand)
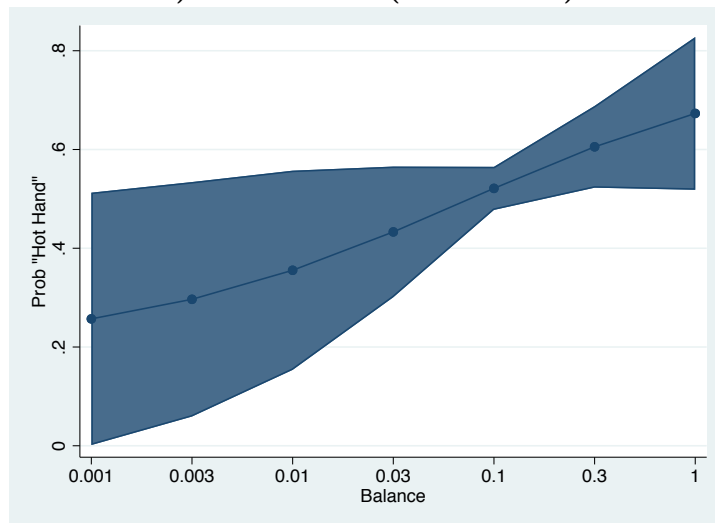
Figure 2.7: Positive classical structural balance and having the "Hot Hand." (a) Shows coefficient estimates from an individual trader and period fixed effects for Logit regression (b) Margins plot of the predicted relationship between the level of structural balance and having the hot hand based on the non-parametric regression. Values are means and 95% CI. Balance presents a superlinear effect. Positive relationship represents 75% of data. Traders trade best (i.e., have the hot hand) when their balance is relative high. The increase from medium to high balance has relatively high association of profits of nearly 30%. x-axis is reported as $e^{log(balance)}$.

et al.[67].

The development of structural balance theory has strictly focused on the structure and evolution of sentiment networks. This focus is motivated by a beautiful correspondence between its elementary axiom set and the macro-topology of a sentiment network. An untested premise of SBT is that it is related to performance, an implication with important consequences for the organization and economics of teams, networks, and other collectives. Research on organizations suggests that individuals choose balance at the expense of talent because individuals favor liking and trust ("lovable fool") over talent and skills ("competent jerk") [47]. By contrast, our test found that the hot hand is more likely to take place when an individual is in structural balance than out of structural balance. One explanation for the finding is that high balance and talent are not mutually exclusive. If balanced relationships result in more trustworthy information even if not with the best informed or most skillful individual, they may reduce verification costs. In our context, lower verification costs can mean trading is more responsive to market opportunities [127]. Further, balanced ties may offer more social support, reducing the emotional highs and lows that undermine risky decision-making or periods of poor trading [146, 147]. In particular, both the information needs of successful trading decisions, facilitated through instant e-communication, and the emotive nature of trading relationships emphasize the need to develop balanced ties to support collaboration and communication among traders over individualism or isolation. Conversely, traders with more strained relationships may need to expend a greater proportion of their energy managing their non-cooperative relationships. In our study, we find evidence suggesting that the expulsion of energy towards managing non-cooperative relationships can detract from people's abilities to effectively utilize their balanced relationships. More broadly, beyond the context of risky decision-making, these findings suggest that future research should further investigate the mechanisms by which balanced ties might improve or hin-

der other performance outcomes such as creativity and innovation, negotiations, conflict resolution, and pro-social behavior. For example, balanced ties might weaken the creative tensions that promote breakthroughs in science, art, and philosophy [148].

Building on our findings, future work might begin to investigate exogenous drivers of network dynamics. SBT theory has been endogenously focused on internal group dynamics. How and whether external forces are related to balance has been left largely unaddressed despite evidence that external conditions affect how people value and interpret their relationships. Our regression analysis showed that balance was sensitive to the overall volatility in the market. Experiments could be devised to explore the mechanisms by which interpersonal attachments change over time in complex collectives that include social hierarchy, norms and rules for interaction that force the mixing of friend and enemy relationships, or where relationships are utilitarian in nature first.

Chapter 3

Generalized Structural Balance in International Networks

Chapter 2 provides empirical support for the emergence of structural balance theory in a longitudinal setting. The experimental results use classical definition of structural balance [52] since there are a small number of traders and due the work environment, they all know each other. Thus, the assumption for fully connected social network, which is one of the requirements for classical balance theory, is acceptable. However, in a large network, this assumption is no longer valid. Large social networks are naturally sparse. Analyzing the sparse networks require an extension of structural balance theory. This chapter builds upon Chapter 3 and extend the study of triads [149] to large and sparse networks.

To study balance theory on sparse networks, we use a publicly available dataset containing timestamped relationship among many countries in world for more than two decades. This dataset provides a familiar setting based on the literature for testing generalizations of balance theory as many researchers have modeled the relationships among countries using balance theory [150, 151, 152, 153]. Additionally, the dataset

in this chapter is significantly longer than the dataset used in Chapter 3. This factor makes it possible to study the dynamics of Markov transition matrices over time. From the literature including the study in Chapter 3, it is unknown what are the underlying changes in the transition matrices of triads and whether one can use time-varying Markov chains and model the dynamics using a convex optimization scheme.

The key result of this chapter, that enables answering the above stated questions is that we define 138 sparse triads and track their distributions in longitudinal, dynamical, and sparse networks of countries, as well as two datasets of Bitcoin trust networks. We compute the empirical Markov transition matrices of sparse triads. We introduce methods for model-driven estimation of evolution in signed networks using generalization of balance theory. Lastly, we detect shocks in the dynamical networks among countries using time-varying Markov models.

The chapter is organized as follows. In Section 3.1, we motivate and informally define the problem, provide a review of existing works in analysis of network dynamics among countries, literature on structural balance theory, and briefly introduce this chapter's four contributions. Section 3.2 provides the necessary preliminaries including definition of symbols and extensions for balance theory. Section 3.3 is dedicated to the design of the core concept of this chapter—Extracting the the networks, computing the empirical Markov transition probability matrix, and estimating the transition matrices via the proposed objective function using convex optimization. The experimental results are illustrated in Section 3.4. We conclude in Section 3.5 with a discussion and a summary of the results of this chapter, and point out potential directions for future research.

3.1 Introduction

Networks of relationships such as like/dislike, trust/distrust, and praise/blame among individuals or collective actors may alter over time. The investigation of the topology of such signed appraisal networks, their evolution over time, and the development of models of their evolution have attracted sustained interdisciplinary interest. The conducted work posits that changes in the structure of appraisal networks are based on tensions generated by particular configurations of appraisals [52] that violate transitivity (a friend of a friend is a friend), and perhaps other such rules (an enemy of an enemy is a friend, a friend of an enemy is an enemy, an enemy of a friend is an enemy). Appraisal networks may arise in small groups of individuals, in communities, or in very large-scale networks composed of collective actors that are organizations or nations with alliances and animosities.

3.1.1 Related Work

In this chapter, we investigate large-scale appraisal networks of collective actors where nodes represent nations, states, or regions of a country [51, 61, 62, 150, 3, 154, 155]. The motivations for exploiting such data include an understanding of the origins of war, the formation of alliances, and the balance of powers. Similarly motivated research includes [3, 51, 61, 62, 150, 154, 155]. Some of this research on international appraisals has been guided by a network science theory of structural balance [52, 53] in which signed networks evolve toward either a network of all positive appraisals or a network composed of two components of actors with all positive within-component appraisals and all negative between-component appraisals. Gellman *et al.* [152] used structural balance theory to analyze the origins of WWI, and Antal *et al.* [153] similarly used balance theory to explore the evolution of major changes among the protagonists prior to WWI during the period 1872 to 1907. Moore *et al.* [151] used balance theory to analyze the

conflict over Bangladesh's separation from Pakistan in 1972. Harary *et al.* [150] also analyzed international relations among nations and different states of equilibrium and disequilibrium, using structural balance theory for the crisis in the Middle East in 1956. Harary *et al.* [150] showed how ten countries, after each international shock, sought a new equilibrium alignment consistent with what balance theory predicts.

Structural balance theory has deep roots in sociology [57] and social psychology [52]. Its applications include research on consumer-branding [59], sports [60], virtual worlds [156], and social animals [64]. It posits that networks of positive or negative interpersonal appraisals evolve towards stable topologies [53, 52, 67, 69, 65]. The formal development of structural balance theory was set in motion with Cartwright and Harary's [53] definition of attractive and repulsive configurations. Their approach, which has become the standard model of structural balance, assumes a complete appraisal network in which all individuals have either a positive or negative appraisal of any other individual in the network. Thus, any three individuals' interpersonal appraisals of one another must be one of 16 configurations some of which are posited to generate tensions that trigger a structural change. Notably, the classical structural balance theory model, which satisfies Cartwright and Harary's criterion of structural balance, permits only 2 of the 16 feasible types. On this basis, a group's network topology must be either a complete network of all-positive appraisal or a network partitioned into two antagonistic subgroups with no negative within-group appraisals and all negative between-group appraisal. The theory asserts that a network of positive and negative interpersonal relations evolves towards either a cohesive group or to a partition into two antagonistic subgroups [70, 74].

Despite numerous theoretical advancements and empirical studies on balance theory, the dynamic predictions of network state changes have rarely been tested with empirical investigations of longitudinal data [156, 149]. There have been a large number of empirical studies on static networks [157, 158, 159]. Longitudinal studies have been limited to small

populations of actors and to a small number of temporal states of the network [51, 160]. In contrast, this chapter presents results on the most extensive set of longitudinal data yet assembled that allows research on the question of whether the evolution of appraisal networks is mainly driven by reductions of intransitive relations.

To tackle those shortcomings in the literature, we use Integrated Crisis Early Warning System (ICEWS) dataset that is a comprehensive, automated, and validated system to monitor national, sub-national, and internal crises [161]. Its event data is publicly available and consists of coded interactions between socio-political actors (i.e., friendly or hostile actions between individuals, groups, sectors, and nation-states). Geographical-temporal metadata are extracted and associated with the relevant events within a news article. The data structure is a list of events. Every event has an occurrence date, a source actor, and a target actor. Every event is also annotated with a value in the $[-10, +10]$ interval that indicates the orientation of the source to the target actor: -10 (completely offensive) to $+10$ (completely supportive). For instance, the news event "Japan said on Tuesday it had halted economic aid to Yugoslavia in line with Western efforts to end the fighting there" is coded as a directed edge from Japan to Yugoslavia with weight -5.6, that is calculated based on the content of the news and the type of event (which in this case was "reduce or stop economic assistance"). Generally, the actors have political positions in a particular country, such as government administration, military, police, etc. In our analysis, we consider every country as a node and focus our analysis on international events in which the source and target nodes belong to different countries.

In the span of 23+ years from 1995-01-01 to 2018-09-30, the ICEWS data includes 250 countries and 8,073,921 international events, each of which are positive or negative appraisals generated from a source country to some other target country. Each appraisal is a value in the interval $[-10, +10]$ that indicates the orientation of the source to the target actor in a news event that occurred at particular time: -10 (completely offen-

sive) to +10 (completely supportive). The event data present positive, negative, and null international edges. The null edges are either a source-target news event that cannot be given a sign or an indicator that no source-target news event has been published. Precisely, there are 5,974,283 positive international edges (74%), 1,333,646 negative international edges (17%), and null instances of 765,992 neutral edges (with weight zero) (9%). In the ICEWS data, null relations appear when there are neither amicable nor hostile events between two countries. While it may be assumed that all countries are aware of each other's existence, such awareness need not be coupled with an amicable or hostile relation.

Unlike classical balance theory's prediction [53], our empirical evidence does not support the prediction that a network of friends and enemies must evolve either to a network of all friends or to a network of composed two antagonistic components of actors with all positive within-component appraisals and all negative between-component appraisals. Instead, the evidence supports the conclusion that the evolution of appraisals is mainly driven by reductions of intransitive relations among actors, which allow the emergence of complex network topologies with more than two mutually antagonistic sets of countries and hierarchically structured positive relations between countries [162]. Intransitive relations occur when there is evidence of a positive chain of international relations $i \xrightarrow{+} k \xrightarrow{+} j$ and evidence of a negative $i \xrightarrow{-} j$ relation. Such intransitive relations are assumed to be sources of international tensions that lead to transformations of positive relations to negative relations, and vice versa.

Furthermore, the empirical evidence does not support balance theory's assumption that every actor has either and positive or negative orientation to every other actor, and a line of research has developed that relaxes this assumption [53, 163, 164, 165, 54, 166, 55, 62, 104]. In large-scale networks, incomplete networks that include indifference relations are the rule. In this chapter, to the best of our knowledge, for the first time in

a longitudinal setting, we are able to address three important limitations of the line of research on the evolution of international appraisals have has been motivated by structural balance theory. These data provide a unique opportunity to (i) construct networks of international amicable and hostile relations among nation-states that occur in specific time-periods and (ii) investigate the global evolution of the network of such international appraisals over a lengthy span of time.

3.1.2   Contributions

Our contributions in this chapter are as follows. In this chapter, we advance the line of research on the evolution of the network of amicable and hostile relations among countries, and also the basic science on structural balance theory. To the best of our knowledge, this chapter reports empirical findings from the largest longitudinal data yet assembled on structural balance theory.

1. We address the existing lacuna on balance theory dynamics in large-scale networks that include null (indifference) relations. In networks that include large numbers of null relations, we find startling evidence of changes in international relations that are predominately restricted to only 10 types of configurations in the possible set of 138 configurations of null, positive, or negative relations among any three countries.

2. We find surprising evidence that does not comport with balance theory's prediction of a general tendency toward configurations of international relations that do not violate the theory's assumptions. Instead, we find a trajectory that involves a short period of increasing numbers of violations of balance theory's expectations, as indifference relations convert to negative or positive relations, followed by a longer trajectory that involves decreasing numbers of violations of transitive relations. This is an artifact of the dataset from year 1995 to 2006 as due to increasing

relationships among countries, the number of positive ties increases and therefore temporarily the number of intransitive triads increases. However, by investigating the Markov transition matrices of triads during the entire course of this evolution, we find that balanced triads are likely to stay balanced and those unbalanced triads are likely to transition to balanced ones.

3. We introduce a novel convex optimization model with a convergence guarantee for quantitatively estimating time-varying Markov chains of the transitions of the structure of international relations. Empirical Markov transition matrices show diminishing variability over our longitudinal data and emergent dynamic stability.

4. We conclude with evidence suggesting that the evolution of the network structure toward dynamic stability is subject to disturbances that appear to be related to disruptive international events and changes in the global economy. This finding provides a empirical support on a longitudinal setting for earlier research regarding the effect of global trades on international conflicts [3].

3.2 Preliminary

3.2.1 Definitions

In Table 3.2.1, we summarize the major notations used throughout the present section. In Table 3.2, we provide formal definitions for balanced triads in sparse networks inspired from three aforementioned historical models.

Symbols	Definition
V	The set of nodes in a network
E	The set of edges in a network
e_{ij}	Directed edge from node i to node j
A_t	Adjacency matrix of directed and signed network at time t
P_t	Markov transition probability matrix from time t to $t+1$
$\hat{P}_t$	Empirical Markov transition probability matrix from time t to $t+1$
$\widetilde{P}_t$	Estimated time-varying Markov transition probability matrix
T	The number of available time periods

Table 3.1: Summary of basic symbols.

Balance Model	Heider Axioms	Structural Equation (condition)
classical [53]	A1, A2, A3, A4	$\forall i, j, k \in V,$ for every combination: if $e_{ik} \neq 0$ and $e_{kj} \neq 0$ then $e_{ij} = e_{ik}e_{kj}$ should be valid
clustering [67]	A1, A2, A3	$\forall i, j, k \in V,$ for every combination: if $e_{ik} \neq 0$ and $e_{kj} \neq 0$ and $(e_{ik} > 0$ or $e_{kj} > 0)$ then $e_{ij} = e_{ik}e_{kj}$ should be valid
transitivity [69]	A1	$\forall i, j, k \in V,$ for every combination: and $e_{ik} > 0$ and $e_{kj} > 0$ then $e_{ij} = e_{ik}e_{kj}$ should be valid

Table 3.2: Sparse balance theory conditions. Definitions of sparse structural balance theory that generalize existing definitions of balance. Transitivity is the most general model that only requires the first axiom. V represents list of nodes in the network and e_{ij} represents the directed edge from node i to node j. For every three nodes of i, j, k and any combinations of which in the network, the condition should hold to be considered structurally balanced. Fig. 3.2 shows all 138 triads and if each triad is considered balance under any of these definitions.

3.2.2   Generalized Structural Balance

Classical balance theory assumes a fully connected network [52, 67, 65, 104]. While it is rational to make that assumption for small networks [75], in this chapter, due to the scale of the networks, the assumption of classical balance theory breaks as in networks with hundreds of nodes, it is unlikely that all nodes are aware of every other node. Even if they are, they may not need to communicate, work, or trade with each other. In such cases, there is no tension toward changing the configuration of appraisal relationships. Since classical balance cannot model the behavior of such large communities, we introduce a generalization of balance theory called sparse balance theory. We generalize three definitions of balance, based on the above axioms, to networks with null edges. Assume e_{ij} represents a directed edge from node i to node j. The value of e_{ij} can have negative, positive or zero (null) value. Out of 138 possible triads, 93 are transitive-balanced (67%), 44 are cluster-balanced (32%), and 24 are classical-balanced (17%). Remarkably, we find a large set of forbidden triad types are transitioning to a relatively small set of permissible triad types (Fig. 3.7). In balance theory literature, the concept of sparse balance theory has been before addressed as incomplete awareness [167, 165]. The concept has been motivated by the empirical evidence that affective relations are signed but seldom complete — actors may be neutral toward each other or there may be null or unobserved edges. Cartwright and Harary [53] define balanced cycles on networks with missing edges such that the only condition is as cycles containing an even number of negative edges. In this chapter, we extend the analysis of networks with null edges to the general case of sparse triads (formal definitions in Table 3.2). Assume every directed edge e has value $\in \{-1, 0, +1\}$. For every three distinct nodes i, j, k, to be considered as a balanced triad, the following condition, for any permutation of the nodes is needed.

3.3   Methods and Materials

3.3.1   Network Extraction

Networks are extracted by aggregating edges in predetermined periods. If the period length is too short we would not obtain sufficient information, while too long periods would decrease the granularity of the observations. We use 12 weeks ($\sim$1 quarter) as the period duration. Note, Fig. 3.5 shows results based on transition matrices are robust with respect to the choice of period length. Consequently, for ICEWS dataset, we have 103 networks. For a given network, the appraisal between nodes i and j is determined by the sign of summed edge weights of all directed edges observed between them (edge (i, j)), during that time period, as described by

$$A_{ij}(t_k) = \text{sign} \left(\sum_{t_k \leq t \leq t_{k+1}} w_{ij}(t) \right), \tag{3.1}$$

where $A(t_k)$ shows the adjacency matrix of directed and signed network at time at period t_k.

3.3.2   Empirical Markov Transition Matrices

We use Maximum Likelihood estimation (MLE) for estimating empirical Markov transition matrices. $\mathbf{P}_t$ represents a Markov transition probability matrix from time t to $t+1$. More precisely, for each consecutive observation period $(t,\ t+1)$, we compute $\mathbf{P}_{ij}(t)$, the number of triads of type i that moved to type j from period t to $t+1$. In fact, for every three nodes in the network, we find the corresponding triad type, at time t and time $t+1$, say triad type i and triad type j, respectively. Then increment the number of transitions happening from $\mathbf{P}_{ij}(t) \leftarrow \mathbf{P}_{ij}(t) + 1$. Thus, row i sums to $\mathbf{P}_{i\star}(t)$, the number of triads of type i at time t, while $\mathbf{P}_{\star j}(t+1)$ is the number of triads that have transitioned to type j

at time $t + 1$. Using the transition matrix $\mathbf{P}_{ij}(t + 1)$, the transition probabilities can be estimated to obtain the transition probability matrix. These quantities can be arranged in a matrix and normalized by the sum of every row. Therefore, we have row-stochastic transition matrix $\mathbf{P}$ where each $\mathbf{P}_{ij}(t)$ is conditional on i only, and not on prior states occupied by the triad. By the Markov property, they are identical for all triads, and they converge to a stationary probability distribution.

It is implicit in the evolution of structural balance that the triads share edges in a network and that might affect the estimating the empirical Markov transition probabilities. However, based on Markov property, the only requirement is that the next state only depend on the current state as we compute the transition probability matrix from two consecutive time periods. This phenomenon introduces additional structures in the transition matrix. As a consequence, some transitions can rarely happen as some entries of the transition matrix will be close to zero. We mitigate this potential dependency among triad transitions by applying smoothness which also helps to estimate the correct transition matrix with fewer number of data points.

3.3.3   Estimating Time-varying Markov Transition Matrices

Estimating Markov transition matrices via counting the observed transitions only takes into account the subsequent periods and therefore does not take advantage of any other similarity among transition matrices. The goal is to have a method that while keeping the Markov attribute of the system, allows for transition matrices to transfer information based on the existing assumptions in the literature, such as applying smoothness to estimate a more accurate set of transition probability matrices. Hence, we use time-varying Markov chains to capture the most out of the observed transitions in the data. The length of the longitudinal data, in this chapter, entails having statistical

sufficiency to apply a nonparametric convex method to accurately estimate the transition probability matrices directly from the data.

Model Formulation

For a network A_t at time t, we count the occurrences of each of three nodes, and classify each into one of 138 possible triads. T represents the number of available time periods and there exists T networks.

There are m entities (triads in a dynamic network), that in parallel, change states for T periods of time. As discussed before, there are 138 triad types. The empirical Markov probability transition matrix from time $t - 1$ to t, represented as $\hat{\mathbf{P}}_t$, is computed as follows

$$\hat{\mathbf{P}}_t = \frac{\sum\limits_{r=1}^{m} \mathbb{1} \left\{ S_t^{(r)} = j, \ S_{t-1}^{(r)} = i \right\}}{\sum\limits_{r=1}^{m} \mathbb{1} \left\{ S_{t-1}^{(r)} = i \right\}}, \tag{3.2}$$

where each $\hat{\mathbf{P}}_t$ is a 138×138 Markov transition matrix and there exist $\hat{\mathbf{P}}_1, \ldots, \hat{\mathbf{P}}_{T-1}$ as empirical transition matrices. m represents the number of possible sub-graphs of three. $\mathbb{1}$ shows indicator function which in this equation depicts counting the number of transitions from time $t - 1$ to time t. $S_t^{(r)}$ shows the type of triad (state) of sub-graph r at time t. In Eq. 3.2, the numerator accounts for the number of transitions from triad type i to j, and the denominator captures the number of transitions from triad type i to any triads. Fig. 3.5 shows the average empirical Markov transition matrices for different choice of period length. Now, we formalize an optimization problem to account for potential error in each empirical transition matrix as being optimized to be close to the true underlying

time-varying Markov transition matrix as

$$\mathbf{P_t} \sim \hat{\mathbf{P}}_{\mathbf{t}}. \tag{3.3}$$

The algorithm considers these empirical transition matrices as the input, and estimates all latent transition matrices, simultaneously. By definition, a Markov transition matrix, $\mathbf{P_t} : 138 \times 138$, should be ergodic, aperiodic and irreducible. Simply put, in the considered Markov chain, it should be possible to be in any state and also should be possible to get to any state from any state. Thus, there are T probability Markov transition probability matrices and every $\mathbf{P_t}$ needs to satisfy

$$0 < (\mathbf{P_t})_{ij} \leq 1, \quad \forall i, j \in \{1, \ldots, 138\} \text{ and } t \in \{1, \ldots, T-1\}. \tag{3.4}$$

By definition, Markov transition probability matrices should be row-stochastic — every row is sum up to 1. That is

$$\mathbb{1}_n^T \mathbf{P_t} = \mathbb{1}_n^T. \tag{3.5}$$

Regarding the objective function, based on previous studies dealing with time-varying Markov chains [168], we make an assumption that subsequent transition matrices are similar to each other; the changes happen smoothly.

$$\mathbf{P_t} \sim \mathbf{P_{t-1}}. \tag{3.6}$$

Optimization Problem

To estimate all unknown transition matrices simultaneously ($T-1$ matrices of size 138×138), we setup an appropriate optimization problem; we shall solve the optimization

problem using convex optimization methods.

$$
\widetilde{\mathbf{P}}_1, \ldots, \widetilde{\mathbf{P}}_{T-1} =
$$

$$
\underset{\mathbf{P_1}, \ldots, \mathbf{P_{T-1}}}{\arg\min} \qquad \frac{1}{2T-1} \sum_{t=1}^{T-1} \left\| \hat{\mathbf{P}}_\mathbf{t} - \mathbf{P}_\mathbf{t} \right\|_F^2 + \sum_{t=2}^{T-1} \psi\left(\mathbf{P_t} - \mathbf{P_{t-1}} \right),
$$

$$(3.7)$$

$$
\text{subject to} \qquad (\mathbf{P_t})_{ij} > 0, \ \forall i, j \in [1, 138],
$$

$$
(\mathbf{P_t})_{ij} \leq 1, \ \forall i, j \in [1, 138],
$$

$$
\mathbb{1}_n^T \mathbf{P_t} = \mathbb{1}_n^T,
$$

where function ψ represents regularization terms for time-varying transition matrices estimation. This function is defined as $\psi(\mathbf{X}) = \lambda_1 \|\mathbf{X}\|_1 + \lambda_2 \|\mathbf{X}\|_2$ for any matrix $\mathbf{X} \in R^{138 \times 138}$. These terms together penalize both the magnitude and number of changes in the Markov transition matrices between periods. In this equation, $\mathbf{P}_t : t = 1, \ldots, T-1$ are the variables to be estimated using convex optimization, $\hat{\mathbf{P}}_t : t = 1, \ldots T$ are the empirically estimated transition matrices using counting each triad's transitions, and $\widetilde{\mathbf{P}}_t : t = 1, \ldots, T-1$ are the estimated transition matrices. The values of $\widetilde{\mathbf{P}}_t$ are shown in Fig. 3.7. More precisely, using function ψ in Eq. 3.7, we apply two forms of smoothness on subsequent Markov transition matrices: $l2$-norm (Frobenius norm), also called group lasso that enforces a small amount of change in transition matrices, and $l1$-norm, also called fused lasso that induces a sparse solution with respect to the changes in matrices. In optimization literature, this criterion is called sparse group lasso [169]. Together they encourage subsequent Markov transition matrices to only deviate from each other with small values and in only a few cells.

This formulation allows for learning a separate model for each transition between time periods while inferring information globally across all periods. Non-parametric estimating all transition matrices together via an optimization problem decreases the

chance of overfitting. This method also allows for finer time windows than otherwise, and provides a better inference granularity in time. Consequently, even with few observations of the data, we end up with an accurate estimation for time-varying transition matrices. Algorithm 1 illustrates the steps for estimating the time-varying Markov chains.

The problem in Eq. 3.7 is convex. The reason is that the objective function is a summation of two norms which are convex, all of the inequality constraints are convex, and all equality constraints are affine. Therefore, the problem is convex [170], it has a globally optimal solution, and we solve this equation by a convex optimization solver, CVXPY [171].

Algorithm 1 Time-varying Markov algorithm. Non-parametric estimation of all time-varying transition matrices simultaneously using a convex objective function.

Input: Signed directed networks over time $\{A\}_{t=1}^{T}$
Output: Estimated transition matrices $\{\widetilde{P}\}_{t=1}^{T-1}$

Tune the hyper-parameters λ_1, and λ_2
for *time starting from $t = 2$ to $T - 1$* **do**
    $\hat{\mathbf{P}}_{\mathbf{t}} :=$ zero matrix$[138, 138]$
    for *every triplet of nodes i, j, k in set of nodes V* **do**
        triad1 $:= \text{type}(A_{t-1}(i, j, k))$
        triad2 $:= \text{type}(A_t(i, j, k))$
        $\hat{\mathbf{P}}_{\mathbf{t}}[\text{triad1}, \text{triad2}] := \hat{\mathbf{P}}_{\mathbf{t}}[\text{triad1}, \text{triad2}] + 1$
    end
    $\hat{\mathbf{P}}_{\mathbf{t}} := \hat{\mathbf{P}}_{\mathbf{t}} / (\mathbb{1}_n^T \hat{\mathbf{P}}_{\mathbf{t}})$
end
Solve the convex optimization problem in Eq. 3.7

Model Comparison

In order to test the predictability of the estimated transition matrices, we predict unseen proportion of the unseen triads using the proposed algorithm as compared to competitive baseline methods. For instance, assume we have T periods. We hold out the proportion of triads at time T and train on periods of 1 up to $T - 1$ using Algorithm 1.

Consequently, the estimated transition matrix for time $T - 1$ to T is multiplied with proportion at $T - 1$ to give us the predicted proportion at T. We apply one step-ahead forecast, for multiple times, in each time retraining the model up to the last held out time. To this end, we have a more descriptive picture of the prediction power of the proposed method. As the forecast metric, we compute Root Mean Squared Error (RMSE) of the difference between the predicted proportion with the ground truth. Random prediction is neglected due to its significantly worse accuracy compared to other baselines. Consequently, we compare our forecast to a baseline of simply predicting the last time steps proportions, and versus an average of all preceding time steps' proportions.

In this dataset, we modify the proposed model in Eq. 3.7 to apply the optimization only on a desired time window with length δ. This hyperparameter would be tuned to determine how many past transition matrices are used for optimizing the current time points. The reason is long-range interactions in the objective function could cause unwanted effects if the dynamics are changing so heavily over time. Especially, when we observe in Fig. 3.9 the changes are dramatically decreasing over time. Using two years as the time window ($\delta = 8$), we compare the proposed model using Time-varying Markov model to the baselines in Fig. 3.1.

Fig. 3.1 depicts that the proposed algorithm outperforms the baselines and makes accurate forecasts of the proportion of triads in the subsequent time period in the ICEWS dataset. Baselines consist of predicting last proportion of triads (Last Proportion), average of previous proportions of triads (Average Proportion), and using previous Markov Transition matrix without applying time-varying estimation to estimation the current proportion (Time-invariant Markov). The proposed Time-varying Markov model clearly surpasses the baselines in almost every year forecast. We also apply on a validation set of the periods, to carefully tune the hyperparameters of algorithm 1. In this chapter, we also set $\lambda_1 = 0.01$ and $\lambda_2 = 0.005$.
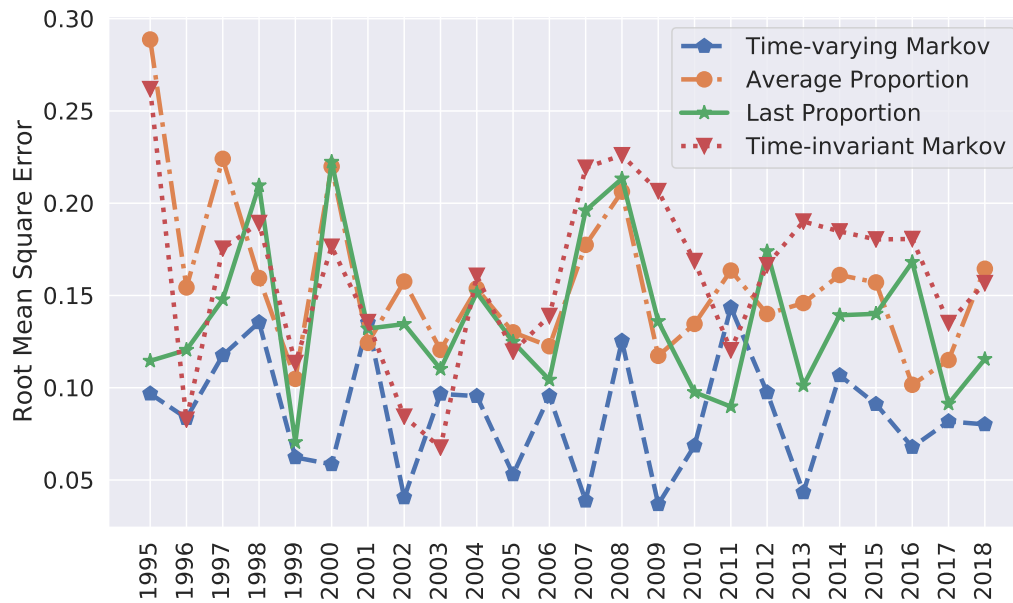
Figure 3.1: Model comparison. Root Mean Square Error (RMSE) of different baseline algorithms and the proposed *Time-varying Markov model* (dashed blue) in predicting unseen triad proportions in Integrated Crisis Early Warning System (ICEWS) dataset (the smaller RMSE the better). *Average Proportion* (dash-dotted orange) computes the average of each triad type proportion up to the current time. *Last Proportion* (solid green) assumes the new proportion is exactly the last one, and due to the origin of being smooth, it is highly competitive. The proposed *Time-invariant Markov* (dotted red) chain method minimises the RMSE thus providing the most accurate proportion of triads. The results show that the proposed method almost for every year surpassed the baselines' accuracy in forecasting the proportion of the triads.

3.3.4   Details and Proofs for Time-varying Markov Model

Fig. 3.2 shows all 138 sparse triads. The title includes (B) and (N) whether if each triad is balanced with respect to classical-, clustering-, and transitivity-balanced, respectively. These definitions are generalizations based on the literature when we require different subset of Heider's axioms [52] (Friend of friend is friend and etc.). The classical version is the most restrictive by requiring four axioms while transitivity requires only one axiom and is the least restrictive.

In the following of this section, we provide proofs for the time-varying Markov model.

Settings: There are $n = 138$ states, named $l_1, \ldots, l_n$. There are m entities (triads in the network), that in parallel, change states for $T + 1$ periods of time. Each empirical Markov probability transition matrix, $\hat{P}_t$, is computed as follows

$$\hat{P}_t(i,j) = \frac{\sum_{r=1}^{m} \mathbb{1}\left\{S_t^{(r)} = j, \ S_{t-1}^{(r)} = i\right\}}{\sum_{r=1}^{m} \mathbb{1}\left\{S_{t-1}^{(r)} = i\right\}} \tag{3.8}$$

where each $\hat{P}_t$ is a $n \times n$ matrix and there exist $\hat{P}_1, \ldots, \hat{P}_T$. m represents the number of possible sub-graphs of three. $\mathbb{1}$ shows indicator function which in this equation depicts counting the number of transitions from time $t-1$ to time t. $S_t^{(r)}$ shows the type of triad (state) of sub-graph r at time t.

Assumptions: The assumption is that there is an error in empirical transition matrices such that

$$\hat{P}_t = P_{0,t} + z_t \tag{3.9}$$

where $P_{0,t} : t = 1, \ldots, T$ are the true unknown transition matrices, $\hat{P}_t, t = 1, \ldots, T$
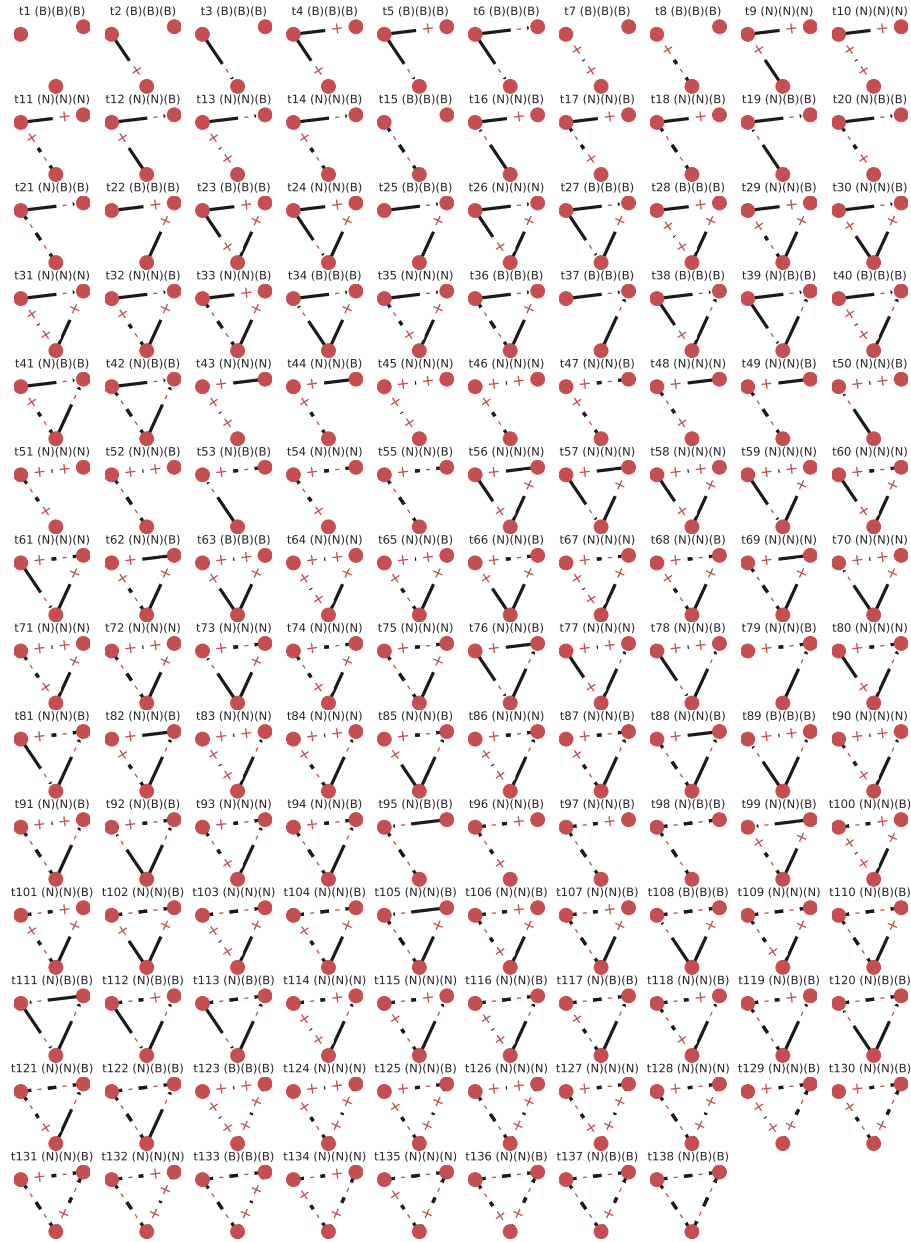
Figure 3.2: Total 138 sparse triads. Title of each triad shows its #ID, and whether if it is balanced with respect to classical-, clustering-, and transitivity-balanced, respectively. The title includes (B) if it is balanced, and (N) if not, for every definition. Notably there exists 24 triads out of 138 ones which are classically-balanced. 44 triads out of 138 are clustering-balanced. Also, 93 triads out of 138 are transitivity-balanced.

the empirical transition matrices, and $z_t, t = 1, \ldots, T$ are i.i.d sub-Gaussian errors with zero mean. The probability transitions are between $[0, 1]$; thus, it is easy to show that the error is bounded as there exists a value for $M, \sigma > 0$ such that

$$P(|z_i| > t) \quad \leq \quad M \exp(-t^2/(2\sigma^2)) \ \forall t > 0, \ i = 1, \ldots, n.$$

Hence, z_t is sub-Gaussian. In our results, we also find empirically support for independence of errors as the Pearson correlation of every cells for subsequent estimated matrices are very small and more than 70% are not statistically significant ($p \geq 0.05$).

We also assume the total variation [172] of matrices does not grow too quickly [173], where each $P_{0,t}$ is a matrix with n^2 dimensions, for the constant value of $n = 138$

$$TV(P_{0,t}) = \sum_{i=2}^{T} ||P_{0,t} - P_{0,t-1}||_{1,1} \leq n^2 C_T = \mathcal{O}(T). \tag{3.10}$$

We empirically report the above equation for our data is approximately $0.04T$, and indeed is $\mathcal{O}(T)$.

Problem definition: Instead of having a model for one Markov transition matrix and fit that to the entire period, we define a convex optimization problem to predict all transition matrices altogether using trend filtering for nonparametric regression [174].

$$\widetilde{P_1}, \ldots, \widetilde{P_T} = \underset{P_1, \ldots, P_T}{\arg\min} \quad \frac{1}{2T-1} \sum_{t=1}^{T-1} ||\hat{P}_t - P_t||_F^2 + \lambda_1 \sum_{t=2}^{T-1} ||P_t - P_{t-1}||_{1,1} + \lambda_2 \sum_{t=2}^{T-1} ||P_t - P_{t-1}||_{2,1},$$

$$\text{subject to} \quad (P_t)_{ij} > 0, \ \forall i, j \in [1, n]$$

$$\mathbb{1}_n^T P_t = \mathbb{1}_n^T$$

$$\tag{3.11}$$

where $\widetilde{P}_t : t = 1, \ldots, T$ are the estimated transition matrices. λ_1 and λ_2 are the

hyperparameters which are tuned by applying Grid Search with 5-fold cross-validation.

Convexity Proof

The objective function is a summation of three norms which are convex, all of the inequality constraints are convex, and all equality constraints are affine [170]. Therefore, the problem is convex, it has a globally optimal solution [170]. Thus, we solve this equation by a convex optimization solver, CVXPY [171].

Convergence Rate Proof

For the sake of simplicity, in the following section, we only take into account $l1-$norm smoothness in the optimization problem.

Convergence Rate Theorem:

$$\sum_{t=1}^{T-1} ||\widetilde{P}_t - P_{0,t}||_F^2 = \mathcal{O}_{\mathbb{P}}\left(n^2(\text{nullity}(\Delta) + M\sqrt{\log r}C_T)\right). \qquad (3.12)$$

Proof: Since the objective function in Eq. 3.11, in previous proof is shown to be convex; thanks to the optimiality of *argmin*, $\widetilde{P}$, the solution of the optimization problem minimizes the objective function more than any other matrix, say X,

$$\text{objective}(\widetilde{P}) \ \leq \ \text{objective}(X).$$

We use Eq. 3.11 and rewrite it as

$$\frac{1}{2T-1}\sum_{t=1}^{T-1} ||\hat{P}_t - \widetilde{P}_t||_F^2 + \lambda_1 \sum_{t=2}^{T-1} ||\widetilde{P}_t - \widetilde{P}_{t-1}||_{1,1} \ \leq \ \frac{1}{2T-1}\sum_{t=1}^{T-1} ||\hat{P}_t - X_t||_F^2 + \lambda_1 \sum_{t=2}^{T-1} ||X_t - X_{t-1}||_{1,1}.$$

As a matter of fact X_t, could be replaced by $P_{0,t}$ as follows

$$\frac{1}{2T-1}\sum_{t=1}^{T-1}||\hat{P}_t-\widetilde{P}_t||_F^2+\lambda_1\sum_{t=2}^{T-1}||\widetilde{P}_t-\widetilde{P}_{t-1}||_{1,1} \leq \frac{1}{2T-1}\sum_{t=1}^{T-1}||\hat{P}_t-P_{0,t}||_F^2+\lambda_1\sum_{t=2}^{T-1}||P_{0,t}-P_{0,t-1}||_{1,1}.$$

After multiplying both sides by 2 and expanding the previous inequality by using the assumption in Eq. 3.9, we have

$$\sum_{t=1}^{T-1}||P_{0,t}+z_t-\widetilde{P}_t||_F^2+2\lambda_1T\sum_{t=2}^{T-1}||\widetilde{P}_t-\widetilde{P}_{t-1}||_{1,1} \leq \sum_{t=1}^{T-1}||P_{0,t}+z_t-P_{0,t}||_F^2+2\lambda_1T\sum_{t=2}^{T-1}||P_{0,t}-P_{0,t-1}||_{1,1}.$$

Then, we can write

$$\sum_{t=1}^{T-1}||(P_{0,t}-\widetilde{P}_t)+z_t)||_F^2+2\lambda_1T\sum_{t=2}^{T-1}||\widetilde{P}_t-\widetilde{P}_{t-1}||_{1,1} \leq \sum_{t=1}^{T-1}||z_t||_F^2+2\lambda_1T\sum_{t=2}^{T-1}||P_{0,t}-P_{0,t-1}||_{1,1}.$$

By expanding the power in term $\sum_{t=1}^{T-1}||(P_{0,t}-\widetilde{P}_t)+z_t)||_F^2$ from above inequality, we have

$$\sum_{t=1}^{T-1}||P_{0,t}-\widetilde{P}_t||_F^2 + \sum_{t=1}^{T-1}||z_t||_F^2 + 2\sum_{t=1}^{T-1}z_t^T(P_{0,t}-\widetilde{P}_t) + 2\lambda_1T\sum_{t=2}^{T-1}||\widetilde{P}_t-\widetilde{P}_{t-1}||_{1,1}$$
$$\leq \sum_{t=1}^{T-1}||z_t||_F^2 + 2\lambda_1T\sum_{t=2}^{T-1}||P_{0,t}-P_{0,t-1}||_{1,1},$$

where rearranging the terms yields

$$\sum_{t=1}^{T-1}||\widetilde{P}_t-P_{0,t}||_F^2 \;\leq\; 2\sum_{t=1}^{T-1}z_t^T(\widetilde{P}_t-P_{0,t})+2\lambda_1 T\sum_{t=2}^{T-1}||P_{0,t}-P_{0,t-1}||_{1,1}-2\lambda_1 T\sum_{t=2}^{T-1}||\widetilde{P}_t-\widetilde{P}_{t-1}||_{1,1}.$$

Using orthogonal decomposition on the left term we have

$$\sum_{t=1}^{T-1}||\widetilde{P}_t-P_{0,t}||_F^2 = \sum_{t=1}^{T-1}||z_t||_{R_\perp}^2 + \sum_{t=1}^{T-1}||\widetilde{P}_t-P_{0,t}||_R^2, \tag{3.13}$$

where the null space term is of the order

$$\sum_{t=1}^{T-1}||z_t||_{R_\perp}^2 = \mathcal{O}(n^2\text{nullity}(\Delta)), \tag{3.14}$$

and the row space term of inequality Eq. 3.13 is rewritten as following

$$\sum_{t=1}^{T-1}||\widetilde{P}_t-P_{0,t}||_R^2 \;\leq\; 2\sum_{t=1}^{T-1}z_t^T P_R(\widetilde{P}_t-P_{0,t})+2\lambda_1 T\sum_{t=2}^{T-1}||P_{0,t}-P_{0,t-1}||_{1,1}-2\lambda_1 T\sum_{t=2}^{T-1}||\widetilde{P}_t-\widetilde{P}_{t-1}||_{1,1}.$$

In the first term we use $P_R = \Delta^\dagger\Delta$ where $\Delta \in \mathbb{R}^{r\times n}$ is an arbitrary linear operator, with r rows. We have

$$\sum_{t=1}^{T-1}||\widetilde{P}_t-P_{0,t}||_R^2 \;\leq\; 2\sum_{t=1}^{T-1}z_t^T\Delta^\dagger\Delta(\widetilde{P}_t-P_{0,t})+2\lambda_1 T\sum_{t=2}^{T-1}||P_{0,t}-P_{0,t-1}||_{1,1}-2\lambda_1 T\sum_{t=2}^{T-1}||\widetilde{P}_t-\widetilde{P}_{t-1}||_{1,1}. \tag{3.15}$$

Based on Hölder's inequality [175], we know for any $p,q \geq 1$ such that $\frac{1}{p}+\frac{1}{q}=1$ then for any two functions f and g the following inequality always holds

$$\|fg\|_1 \;\leq\; \|f\|_p\|g\|_q.$$

By applying Hölder's inequality on the term $z_t^T \Delta^\dagger \Delta(\widetilde{P}_t - P_{0,t})$ from Eq. 3.15, with $p = \infty$ and $q = 1$, we see

$$z_t^T \Delta^\dagger \Delta(\widetilde{P}_t - P_{0,t}) \leq ||z_t^T \Delta^\dagger \Delta(\widetilde{P}_t - P_{0,t})||_1 \leq ||(\Delta^\dagger)^T z_t||_\infty ||\Delta(\widetilde{P}_t - P_{0,t})||_1,$$

in which $\Delta(\widetilde{P}_t - P_{0,t}) = (\widetilde{P}_t - \widetilde{P}_{t-1}) - (P_{0,t} - P_{0,t-1})$. We can rewrite the inequality as

$$z_t^T \Delta^\dagger \Delta(\widetilde{P}_t - P_{0,t}) \leq ||(\Delta^\dagger)^T z_t||_\infty ||(\widetilde{P}_t - \widetilde{P}_{t-1}) - (P_{0,t} - P_{0,t-1})||_1. \qquad (3.16)$$

We claim that variation in every step from its previous value has the same sign in the ground truth and the estimated matrix. In other words, sign of $P_{0,t} - P_{0,t-1}$ and $\widetilde{P}_t - \widetilde{P}_{t-1}$ are always the same. Thus, we can use the inequality $||x - y|| \leq ||x + y||$ where $xy \geq 0$. Therefore, we have

$$z_t^T \Delta^\dagger \Delta(\widetilde{P}_t - P_{0,t}) \leq ||(\widetilde{P}_t - \widetilde{P}_{t-1}) - (P_{0,t} - P_{0,t-1})||_1 \leq ||(\widetilde{P}_t - \widetilde{P}_{t-1}) + (P_{0,t} - P_{0,t-1})||_1$$

Based on triangle inequality ($||x + y||_1 \leq ||x||_1 + ||y||_1$ for any x, y), we know the right term in previous equation is

$$z_t^T \Delta^\dagger \Delta(\widetilde{P}_t - P_{0,t}) \qquad (3.17)$$
$$\leq ||(\Delta^\dagger)^T z_t||_\infty \left\| (\widetilde{P}_t - \widetilde{P}_{t-1}) + (P_{0,t} - P_{0,t-1}) \right\|_1$$
$$\leq ||(\Delta^\dagger)^T z_t||_\infty \left(||\widetilde{P}_t - \widetilde{P}_{t-1}||_1 + ||P_{0,t} - P_{0,t-1}||_1 \right)$$

Note z_t are all independent, and thus their summation is treated as a constant. Therefore, using equations Eq. 3.16 and Eq. 3.17 and after applying summation, we have

$$\sum_{t=1}^{T-1} z_t^T \Delta^\dagger \Delta(\widetilde{P}_t - P_{0,t}) \leq \sum_{t=1}^{T-1} ||(\Delta^\dagger)^T z_t||_\infty \left(\sum_{t=2}^{T-1} ||\widetilde{P}_t - \widetilde{P}_{t-1}||_1 + \sum_{t=2}^{T-1} ||P_{0,t} - P_{0,t-1}||_1 \right).$$

By picking the right value for $\lambda_1 \geq \frac{1}{T} \sum_{t=1}^{T-1} ||(\Delta^\dagger)^T z_t||_\infty$, then above equation can simplified as

$$\sum_{t=1}^{T-1} z_t^T \Delta^\dagger \Delta(\widetilde{P}_t - P_{0,t}) \leq \lambda_1 T \sum_{t=2}^{T-1} ||\widetilde{P}_t - \widetilde{P}_{t-1}||_1 + \lambda_1 T \sum_{t=2}^{T-1} ||P_{0,t} - P_{0,t-1}||_1.$$

Consequently, we use above inequality in Eq. 3.15, and rewrite it as in the following

$$\sum_{t=1}^{T-1} ||\widetilde{P}_t - P_{0,t}||_R^2$$
$$\leq 2\lambda_1 T \sum_{t=2}^{T-1} ||\widetilde{P}_t - \widetilde{P}_{t-1}||_1 + 2\lambda_1 T \sum_{t=2}^{T-1} ||P_{0,t} - P_{0,t-1}||_1$$
$$+ 2\lambda_1 T \sum_{t=2}^{T-1} ||P_{0,t} - P_{0,t-1}||_{1,1} - 2\lambda_1 T \sum_{t=2}^{T-1} ||\widetilde{P}_t - \widetilde{P}_{t-1}||_{1,1}.$$

And thereupon

$$\sum_{t=1}^{T-1} ||\widetilde{P}_t - P_{0,t}||_R^2 \leq 4\lambda_1 T \sum_{t=2}^{T-1} ||P_{0,t} - P_{0,t-1}||_{1,1}. \tag{3.18}$$

Similar to previous studies [176], we know $||(\Delta^\dagger)^T z_t|| = \mathcal{O}_\mathbb{P}(M\sqrt{\log r})$ by a standard result on the maximum of Gaussians (derived using the union bound, and Mills' bound

on the Gaussian tail), where M is the maximum $l2-$norm of the columns of $\Delta^\dagger$. Thus, for the hyperparameter λ_1 we know

$$\lambda_1 \geq \frac{1}{T}\sum_{t=1}^{T-1}||(\Delta^\dagger)^T z_t||_\infty = \mathcal{O}_\mathbb{P}(\frac{M}{T}\sqrt{\log r}).$$

And based on the total variation growing condition in Eq. 3.10 and the aforementioned choice of λ_1, inequality in Eq. 3.18 gives the below inequality

$$\sum_{t=1}^{T-1}||\widetilde{P}_t - P_{0,t}||_R^2 \leq 4(\frac{M}{T}\sqrt{\log r})Tn^2 C_T = 4n^2 MC_T\sqrt{\log r}. \tag{3.19}$$

The convergence rate for the entire problem, by using Eq. 3.19 and Eq. 3.14, would be the big o probability of the following

$$
\begin{aligned}
\sum_{t=1}^{T-1}||\widetilde{P}_t - P_{0,t}||_F^2 &\leq \sum_{t=1}^{T-1}||\widetilde{P}_t - P_{0,t}||_{R_\perp}^2 + \sum_{t=1}^{T-1}||\widetilde{P}_t - P_{0,t}||_R^2 \\
&\leq n^2\text{nullity}(\Delta) + 4n^2 MC_T\sqrt{\log r},
\end{aligned}
$$

And thus,

$$\sum_{t=1}^{T-1}||\widetilde{P}_t - P_{0,t}||_F^2 = \mathcal{O}_\mathbb{P}\left(n^2(\text{nullity}(\Delta) + M\sqrt{\log r}C_T)\right)$$

∎

3.4 Experimental Results

3.4.1 Empirical Dynamic Networks

To investigate the evolution of the international appraisals, these data are disaggregated into time periods. Each time period is associated with the subset of published events that occurred during the period. Each network is comprised of 62,250 ($250^2 - 250$) directed positive, negative, and null edges among the 250 countries. A particular source-target ordered pair of countries may be associated with multiple events during a particular time period, and we take the sign of the summed value of these multiple events as the measure of the orientation of the source to the target. Hence, for 3 month periods, we have 101 snapshots of signed and directed networks among countries. We attend to different definitions of period length as a check on the robustness of our findings.

We find that the network structures are in the class of classical core-periphery (also called center-periphery) structures [177, 178]. Such structures of n nodes are composed of one strong component of k nodes (the core) in which one or more paths of positive appraisals exits from every member of the core to every other member of the core. The remaining set of $n - k$ nodes (the periphery) is composed of nodes each which has at least one positive appraisal to a node (or nodes) in the core. We find, in the first period of the data, that there are exactly 111 countries in the core and 23 countries in the periphery. These peripheral countries were Afghanistan, Angola, Guinea, Haiti, Sierra Leone, Zimbabwe, Bolivia, Paraguay, Rwanda, Armenia, Azerbaijan, Congo, Grenada, Guatemala, Guyana, Kuwait, Malawi, Mozambique, Nicaragua, Nigeria, Panama, Sudan, Timor-Leste. We find that over time (in about 4 years), all of the first period peripheral countries moved into the core. That is, the size of the core grew to $n = 134$ and was maintained as a single strong component of 134 nodes. The remaining 116 countries do not exist in all network periods. Thus, we focus on the network dynamics of these 134

countries in our analysis. Using quarterly periods, the percentage of positive ties in the core increases from 4% to 18%, and the percentage of negative ties increases from 1% to 4%. This trend is shown in Fig. 3.3 (a).

This theory predicts an evolution of the structure of signed networks toward a state in which all violations are eliminated. In this theory, triads —subsets of three nodes— are considered the building blocks of relationships. Every possible triad of three countries among the core countries (134 countries) involves six edges. Classical structural balance theory assumes the absence of null edges, as every edge can be only positive or negative. In this case, there are 16 possible type of triads [75, 104, 149, 70, 179]. As large networks are rarely fully connected, in this chapter, we consider an generalization of structural balance theory in which each edge is either positive, negative or null. We call it sparse structural balance theory. In this model since null arcs are allowed, there are 138 possible types of triads (Fig. 3.2 shows total 138 possible triads). The underlying idea behind this generalization is that at any given time, if an edge has not been existed until now, it means there exists no social tension between those two nodes and that edge should not be considered as a violation by the balance theory axioms. To follow a tremendous literature on structural balance theory, we extend it on sparse networks using three existing models classical [53], clustering [67], and transitivity [69] (from least to most general respectively). Each model permits different triad set to be considered structurally balanced. The extension of these models are formally defined in Methods. Unlike the past research in sparse balance theory [180, 181], our study is more general, concise, and uses a set of more detailed and longitudinal real-world datasets.

Remarkably, we find that 91% of the 392,084 observed triads in 23+ years are concentrated on only 10 triad types (out of 138). Fig. 3.3 (d) displays this operative set of triad types (most frequent triads). The types 6, 8 and 9 include one or more violations of transitivity, and the others do not. Fig. 3.3 (c) shows the average distribution of oper-

ative triads over time and Fig. 3.3 (b) depicts the temporal trajectory of the percentage of transitive triads. It is evident that structural balance does not always increase. Our finding based on Fig. 3.3 (b) is that after a decrease of structural balance during the first periods, the network's trend is toward greater balance since 2006 onward. The main basis of the initial decline are conversions of null relations to positive relations and the associated proliferation of intransitive triad 9 configurations. Overtime, many of these violations of transitivity are then resolved by conversions to triads that do not violate transitivity (triads 1, 4 or 10). This increase in the number of triads 6, 8 and 9 before 2006 is not due to any particular major global occurrences but in fact is the inherent property of inception of many connections among countries around this era. After analyzing the Markov transition matrices of all these triads, we find there is a high probability for transitioning from all these three not balanced triads to the balanced triads consistently using any period length. This shows staying in these not balanced triads is temporary. Also, looking at distribution of triads (Fig. 3.3 (c)), we see only about 8% of triads (summation of volume of triads 6, 8 and 9) to be not-balanced over course of more than two decades. The evidence for this result is highlighted in our Markov chain analysis to which we now turn.

3.4.2   Markov Model on Dynamic Networks

Here, we present a Markov model of the dynamical system of the temporal transitions of the networks' triads that is not restricted to the operative set of triad types. This model provides a deeper image of the probabilistic micro-dynamics of the alterations of international appraisals during the 1995-2018 span of the available data. Fig. 3.4 shows the average probability transition matrix of the 138 possible triad types from 103 networks aggregated over a three-month period (seasonally). Interestingly, most of probabilities in

(a)

(b)

(c)

(d)
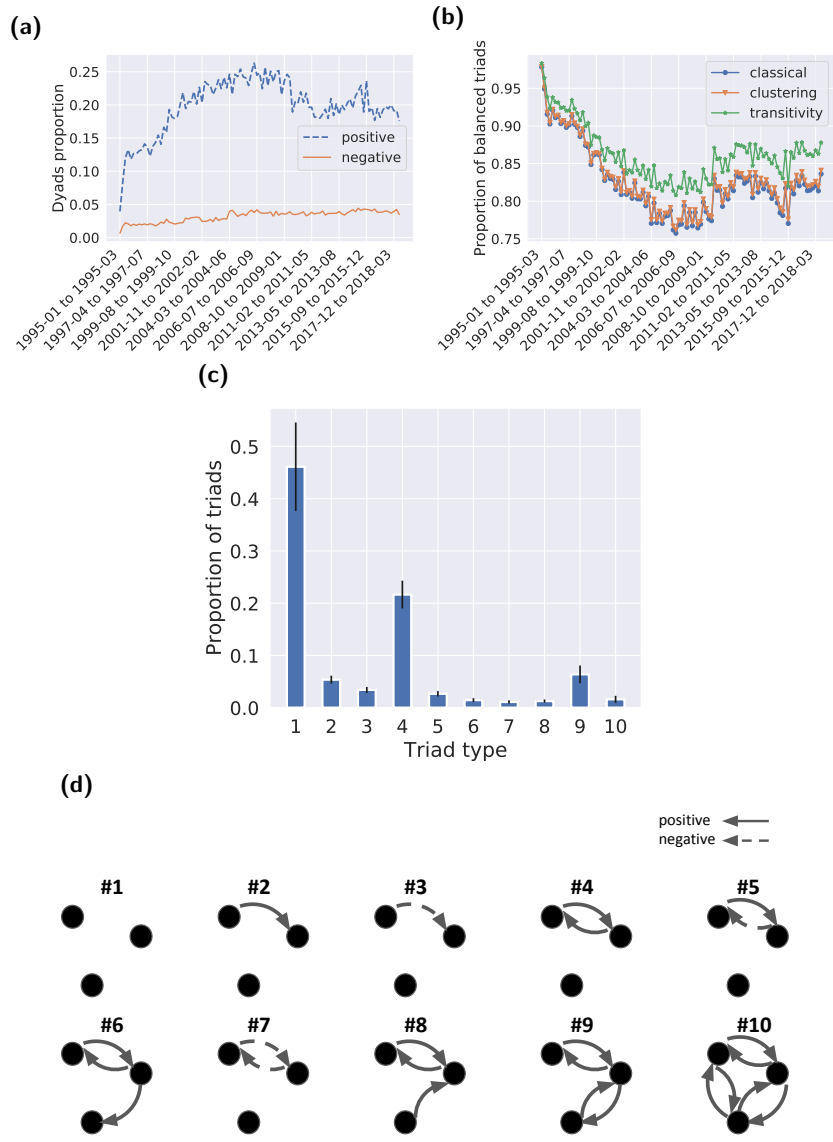
Figure 3.3: Network dyads and triads over time. This figure presents the dynamics of Integrated Crisis Early Warning System (ICEWS) network over time. a) Proportion of positive and negative dyads (edges) over time in the strongly connected component. b) Proportion of balanced triads over 23+ years. The three lines represent different subsets of Heider axioms as structural balance criteria in which they all show a similar trend. Triads are counted in networks built by aggregating three months of news articles. We find that changing the period length to monthly, biweekly and weekly does not change the trend in this figure. c) Average proportion of triads over 23+ years. Error bars correspond to one standard deviation and are computed using $n = 103$ network snapshots of quarters. d) The set of ten operative triads (most frequent triads out of 138 possible ones).

this matrix are very close to zero and the dynamics of the system can be described only by a few states. For the sake of visualization, we can focus on the operative set of 10 triad types (described in Fig. 3.3 (e)) and we show their transition probabilities in Fig. 3.5 (a). The probability transition matrix is robust with respect to the choice of period. In Fig. 3.5, each panel shows the transition matrix for period lengths: (a) seasonally (b) monthly (c) biweekly (d) weekly. The probability transition matrices look very similar. Quantitatively, the Pearson correlation between the flatten format of transition matrix in (a) with (b), (a) with (c), and (a) with (d) is 0.99, 0.98, and 0.86, respectively where all are statistically significant ($p < 0.05$). Based on these transition matrices, one can see the triads 1, 4, 9 and 10 have large self-transition probabilities (high probability of transitioning from 1 to 1) and, thus, are most likely to persist. More precisely, Fig. 3.5 (e) shows the stationary distribution of the Markov process. The summation of balanced triads in the stationary distribution is larger than 0.85. It appears that regardless of the definition of period, the Markov model predicts our empirical finding of a network evolution toward structural balance.

3.4.3   Time-varying Markov Model on Dynamic Networks

Our results show that the probability of transitions to and remaining in balanced states are statistically significant in every period over the 23+ year data span. This motivates us to apply a more holistic and time-varying Markov model in which the transition matrix can smoothly change and is learned via a convex optimization scheme (see Methods for details). Fig. 3.6 describes the analysis pipeline of this model. Our Fig. 3.7 results further support the conclusion that structural balance drives the dynamics of the system. All unbalanced triads have an estimated high mean probability and small standard deviation on transitions into balanced triads, and the balanced triads have an
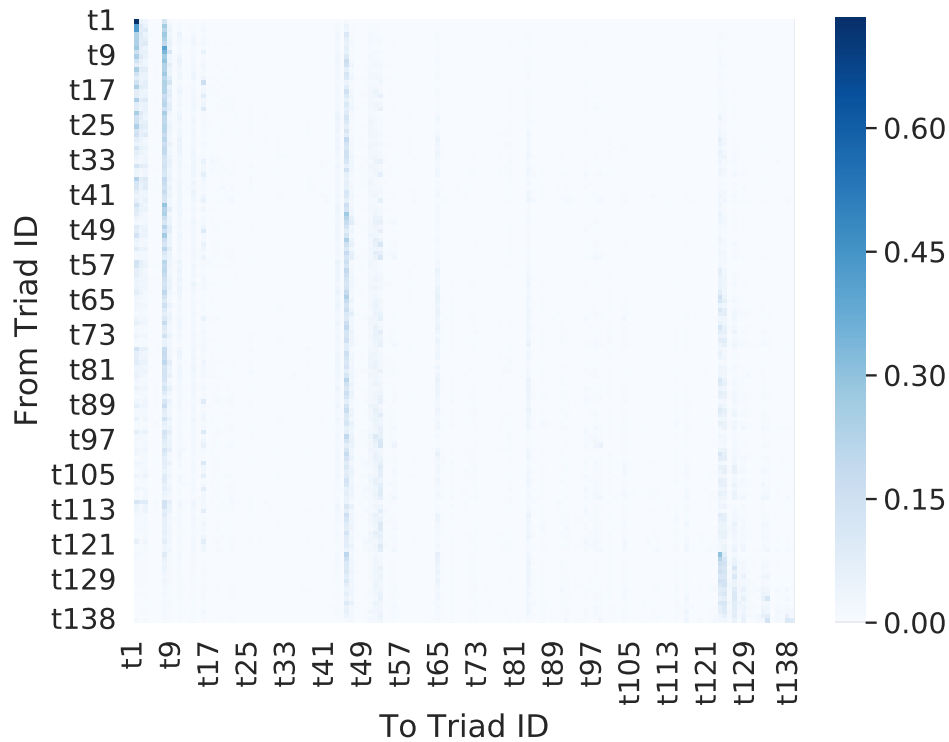
Figure 3.4: Transition matrix for the all triads. Average probability transition matrix in the Integrated Crisis Early Warning System (ICEWS) dataset. The average is computed from 101 transition matrices between states which are the 138 possible sparse triads (Fig. 3.2 depicts all these triads). The transition matrix is row-stochastic and its elements falls into $(0, 1]$. This figure shows there exist only a small number of triad transitions as most elements of this matrix are close to zero. It also depicts most transitions only happen toward a few of triads. The transition matrix for the top ten most frequent triads is further analysed in Fig. 3.5.
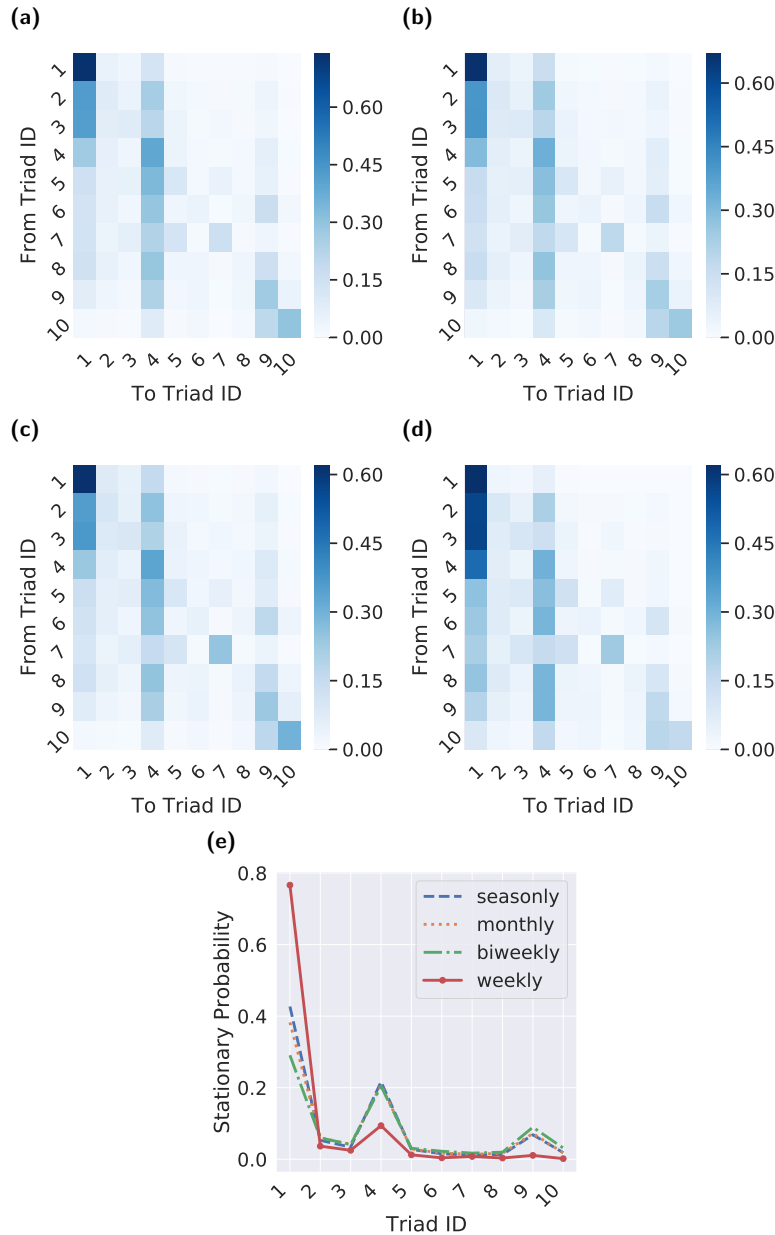
Figure 3.5: Transition matrix for the core triads. Average probability transition matrix only for the core triads (3.3) in the Integrated Crisis Early Warning System (ICEWS) dataset by aggregating dynamic networks of a) seasonally b) monthly c) biweekly d) weekly period. The transition matrix is row-stochastic and its elements falls into $(0, 1]$. There are 138 possible triads; only the sub-matrix of the 10 operative triads is shown (given in Fig. 3.3 (e)). Panel e) shows probability stationary distribution of the transition matrices, with the different aforementioned periods. The stationary distribution shows the state of the system under the condition that the Markov model persists. It appears that the probability transition matrix and stationary distribution are robust with respect to choice of period length.

estimated high mean probability and small standard deviation of remaining balanced. Note the distinctive separation of the transition probabilities.

Applying this experiment on other datasets we posit this result not only holds in our focal network of international relations, but also in two longitudinal datasets on financial Bitcoin trust networks [182, 183]. Table 3.3 provides details about all datasets including the Bitcoin trust networks and Fig. 3.8 shows the results in all datasets. Results show although international and financial networks are very different, our findings on transition toward balance generalize across all three datasets. Therefore, it appears that transitions toward balance are ubiquitous (i) regardless of the definition of balance, (ii) regardless of the setting (international news networks or financial networks), and (iii) regardless of the type of actor (individuals or countries).

To buttress the finding of high transition probability toward and staying in more balanced triads, we apply our experiments on two other datasets. We report the results of the time-varying Markov model on estimating the underlying probability transitions for all three datasets: Integrated Crisis Early Warning System (ICEWS), Bitcoin Alpha, and Bitcoin OTC.

Bitcoin Alpha trust weighted signed network: This is a who-trusts-whom network of people who trade using Bitcoin on a platform called Bitcoin Alpha. Since Bitcoin users are anonymous, there is a need to maintain a record of users' reputations to prevent transactions with fraudulent and risky users. Members of Bitcoin Alpha rate other members on a scale of -10 (total distrust) to +10 (total trust) [182, 183].

Bitcoin OTC trust weighted signed network: Very similar to the previous dataset, Bitcoin OTC is another platform for trading Bitcoin and has similar trust edges over time [182, 183]. The statistics about all datasets are depicted in Table 3.3.

Figure 3.7 shows the evidence for the network dynamic toward balance for these three datasets. The probability of transitions from unbalanced to balanced triads is
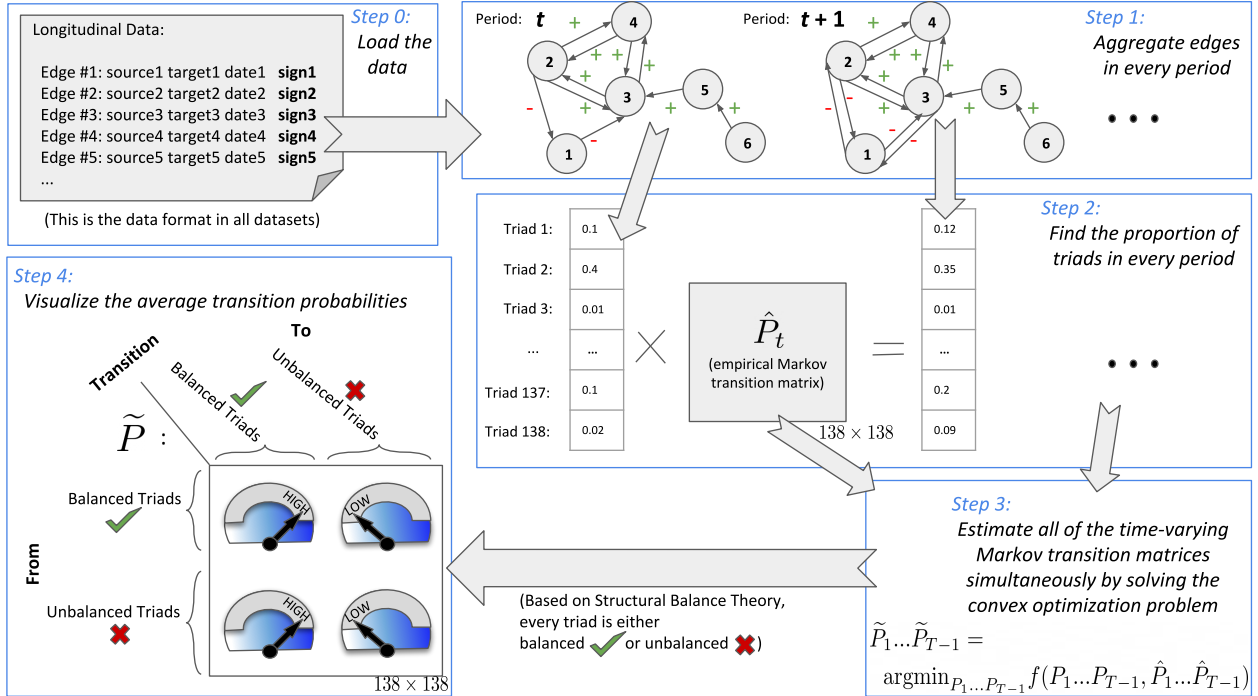
Figure 3.6: Pipeline description. Estimation of transition probability matrices between balanced and unbalanced triads over a sequence of time periods. This figure illustrates the preprocessing steps, the optimization problem, and the results. Step 1: for all time periods t from 1 to $T-1$ (where T is the maximum number of periods in that dataset), each edge is labeled using aggregated majority in that period as positive ($+$) or negative ($-$). Step 2: we compute the proportion of triads in every period and estimate the transition matrix at time t as the unknown matrix that multiplied by the vector of proportion of triads at period t gives the corresponding vector at period $t+1$. Step 3: we estimate all transition matrices together using a time-varying Markov model. This step ensures that the results provide a holistic view of the available longitudinal data. Step 4: we visualize the probability of transition from balanced and unbalanced triads in time-varying estimated transition matrices. By allowing null ties, there are 138 types of triads. P_t represents the unknown transition matrix at time t and $\hat{P}_t$ represents the empirically estimated transition matrix at time t, and $\widetilde{P}_t$ represents the time-varying estimated transition matrix at time t. The four quadrants of $\hat{P}_t$ show the average estimated transition probabilities (see Methods for details). The result of this experiment is shown in Fig. 3.7.

(a)

(b)

(c)
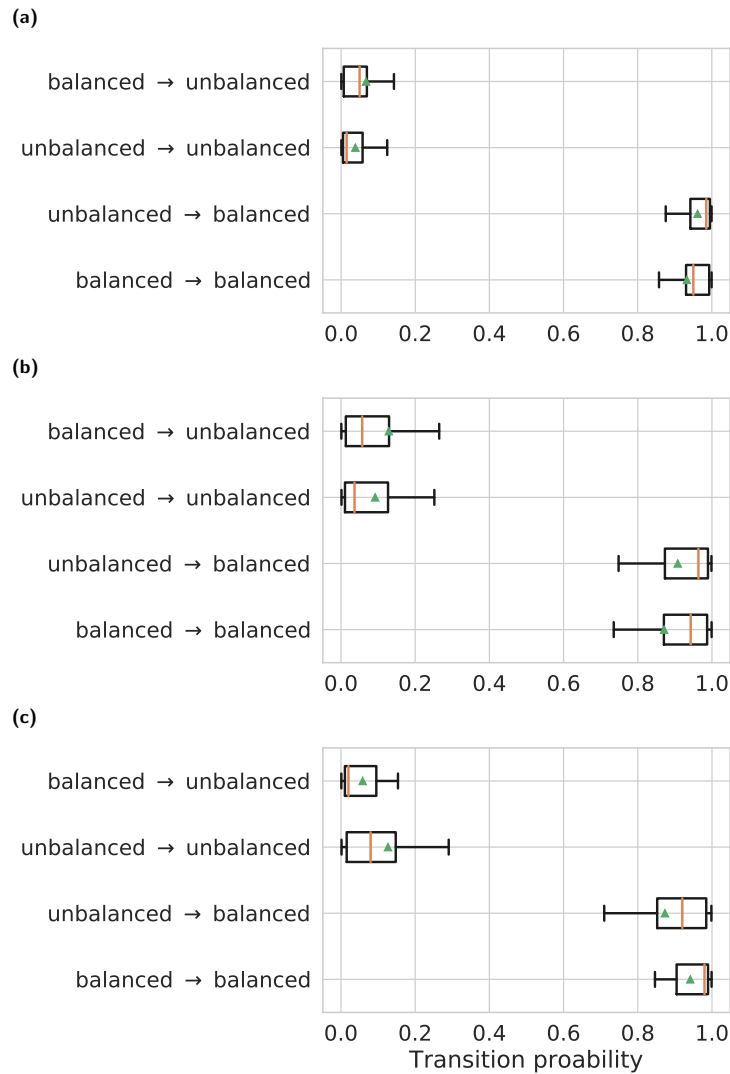
Figure 3.7: Probability of kinds of transitions. Estimated transition probability for a) transitivity-, b) clustering-, and c) classical-balanced and -unbalanced triads in Integrated Crisis Early Warning System (ICEWS) dataset (the pipeline is described in Fig. 3.6). The Y-axis indicates the kind of transition and the X-axis shows the estimated probability (computed by solving Eq. 3.7), the box is the interquartile range of the probability distribution, the orange line is the median and green dot is the average of the distribution, and the whisker shows minimum and maximum of the range of the distribution. This figure shows that the probability of transitions from unbalanced triads to balanced ones is significantly higher than the opposite transitions. Also, the probability of remaining balanced is more likely than the probability of remaining unbalanced. These findings hold regardless of the definition of balance. Box plots are computed using $n = 103$ network snapshots of quarters. Fig. 3.8 extends this analysis to two Bitcoin datasets showing that movement toward balance is not a peculiarity of the ICEWS dataset.

Name	Integrated Crisis Early Warning System (ICEWS)
#Nodes	250
#Edges	8,073,921
#Positive edges	32,029 (90%)
#Negative edges	3,563 (10%)
Edge weight	-10 to +10
Spans through	1995-01-01 to 2018-09-30 (23+ years)

Name	Bitcoin Alpha
#Nodes	3,783
#Edges	24,186
#Positive edges	22,650 (94%)
#Negative edges	1,536 (6%)
Edge weight	-10 to +10
Spans through	2010-11-07 to 2016-01-21 (5+ years)

Name	Bitcoin OTC
#Nodes	5,881
#Edges	35,592
#Positive edges	32,029 (90%)
#Negative edges	3,563 (10%)
Edge weight	-10 to +10
Spans through	2010-11-08 to 2016-01-24 (5+ years)

Table 3.3: Datasets' Information. Brief statistics about the datasets used in this chapter.

significantly higher than transitions from balanced to unbalanced triads. The probability of remaining balanced is more likely than the probability remaining unbalanced. These findings are most strongly expressed in the data on transitivity-balance. This especially strong expression of transitivity-driven evolution is consistent with its status as the most important axiom of structural balance theory [52, 69].

Interestingly, Figure 3.7 shows that transition toward and staying in structurally balance hold regardless of the definition of balance and the setting (international or financial networks), but notably, they have the strongest expression with transitivity-balance.

3.4.4 Qualitative Relation with Exogenous Shocks

The transition matrices are stable over time, as measured by the Frobenius norm difference of consecutive matrices (Fig. 3.9). Interestingly, the Frobenius norm of transition matrices declines smoothly over time. We call this phenomenon, the stability of the dynamics. This finding is aligned with the fact that the number of wars per pair of countries in the past 50 years was roughly a 10th as high as it was from 1820 to 1949. Fig. 3.9 (a) suggests that the disruptions to this trend are associated with important shocks such as the September 11th, 2001 attacks (9/11).

3.4.5 Quantitative Relation with International Trade Activity

Additionally, inspired by previous research [3, 4, 5, 6, 7], using the data on international trades among nations since 1995, in Fig. 3.9 (b), we find a statistically significant correlation between the Frobenius norm difference of consecutive matrices and inverse of global trades. World trade data shows the global trades among all countries in world as of the percentage of each countries' GDP, which is extracted from The World Bank
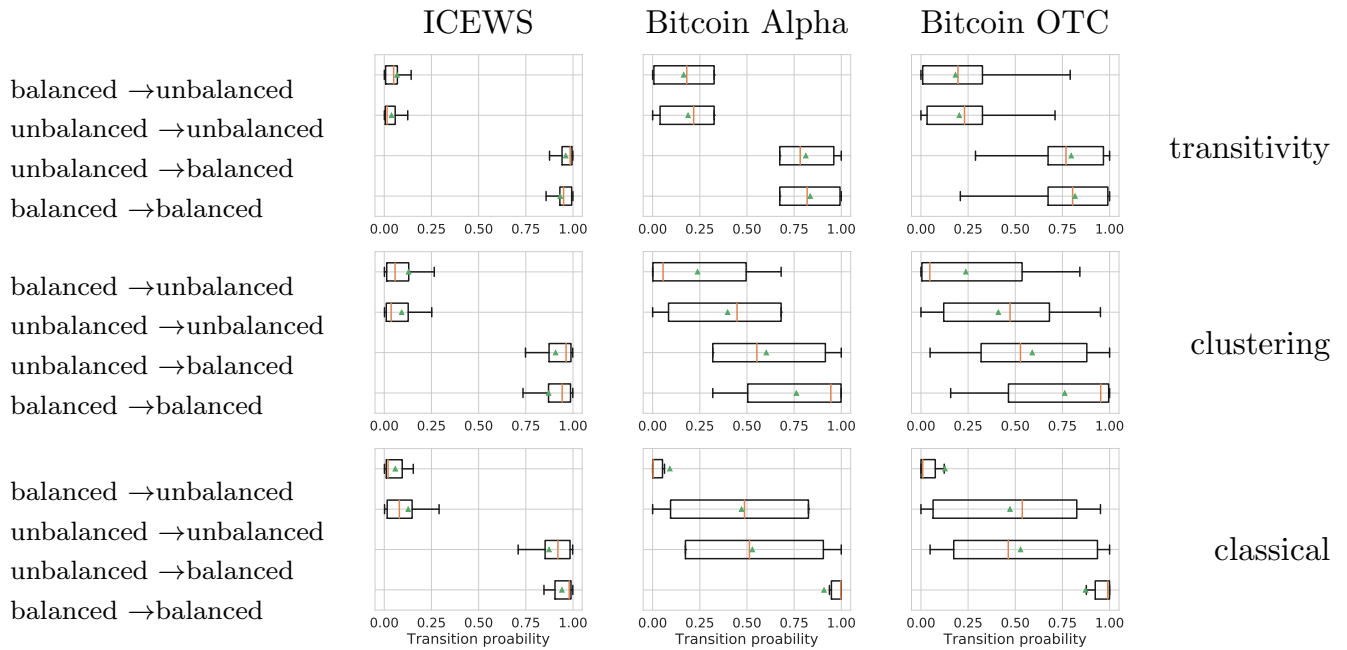
Figure 3.8: Probability of kinds of transitions in different datasets. Estimated transition probability for classical-, clustering-, and transitivity-balanced and -unbalanced triads in all three datasets (the pipeline is described in Fig. 2.2 and datasets in Table 3.3). The x-axis shows the estimated probability (computed by solving Eq. 3.7), the box is the interquartile range of the probability distribution, the green dot is the average and the orange line is the median of the distribution, and the whisker shows minimum and maximum of the range of the distribution. This figure shows that the probability of transitions from unbalanced triads to balanced ones is significantly higher than the opposite transitions. Also, the probability of remaining balanced is more likely than the probability of remaining unbalanced. Surprisingly, these findings are robust with respect of multiple definitions of balance and different settings. Box plots are computed using $n = 103$ network snapshots for Integrated Crisis Early Warning System (ICEWS) dataset, $n = 66$ network snapshots for Bitcoin Alpha dataset and $n = 66$ network snapshots for Bitcoin OTC dataset.

national accounts data (see Data Availability for details). The stability of dynamics and global trades are correlated in past 23+ years (Pearson correlation coefficient of 0.88 ($p <$ 1e-07)). Fig. 3.9 shows that as relationships among countries have become stable over the years, the volume of trades has been increased.

Moreover, our causality test shows evidently the more global trades there are, the more stable the relational dynamics become and vice versa over the course of two decades. Granger causality test [2] shows an statistically significant effect of global trades on the stability of the dynamics ($p <$ 1e-03), and also shows a feedback effect ($p <$ 1e-02). The causality tests are found to be statistically significant using both F-test and chi2-test with #lags = 1.

This result simply means as the relations among countries become more stable, they are more willing to trade for economical benefits, and on the other hand when they internationally trade with one another, they are willing to have a stable relationship with one another. In this chapter, stability is captured with Markov transition matrices of triads over the course of two decades. This finding comports with the seminal study by Jackson *et al.* [3] and its finding on stabilizing the international conflicts by the decrease of the number of wars among nations as the same rate as the increase in global trades.

3.5   Conclusion and Future Works

Balance theory has triggered a literature of efforts to specify the mechanisms that alter interpersonal appraisal networks [52, 53, 103] towards states of structural balance. This theory is also associated with research on international relations. However, despite the need for longitudinal data to recover the underlying dynamics of balance theory, such investigations have been rare. We have leveraged an extensive longitudinal dataset to advance the research on the evolution of the network of global international relations, and
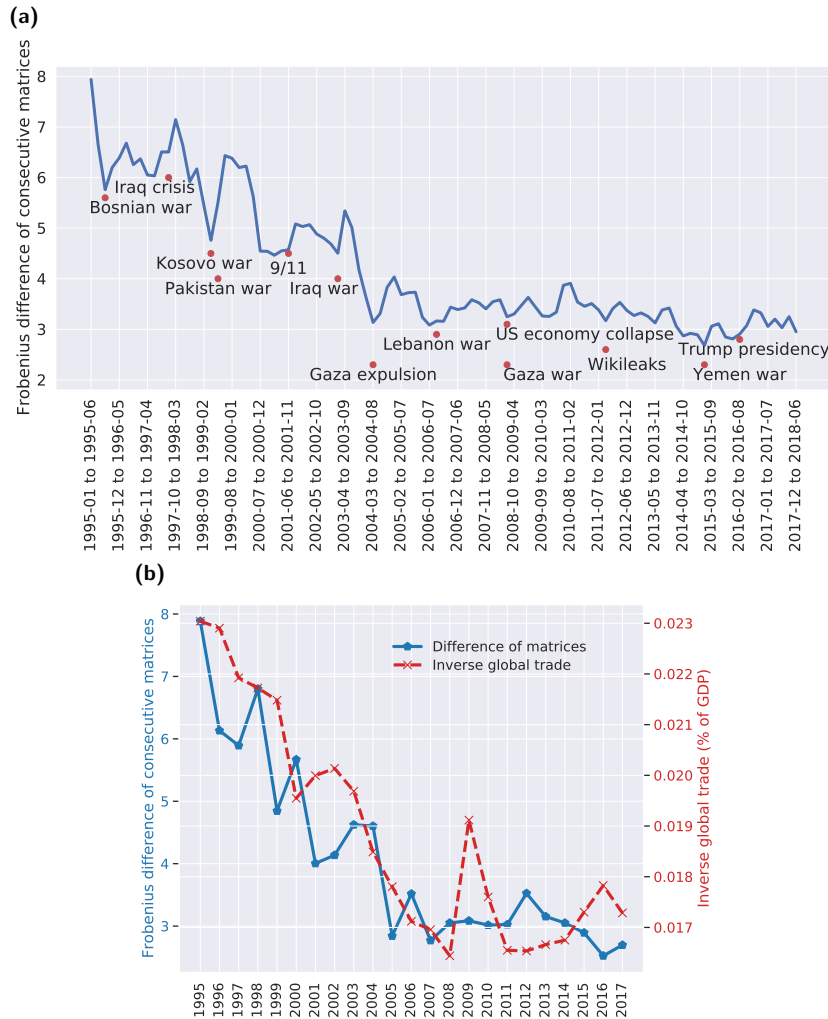
Figure 3.9: International relationship stabilization. a) The Frobenius norm difference of consecutive empirical transition matrices (blue line) becomes stable over time corresponding to the Markov chain of triads becoming stable over time. Most global exogenous events (red dots) such as wars trigger disturbances in the dynamics of relationships. b) Comparison of the Frobenius norm difference of consecutive empirical transition matrices (full blue line), versus international trades in % of each country's GDP (dashed red line) highlights a reverse relation between changes in the system and international trades. We find Frobenius norm difference of consecutive empirical transition matrices and international trades are statistically and negatively correlated (Pearson coefficients $r = -0.88$ and $p < 1\text{e-}07$). Moreover, we find the international trades statistically Granger cause [2] the stability of relationships among countries ($p < 1\text{e-}03$). This result means the more international trades existed the less changes in the relationships among countries have happened. Aligned with this finding, earlier research [3, 4, 5, 6, 7] also claimed increased trades have decreased countries' incentive to attack each other, leading to a stable and network of alliances. Statistical significance is computed using $n = 23$ years of global trades and Frobenius norm difference of transition matrices.

the basic science on balance theory. We find consistently high probabilities of transition toward and remaining in balanced triads and not vice versa. We believe that balance theory's prediction of a structural evolution toward balanced states is sound. Also, we find that the network dynamics of international relations over the past 23+ years have been toward structural stability, consistent with balance theory expectations, with occasional shocks of large scale international events on the trajectory of the global network.

A future direction to improve the predictability of the proposed model is to remove the Markov assumption in the modeling. We can let models find the best number of previous periods which should be taken into account for predicting the proportion of triads. Recursive neural networks, such as Long short-term memory (LSTM) networks [184], theoretically can model the non-Markovian aspect inherent in the data.

Chapter 4

Interpersonal Influence Estimation in Small Group Networks

Chapter 2 and Chapter 3 both provide empirical support for the emergence of structural balance theory in signed networks. These networks have edges with positive and negative sign. More precisely, Chapter 2 deals with fully connected signed networks (+/-) where Chapter 3 deals with sparse signed networks (+/-/null). However, if allowed for continuous values on edge weights, these networks would contain more information to analyze. Such entities are called influence networks. Therefore, by building upon Chapter 2 and Chapter 3, in this chapter, we focus on dynamic influence networks which instead of signs contain real values as edge weights. Similar to financial and international datasets used in Chapter 2 and Chapter 3, respectively, the dataset for influence networks in this chapter represent relationships and attitudes among individuals; however, in a much richer representation.

To study the dynamics of influence networks, in this chapter, we collect data from human subjects answering trivia questions in teams of four. After individually answering a question, subjects collaborate on a final answer through a chat system. The participants

are periodically asked to assess their appraisals of each other. We seek to find underlying factors that contribute to the awarded influence. Moreover, we address the influence estimation problem and compare the proposed models with standard baselines.

The key result of this chapter, that enables answering the above stated questions is that we introduce three hypotheses rooted in several theories of sociology and social psychology. These hypotheses claim that social influence originates from individual expertise, social confidence, and ability to recognize and compare other experts. Later, we not only provide statistically significant empirical evidence for the aforementioned hypotheses; but also we bake them into a proposed dynamical model and demonstrate its accuracy and efficiency on empirical data.

The chapter is organized as follows. In Section 4.1, we motivate and informally define the problem of influence estimation, provide a review of existing works related to hypotheses on interpersonal influence and prediction models, and briefly introduce this chapter's three contributions. Section 4.2 provides the necessary preliminaries including definition of symbols, the introduced cognitive science hypotheses, and the experimental design which is used for human subject data collection in this chapter. Section 4.3 is dedicated to the design of the core concept of this chapter—predicting the interpersonal influence matrix using dynamical and machine learning models and mathematically proving their correctness and convergence. The experimental results are illustrated in Section 4.4. We conclude in Section 4.5 with a discussion and a summary of the results of this chapter, and point out potential directions for future research.

4.1 Introduction

Inevitably, relationships among collaborating actors evolve over time, with people changing their opinions or appraisals of one another. Such relationships form a net-

work structure called an influence/appraisal network [185, 186, 187, 188, 189, 190] with signed edges that may portray trust/distrust, friendship/enmity, and like/dislike [51]. In our study, we use the terms *influence* and *appraisal* interchangeably. Investigations of the evolution of such networks draw on a rich body of literature on opinion dynamics. DeGroot *et al.* [191], and Friedkin *et al.* [186] propose widely-established models of opinion change and the conditions of consensus formation. Altafini *et al.* [192]'s model considers diverging opinions under antagonistic interactions. Such models are surveyed in Proskurnikov *et al.* [193]. Influence system specifications play a pivotal role in all of these studies. Note that these opinion dynamic models assume the influence network of a group is given a prior. Our goal is to quantitatively estimate the influence network among individuals in a group, where the influence network within the group is represented by a row-stochastic matrix. The estimation of this matrix paves the way for solving problems such as influence maximization [194, 195]; viral marketing [196, 197]; personalized recommendation [198]; feed rankings [199]; target advertisement [200]; selecting influential tweeters [201, 202]; and selecting informative blogs [203].

4.1.1   Related Work

Classic studies of the antecedents of interpersonal influence include French and Raven's work [204] on the bases of social power, and cognitive biases research [205] showed that individuals are accorded influence based on their job titles, past performance, friends' opinions, etc. There has also been mathematical modeling of the endogenous evolution of appraisal networks. Friedkin *et al.* [206] showed how reflected appraisal mechanisms elevate or dampen the self-weights of group members along a sequence of issues. Jia *et al.* [189] proposed the DeGroot-Friedkin model, where the appraisal network evolves as a function of the social power within the group. Jia *et al.* [207] also studied how over

time, the coevolution of appraisal and influence networks leads to a generalized model of structural balance theory [52, 70, 208, 55, 156, 149]. Mei *et al.* [16] modeled collective learning in teams of individuals using appraisal networks, where the appraisal dynamics change as a function of the performance of individuals within the team.

Research on transactive memory systems (TMS) [209, 11, 12, 10] provide an approach to formation of influence systems. A TMS is characterized by individuals' skills and knowledge, combined with members' collective understanding of which members possess what knowledge [210, 12, 211]. As members observe the task performances of each other, their understanding of "who knows what" tends to converge to an accurate assessment, leading to greater coordination and integration of members' skills. Empirical research [209, 11, 12, 10] across a range of team types and settings demonstrate a strong positive relationship between the development of a team TMS and team performance. The research indicates for the purpose of improving self performance, individuals tend to find experts via demonstrability in their group during intellective tasks [212, 213]. Unlike judgemental issues, for intellective tasks there exists a demonstrable mathematical or verbal correct answer that can be distinguished by high-performing teammates [212].

Research in social comparison theory has shown that individuals tend to evaluate their own abilities by biased comparisons with their peers. In particular, Woods [214] describes several motivations behind biased social comparison such as self-esteem protection [215], lack of appropriate incentives [216], or the existence of dominant individuals who skew member contributions [217, 218]. Davison *et al.* [218]'s experimental results show that low-performing individuals tend to overestimate (resp. underestimate) low-performers (resp. high-performers), i.e. high-performing individuals are better able to recognize other experts than low-performing individuals. To study such psychological cognitive biases, several scientists have conducted group experimental studies by self and peer evaluations [217, 219, 220].

Research on confidence heuristics [13, 14] has shown that the more self-confident individuals are, the more influence they are accorded by others. London *et al.* [221] find that "the single significant behavioral difference between persuaders and persuadees was in the expression of confidence". Confidence heuristics is defined based on a social and psychological norm, whereby more confidently expressed arguments signal better information, allowing an efficient revelation of information and decision-making based on expressed confidence [13].

We build on the above three lines of research. Although the problem of estimating social power [189, 222], and influence networks have been studied before [223, 224, 225], existing research lacks empirical studies as they are mostly based on theory and grounded on simulation-based analyses [16]. Moreover, previous studies on influence estimation has focused on proxies of influence such as propagation of hashtags, quotes, and retweets [225, 226, 227, 228, 229, 230]. An impactful study by Almaatouq *et al.* [231] finds that social influence is significantly correlated with confidence and correctness. However, no estimation method is proposed that mathematically formulates how these factors contribute to the underlying dynamics of influence. Furthermore, we find these two factors alone do not lead to the most accurate predictions of self-reported influence for small teams with static networks in this empirical setting. Studies on the empirical estimation of the weighted network of who-influences-whom are rare [232, 233]. In the present work, we probe more deeply into the foundations of the links between individual performance, self-confidence and social comparison on interpersonal influence. Our work bridges the gap between empirical and simulation-based results by utilizing sociology-inspired mechanisms and machine-learning based models to estimate the social influence in groups. Overall, to the best of our knowledge, this study is the first to estimate the influence matrices in a text-based shared media among individuals, collected from a human subject experiment, where teammates communicate via a broadcast system to solve intellective

tasks.

4.1.2 Contributions

Our contributions in this chapter are threefold.

1. We find empirical support for widely established theories in psychology, sociology and management regarding the effect of TMS [209, 11, 10], confidence heuristics [13, 14] and social comparison theory [218, 214] on individuals' influence over their teammates.

2. We introduce a novel cognitive dynamical model based on the aforementioned theory regarding how influence is accorded from others. This cognitive model is validated against the empirical data and can be used to estimate influence matrices using past reported influence matrices and individual performance. We provide analytical and simulation results on the asymptotic behavior of the model for the case with identically performing individuals.

3. We propose a machine learning-based model for estimating influence networks using any features such as individual performance, past influence matrices, and communication contents as well as communication timestamps. Extensive experiments show that our proposed neural network model surpasses all baseline algorithms with statistical significance on multiple merits.

4.2 Preliminary

4.2.1 Definitions

Table 4.1 summarizes the major notations used throughout the present manuscript.

Symbols	Definition
n	Number of individuals in a team
N	Number of teams
T	The number of available time periods (game rounds)
$\mathbb{1}_n$	n-dimensional column vector of ones
$\mathbb{I}_n$	$n \times n$-dimensional identity matrix
$M = \{M_{ij}\}$	Nonnegative and row stochastic influence matrix for every $(ij) \in$ edges with $M\mathbb{1}_n = \mathbb{1}_n$.
$M^{(t)}$	Ground truth influence matrix for any given team at time t
$M^{(m,t)}$	Ground truth influence matrix for team m at time t
$\hat{M}^{(m,t)}$	Estimated influence matrix for team m at time t
A	Connectivity (weighted adjacency) matrix
K	Cardinality of feature set
W, B	Weight and Bias matrices being being evaluated in the linear model
$v_{\mathrm{L}}(X)$	Stationary distribution of matrix X
$\mathrm{diag}(x)$	A matrix with diagonal entries of vector x and zero everywhere else
X_{ij}	Element at row i and column j in matrix X
$X_{i,\cdot}$	Row i in matrix X
$X_{\cdot,j}$	Column j in matrix X
$\mathrm{Tr}(X)$	Trace of square matrix X

Table 4.1: Description of notations.

4.2.2   Hypotheses

The following hypotheses motivated from past research are empirically supported by our experimental results:

Hypothesis 1 *Individuals with higher expertise are accorded higher interpersonal influence from the group.*

Hypothesis 2 *Individuals with lower expertise have diminished ability to recognize experts in the group.*

Hypothesis 3 *Individuals with higher confidence are accorded higher interpersonal influence from the group.*

In this experiment, subjects read and answer every question individually. Ergo, the individual performance (expertise) can be measured by the ratio of correct answers one gives individually, prior to seeing others' answers and the discussion phase. Assuming individuals can potentially keep track of others' expertise by recalling their answers or their chat messages, we study if individual expertise plays a prominent role in the amount of social influence one receives.

4.2.3   Experimental Design

We collected data for 31 teams comprising four human members each. Each team is presented with 45 trivia questions sequentially. Questions fall into three categories of Science and Technology, History and Mythology, and Literature and Media. The team members first answer individually before their answers are revealed to the team. Then, they are asked to collaborate on a single unanimous response. The design incorporates a multi-part incentive for subjects to seek the correct answer on each question: an evolving

team performance score; an option to consult with one of four available AI-agents after the team discussion (the AI-agents may or may not provide a correct answer) which, if exercised, must lower the team's performance score regardless of whether provides a correct or incorrect answer; and feedback to each team on correct and incorrect answers. This multi-part incentive structure operated to concentrate the attention of the team on the evaluation of the relative expertise of their members. Fig. 4.1 shows the stages of experiments for every question.

Subjects are instructed to read the multiple choice question and respond individually.
Individuals' chosen answers are revealed to the group and chat becomes enabled.
Submit button is enabled and the group needs to reach a consensus to be able to submit their answer before the time expires.
Correct answer is revealed and the group score is reported.

0   Stage 1   30   Stage 2   60   Stage 3   120   (seconds)

Figure 4.1: Experimental setup for every intellective question. Questions take two minutes and encompass three stages: subjects answer individually, observe everyone's answers, and discuss their takes. Lastly, the platform reveals the correct answer.

This experimental setting tests the participants' intellective memory. Every team has two minutes to answer each question and then the platform reveals the correct answer immediately after a team submits their answer. Thus, they are provided with immediate feedback on their performance after every response. The experiment is run on the Platform for Online Group Studies (POGS). Each team receives the questions in the exact same order. Each experiment is conducted in nine rounds of five intellective questions each. The teams are surveyed after each round.

At the end of each round, subjects are asked to record the influence of their teammates in their decision-making process as a percent value, such that the sum of all values adds up to 100. Every subject assumes they are given a total of 100 chips and instructed to distribute these chips to indicate the relative importance of each member in deter-

mining their own final answer on all past problems. Thus, the number of chips that a subject allocates to a particular member should indicate the extent to which that member provided information that they personally found useful and cause them to modify their approach to the problem or final solution. The number of chips that subjects allocate to themselves should indicate the extent to which their final answer was not affected by the conversation. If an individual felt that all conversations so far provided no influence to their choice of answer, then they would put 100 besides their own name. If the conversation caused them to abandon their approach to the problem, then they are instructed to put zero beside their own name and allocate all the chips to one or more of the other members.

After normalization, the self-reported interpersonal influences form a row-stochastic influence matrix for every round, containing only non-negative entries (in a row-stochastic matrix every row sums up to one). The platform ensures that in each inquiry, the reported influence matrix has non-negative entries and is row-stochastic. The platform collects a log of all the instant messages including time of message and content during every question, the individual and group answers, and the self-reported influence matrices.

Since the platform displays the correct answer to every question immediately after the group submits its response, attentive subjects can use the individual responses and text discussion to keep track of which individual teammates may have expertise in one or more areas over the course of the experiment. Thus, along the problem sequence, the team may solve problems more efficiently and also more accurately.

4.3   Methods and Materials

Here, we provide mathematical formulation regarding how the proposed dynamical model, linear, and deep neural network model alongside baselines efficiently frame and

solve the influence matrix estimation problem.

4.3.1   Proposed cognitive dynamical models

We propose various discrete time dynamical models that characterize the evolution of the influence network based on various sociological concepts. Let the simplex be defined as $\Delta_n = \{x \in \mathbb{R}_{\geq 0} \mid \mathbb{1}_n^\top x = 1\}$. Given an estimate of a previous row-stochastic influence matrix $\hat{M}^{(t)}$ and an estimate of normalized or perceived expertise $x^{(t)} \in \Delta_n$, our models are in the general form

$$\hat{M}^{(t+1)} = T\big(\hat{M}^{(t)}, x^{(t)}\big) \quad \text{for } t \geq 1,$$

where $\hat{M}^{(t)}$ denote the influence matrix estimate at time t. Let $\hat{M}_d^{(t)} = [\hat{M}_{11}^{(t)}, \ldots, \hat{M}_{nn}^{(t)}]^\top$ denote the vector of self-influence weights. Consider the normalized expertise and per-ceived expertise, defined as follows. *Normalized expertise* $\bar{y}^{(t)} \in \Delta_n$ is defined as

$$\bar{y}^{(t)} = \big(\mathbb{1}_n^\top y^{(t)}\big)^{-1} y^{(t)} \tag{4.1}$$

and *perceived expertise* $\hat{y}^{(t)}(y^{(t)}, \hat{M}_d^{(t)}) \in \Delta_n$ is defined as

$$\hat{y}^{(t)}(y^{(t)}, \hat{M}_d^{(t)}) = \big(\hat{M}_d^{(t)\top} y^{(t)}\big)^{-1} \operatorname{diag}\big(M_d^{(t)}\big) y^{(t)}. \tag{4.2}$$

Then depending on the model, $x^{(t)}$ is equal to either $\bar{y}^{(t)}$ or $\hat{y}^{(t)}$. Our proposed models use also a scaling parameter $\tau \in (0, 1)$ that can be adjusted to change the time-scale of the dynamics. If we have information on past reported influence matrices and expertise levels of team members, these models can be used to predict future influence matrices.

- *Differentiation model (D model):* Motivated by Hypothesis 1, this model assumes

individuals assign influence based on the unweighted, normalized, cumulative correctness-rate, where individuals who perform better are accorded higher influence. The model uses the normalized expertise [4.1] and is defined for all $i, j \in \{1, \ldots, n\}$ as

$$\hat{M}_{ij}^{(t+1)} = (1 - \tau)\hat{M}_{ij}^{(t)} + \tau \bar{y}_j^{(t)}, \tag{4.3}$$

which reads in matrix form as $\hat{M}^{(t+1)} = (1 - \tau)\hat{M}^{(t)} + \tau \mathbb{1}_n \bar{y}^{(t)\top}$.

- *Differentiation, Reversion model (DR model):* Motivated by Hypotheses 1 and 2, this model is based on the D model and assumes high-performing individuals are accorded more influence and low-performing individuals tend to assign influence weights uniformly amongst team members. The model uses the normalized expertise [4.1] and is defined for all $i, j \in \{1, \ldots, n\}$ as

$$\hat{M}_{ij}^{(t+1)} = (1 - \tau)\hat{M}_{ij}^{(t)} + \tau \Big(\bar{y}_i^{(t)} \bar{y}_j^{(t)} + \big(1 - \bar{y}_i^{(t)}\big)\frac{1}{n} \Big), \tag{4.4}$$

which reads in matrix form as

$$\hat{M}^{(t+1)} = (1 - \tau)\hat{M}^{(t)} + \tau \Big(\bar{y}^{(t)} \bar{y}^{(t)\top} + \frac{1}{n} \big(\mathbb{1}_n - \bar{y}^{(t)}\big)\mathbb{1}_n^\top \Big).$$

- **Cognitive model based on Differentiation, Reversion, Perceived expertise model (DRP model)**: Motivated by Hypotheses 1, 2 and 3, this model is an extension of [4.5], where everyone's expertise is misevaluated based on their own self-confidence. The model then uses the perceived expertise [4.2] to learn how much influence is accorded to one another. Fig. 4.8 depicts for both single-round and multi-round prediction, using all three hypotheses baked in this model provides the most accurate

100

and consistent estimation. This model is defined for all $i, j \in \{1, \ldots, n\}$ as

$$\hat{M}_{ij}^{(t+1)} = (1 - \tau)\hat{M}_{ij}^{(t)} + \tau\left(\hat{y}_i^{(t)}\hat{y}_j^{(t)} + \left(1 - \hat{y}_i^{(t)}\right)\frac{1}{n}\right). \tag{4.5}$$

The following Lemma states that the D, DR, and DRP model are well-posed and the dynamics ensures that row-stochastic matrices are mapped to row-stochastic matrices without needing to normalize at each time step.

Lemma 1 (DRP model preserves row-stochasticity) *Consider the D model* Eq. [4.3], *DR model* Eq. [4.4], *and DRP model* Eq. [4.5] *with $\tau \in (0,1)$ and $y^{(t)} = y = [0,1]^n$. If $\hat{M}^{(1)}$ is row-stochastic, then $\hat{M}^{(1)}$ remains row-stochastic for all $t \geq 1$ under the D and DR model.*

If additionally, there exists at least one i such that $M_{ii}^{(1)} > 0$ and $\bar{y}^{(t)} \in (0,1)^n$, then the DRP model is well-posed for finite t and $\hat{M}^{(t)}$ remains row-stochastic for all $t \geq 1$ under the DRP model.

Proof: Let $\hat{M}_d^{(t)} = [\hat{M}_{11}^{(t)}, \ldots, \hat{M}_{nn}^{(t)}]^\top \in [0,1]^n$ denote the vector of self-influence weights of the influence matrix at time $t \geq 1$. Per our assumptions, $y^\top \hat{M}_d^{(0)} > 0$. Additionally, the dynamics of the Differentiation, Reversion, Perceived expertise (DRP) model guarantee that $\hat{M}_{ii}^{(t)} > 0$ for all $i \in \{1, \ldots, n\}$ and finite time t since $\hat{M}_{ii}^{(t)} \geq (1 - \tau)\hat{M}_{ii}^{(t-1)} \geq 0$. For the simplicity in notation, we define a new variable $z^{(t)} = \left(y^\top \hat{M}_d^{(t)}\right)^{-1}\text{diag}(y)\hat{M}_d^{(t)}$. Recall, $\hat{M}^{(1)}\mathbb{1}_n[n] = \mathbb{1}_n[n]$ from our assumptions. Based on the definition of variable z, we know $z^{(t)} = \mathbb{1}_n[n]^\top\hat{y}^{(t)}(y, \hat{M}_d^{(t-1)})^\top = \left(y^\top\hat{M}_d^{(t)}\right)^{-1}y^\top\hat{M}_d^{(t)} = 1$.

Then, we have

$$\hat{M}^{(t+1)} \mathbb{1}_n[n] = (1-\tau)\hat{M}^{(t)} \mathbb{1}_n[n] + \tau \Big(\operatorname{diag}(z^{(t)}) z^{(t)\top} \mathbb{1}_n[n] + \frac{1}{n} \operatorname{diag}\big(\mathbb{1}_n[n] - z^{(t)}\big) \mathbb{1}_n[n]^\top \mathbb{1}_n[n] \Big)$$

$$= (1-\tau)\mathbb{1}_n[n] + \tau \Big(\operatorname{diag}(z^{(t)}) + \operatorname{diag}(\mathbb{1}_n[n] - z^{(t)}) \Big)$$

$$= (1-\tau)\mathbb{1}_n[n] + \tau \mathbb{1}_n[n] = \mathbb{1}_n[n].$$

Additionally $\hat{M}_{ij}^{(t+1)} \geq 0$ for all $i, j \in \{1, \ldots, n\}$. Therefore, $\hat{M}^{(t)}$ remains row-stochastic for all time $t \geq 1$. ∎

Given constant expertise y, it is clear that the affine D and DR models converge. Additionally, in simulations, we observe that the DRP model convergence behaviors to a unique equilibrium. In particular, the next Lemma rigorously shows that the DRP model converges to the uniform-weighted influence matrix, for $y = c\mathbb{1}_n$ where $c > 0$.

Lemma 2 (Equilibrium and convergence of DRP model) *Consider the DRP model* [4.5]. *Assume for $\tau \in (0,1)$, constant uniform expertise values $y^{(t)} = c\mathbb{1}_n$ with $c > 0$, $\hat{M}^{(1)}$ row-stochastic, and that there exists at least one i such that $M_{ii}^{(1)} > 0$. Then $\lim_{t\to\infty} \hat{M}^{(t)} = \frac{1}{n}\mathbb{1}_n\mathbb{1}_n^\top$.*

4.3.2 Proposed linear model

Using machine learning models we can take advantage of all available data to estimate influence matrices. Combining text, connectivity network, expertise, and historical appraisals produce a multi-dimensional prediction model. We have N teams of n individuals that go through T times (rounds). To have a general format, we assume all aforementioned features fall into matrix format (shown by $\mathbf{X}_k^{(m,t)}$ for team m at time t) or vector format (shown by $x_k^{(m,t)}$. For instance, Text embedding and connectivity networks are matrix features, and expertise is represented as a vector. We want to learn weight

variables that combine the features. In total, we assume there are K matrix variables, shown as $\mathbf{W}_k$, and there are K' vector variables shown as $w_{k'}$. Ergo, a convex objective function for estimating the influence matrix is defined as follows,

$$
\begin{aligned}
\min_{\substack{\mathbf{W}_k:\, k=1 \text{ to } K, \\ w_{k'}:k'=1 \text{ to } K', \\ B}} & \sum_{m=1}^{N}\sum_{t=1}^{T}\Big(\\
& \|\sum_{k=1}^{K}\mathbf{X}_k^{(m,t)}\mathbf{W}_k + \sum_{k'=1}^{K'}x_{k'}^{(m,t)}w_{k'}^{T} + \mathbf{B} - \mathbf{M}^{(m,t)}\|_F^2\Big) \\
& + \lambda\Big(\sum_{k=1}^{K}\|\mathbf{W}_k\|_{1,1} + \sum_{k'=1}^{K'}\|w_{k'}\|_1 + \|\mathbf{B}\|_{1,1}\Big), \\
\text{Subject to } & \sum_{m=1}^{N}\sum_{t=1}^{T}\sum_{k=1}^{K}\mathbf{X}_k^{(m,t)}\mathbf{W}_k + \sum_{k'=1}^{K'}x_{k'}^{(m,t)}w_{k'}^{T} + \mathbf{B} \geq 0, \\
& \mathbb{1}_n^{T}\Big(\sum_{m=1}^{N}\sum_{t=1}^{T}\sum_{k=1}^{K} \\
& \mathbf{X}_k^{(m,t)}\mathbf{W}_k + \sum_{k'=1}^{K'}x_{k'}^{(m,t)}w_{k'}^{T} + \mathbf{B}\Big) = \mathbb{1}_n^{T}.
\end{aligned}
\tag{4.6}
$$

where $\mathbf{M}^{(m,t)}$ is the ground truth influence matrix, self-reported by the members of team m at time t. Depending on the application, for the history of the influence matrix, we may use only the first matrix, the average of all previous ones, or only the previous matrix. Variables to be calculated via optimization are the $n \times n$ weight matrices $\mathbf{W}_k$ and $n \times 1$ weight vector $w_{k'}$. $\mathbf{B}$ is the $n \times n$ bias matrix also to be estimated. We also use an $l1$-norm regularization to introduce sparsity to the estimated parameters that is commonly used in many real applications and also decrease the potential search space and therefore provides efficiency for the optimization solver.

Lemma 3 *The problem in* Eq. [4.6] *is convex.*

Proof: With respect to variables $\mathbf{W}_k$ for any $k = 1$ to K and B, the loss function $\sum_{m=1}^{N} \sum_{t=1}^{T} \left\| \sum_{k=1}^{K} \mathbf{X}_k^{(m,t)} \mathbf{W}_k^T + \mathbf{B} - \mathbf{M}^{(m,t)} \right\|_F^2$ is a summation of multiple squared Frobenius norms. The regularization term $\sum_{k=1}^{K} \|\mathbf{W}_k\|_{1,1} + \|\mathbf{B}\|_{1,1}$ is also a summation of $l1-$norms. All of which are convex functions [170]. Both constraints $\sum_{m=1}^{N} \sum_{t=1}^{T} \sum_{k=1}^{K} \mathbf{X}_k^{(m,t)} \mathbf{W}_k^T + \mathbf{B} \geq 0$ and $\mathbb{1}_n[n]^T \left(\sum_{m=1}^{N} \sum_{t=1}^{T} \sum_{k=1}^{K} \mathbf{X}_k^{(m,t)} \mathbf{W}_k^T + \mathbf{B} \right) = \mathbb{1}_n[n]^T$ are linear combination of variables and hence affine functions. To this end, all of the inequality constraints are convex, and all equality constraints are affine. Therefore, the problem is convex, it has a globally optimal solution, and we can solve this equation with a convex optimization solver, CVXPY. ∎

Based on the application, when only the probability distribution and the order of influence toward others is more important than exact values, we use cross-entropy as the loss function and KL divergence as the metric. In such a case, we can formulate the matrix estimation problem as the estimation of each row, which is a discrete distribution comprised of four numbers. Cross-entropy for two probability distribution of p and q is defined as $H(p, q) = -\sum_{i=1}^{n} p_i \log q_i$. in this chapter, the two probabilities are

$$
\begin{aligned}
p &= \mathbf{M}_{i,.} &&\forall i \in [1, n] \\
q &= \hat{\mathbf{M}}_{i,.} = \sigma(\mathbf{O}_{i,.}) = \sigma(\mathbf{W}^T \mathbf{X}_{i,.} + b) &&\forall i \in [1, n]
\end{aligned}
$$

where σ represents Softmax function.

Lemma 4 *The optimization problem using the cross-entropy loss function on corresponding rows of two matrices M and $\hat{M}$ can be written as*

$$\min_{\mathbf{W},b} \quad -\sum_{m=1}^{N}\sum_{t=1}^{T}\sum_{j=1}^{n}\sum_{k=1}^{n}\mathbf{M}_{j,k}^{(m,t)}\bigg(\mathbf{X}_{j,k}^{(m,t)}\mathbf{W}_{k,j}+b_j$$
$$-\log\sum_{l=1}^{n}\exp\big(\mathbf{X}_{j,k}^{(m,t)}\mathbf{W}_{k,j}+b_j\big)\bigg)+\lambda\bigg(\|\mathbf{W}\|_1+\|b\|_1\bigg) \qquad (4.7)$$

The loss function using cross-entropy can be derived, step by step, as follows,

Proof: The objective function using cross-entropy can be derived, step by step, as follows,

$$\begin{aligned}
\text{loss} &= \sum_{m=1}^{N}\sum_{t=1}^{T}\sum_{j=1}^{n}H(M_{j,.}^{(m,t)},\hat{M}_{j,.}^{(m,t)}) \\
&= \sum_{m=1}^{N}\sum_{t=1}^{T}\sum_{j=1}^{n}-\sum_{k=1}^{n}M_{j,k}^{(m,t)}\log\hat{M}_{j,k}^{(m,t)} \\
&= -\sum_{m=1}^{N}\sum_{t=1}^{T}\sum_{j=1}^{n}\sum_{k=1}^{n}M_{j,k}^{(m,t)}\log\sigma(O_{j,k}^{(m,t)}) \\
&= -\sum_{m=1}^{N}\sum_{t=1}^{T}\sum_{j=1}^{n}\sum_{k=1}^{n}M_{j,k}^{(m,t)}\log\frac{\exp(O_{j,k}^{(m,t)})}{\sum_{l=1}^{n}\exp(O_{j,l}^{(m,t)})} \\
&= -\sum_{m=1}^{N}\sum_{t=1}^{T}\sum_{j=1}^{n}\sum_{k=1}^{n}M_{j,k}^{(m,t)}\bigg(O_{j,k}^{(m,t)}-\log\sum_{l=1}^{n}\exp(O_{j,l}^{(m,t)})\bigg) \\
&= -\sum_{m=1}^{N}\sum_{t=1}^{T}\sum_{j=1}^{n}\sum_{k=1}^{n}M_{j,k}^{(m,t)}\bigg(X_{j,k}^{(m,t)}W_{k,j}+b_j-\log\sum_{l=1}^{n}\exp(X_{j,k}^{(m,t)}W_{k,j}+b_j)\bigg).
\end{aligned}$$

Therefore, it results to

$$
\begin{aligned}
\text{objective} &= \text{loss} + \lambda\bigg(\|\mathbf{W}\|_1 + \|b\|_1 \bigg) \\
&= -\sum_{m=1}^{N}\sum_{t=1}^{T}\sum_{j=1}^{n}\sum_{k=1}^{n} M_{j,k}^{(m,t)}\bigg(X_{j,k}^{(m,t)}W_{k,j} + b_j - \log\sum_{l=1}^{n}\exp(X_{j,k}^{(m,t)}W_{k,j} + b_j) \bigg) \\
&\quad + \lambda\bigg(\|\mathbf{W}\|_1 + \|b\|_1 \bigg)
\end{aligned}
$$

The final equation for the objective function is the same as Eq. [4.7]. ∎

The problem in Eq. [4.7] does not require any constraints to solve the convex optimization. First, because the Softmax function (σ) in this equation provides a discrete distribution in the format of vectors (all fall into $[0, 1]$ and sum up to 1). Second, since here we format the data points as vectors and not as matrices.

Lemma 5 *The problem in* Eq. [4.7] *is convex.*

Proof: With respect to variables W, b, the problem is a summation of an affine function $(-X_{j,k}^{(m,t)}W_{k,j})$, log-sum-exp term $(\log\sum_{l=1}^{n}\exp(X_{j,k}^{(m,t)}W_{k,j}+b_j))$ and two $l1-$norms regularization terms $\big(- \lambda\left(\|W\|_1 + \|b\|_1\right)\big)$. It has been proved mathematically that the expression $log\sum\exp(r)$ for any real r is convex in R^n [170]. In here, r is an affine function $-X_{j,k}^{(m,t)}W_{k,j}$ with respect to variables W, b. Hence, the problem is a summation of an affine and two convex terms which preserves convexity and produces a convex function [170]. Therefore, the minimization problem is convex, it has a globally optimal solution, and we can solve this equation with the aforementioned convex optimization solver. ∎

4.3.3   Proposed deep neural network-based model

We can also learn the mapping defined by the three weight matrices as deep encoders in a two-tower model [8]. In this regard, we apply end-to-end models to estimate the social influence matrices using multi-layered encoders from raw features to an influence matrix. This is described in Fig. 4.2. Each encoder is comprised of three fully connected Exponential Linear Unit (ELU) [234] layers, initialized by He *et al.* [235] Normal initialization, such that it draws samples from a truncated normal distribution centered on 0 with a standard deviation of $\sqrt{\frac{2}{f}}$ where f is the number of input units in the weight tensor. We use Dropout [236] after each fully connected layer to decrease overfitting. Then, all three outputs are concatenated and fed to another three fully connected layers with the same activation function to decrease the dimensionality of embedding vectors to an $n \times n$ matrix $\tilde{M}^{(m,t)}$, n being the number of individuals. Finally, cosine similarity of the two matrices $M^{(m,t)}$ and $\tilde{M}^{(m,t)}$ is computed and the error is back-propagated using stochastic gradient descent.

The deep method description is shown in Fig. 4.2. In this figure, the weights matrices in Eq. [4.6] are framed as a layers of deep neural networks. This model creates a non-convex problem; however, arguably with the abundance of data, a more effective model.

Fig. 4.3 shows an example of input features to the convex-based model. It shows a set of input features for predicting an influence matrix in a given time from the data. Response network, sentiment and emotion are networks extracted from time of text messages represented as 4×4 connectivity matrix, text embeddings are shown as 4×784 matrix, and individual performance (expertise) is individual correctness rate which is a 1×4 vector.
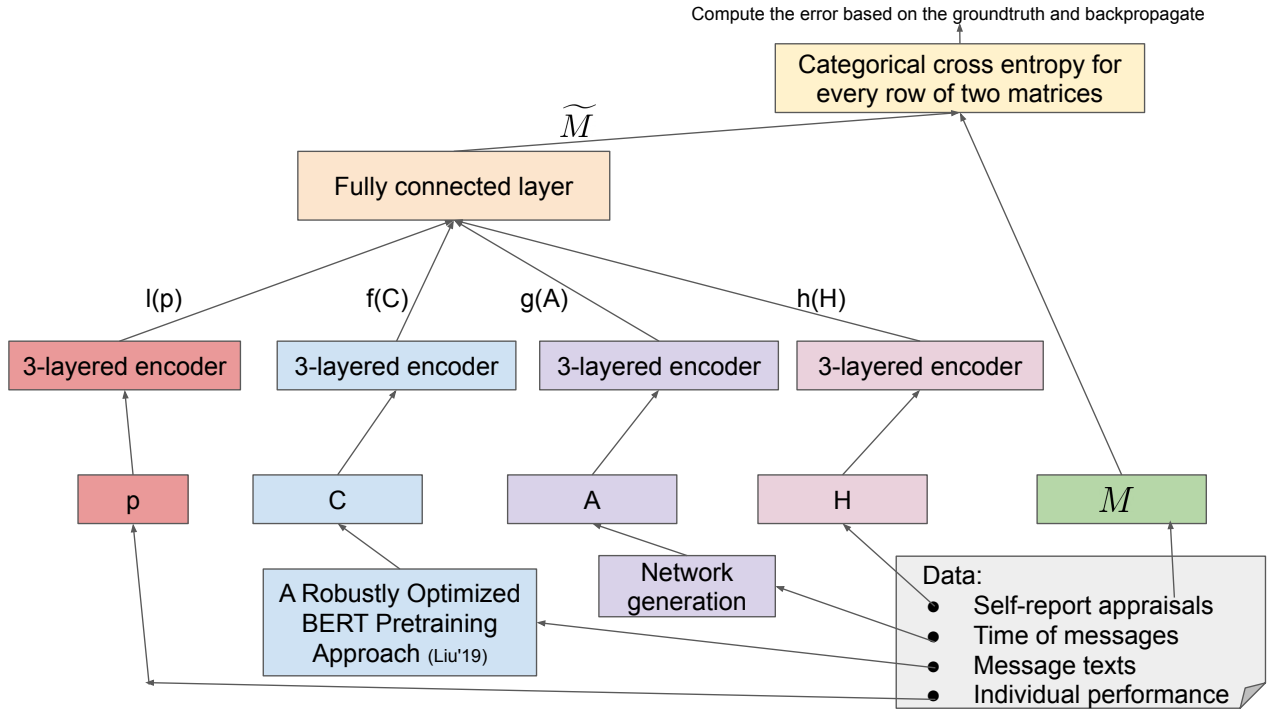
Figure 4.2: Deep learning model architecture. A deep encoder model in a two-tower framework [8] for learning the three mappings of connectivity network, content of messages, and history of appraisals. The final layer computes the cosine similarity with the ground truth influence matrix and back-propagates the error using Stochastic Gradient Descent (SGD).
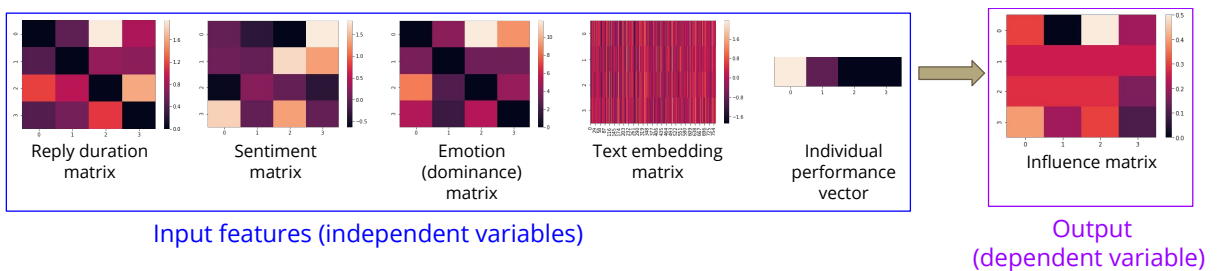
Figure 4.3: An example for one row in the supervised learning problem of estimating influence matrix.

4.3.4   Baseline dynamical models

- *Constant appraisal model:* This is a basic model which assumes the influence matrix remains constant over time. The model reads in matrix form as $\hat{M}^{(t+1)} = M^{(t)}$, or defined element-wise, for all $i, j \in \{1, \ldots, n\}$ as

$$\hat{M}_{ij}^{(t+1)} = \hat{M}_{ij}^{(t)}. \tag{4.8}$$

- *Reflected appraisal model:* The reflected appraisal model is based on the model proposed in Mei *et al.* [16]. The self-influence estimate $\hat{M}_{ii}^{(t+1)}$ increases relative to $\hat{M}_{ij}^{(t)}$ if the expertise of individual i, $y_i^{(t)}$, is larger then average team expertise observed by individual i, $\sum_{i=1}^{n} \hat{M}_{ik}^{(t)} y_k^{(t)}$. If $\hat{M}_{ii}^{(t)}$ increases, then the interpersonal weights $\hat{M}_{ij}^{(t+1)}$ for all $j \neq i$ are decreased so that $\hat{M}^{(t+1)}$ remains row-stochastic. The reflected appraisal model is defined element-wise for all $i, j \in \{1, \ldots, n\}$ and $t > 0$ as

$$
\begin{aligned}
\hat{M}_{ii}^{(t+1)} &= \hat{M}_{ii}^{(t)} + \hat{M}_{ii}^{(t)}(1 - \hat{M}_{ii}^{(t)})\left(\bar{y}_i^{(t)} - \sum_{k=1}^{n} M_{ik}^{(t)} \bar{y}_k^{(t)}\right), \\
\hat{M}_{ij}^{(t+1)} &= \hat{M}_{ij}^{(t)} - \hat{M}_{ii}^{(t)} \hat{M}_{ij}^{(t)}\left(\bar{y}_i^{(t)} - \sum_{k=1}^{n} \hat{M}_{ik}^{(t)} \bar{y}_k^{(t)}\right),
\end{aligned}
\tag{4.9}
$$

which reads in matrix form as

$$\hat{M}^{(t+1)} = \hat{M}^{(t)} + \mathrm{diag}\left((I_n - \hat{M}^{(t)})\bar{y}^{(t)}\right)\mathrm{diag}(\hat{M}_d^{(t)})(I_n - \hat{M}^{(t)}).$$

- *Structural balance theory:* Structural balance theory is a long-established theory describing the dynamics that govern the sentiment of interpersonal relationships. Researchers have consistently delivered various theoretical [70, 208, 55, 52] and empirical support [162, 149, 156] for the emergence of this phenomenon in myriad settings. in this chapter, we use a generalized Structural balance theory model (SBT) that is inspired by

earlier research Kulakowski *et al.* [15]. It predicts the dynamic of influence as introduced in the following

$$\hat{M}_{ij}^{(t+1)} = \frac{1}{n-2} \sum_{k=1,\ \text{when}\ k \neq i,\ k \neq j}^{n} \hat{M}_{ik}^{(t)} \hat{M}_{kj}^{(t)}. \tag{4.10}$$

4.4   Experimental Results

In this section, we start with statistics from the logs in the human subject experiment and we study the dynamics of influence matrices. Then, we study factors leading to influence and eventually provide efficacy results of the proposed models to estimate the influence matrix in every round.

The experimental logs show that most teams reached a consensus when answering the questions. Every team reached a consensus on average 42 times on the sequence of 45 questions posed to them. All self-reported influence networks are found to be unilaterally connected and the majority are strongly connected. More precisely, out of 279 influence matrices reports, only six ($\sim 2\%$) are not strongly connected which happen only when one person assigns all their influence to only themselves. Almost all of the not strongly connected cases were reported early in the experiment. With respect to the convergence of influence, in the last round, in 90% of the teams, at least half of the subjects reported the same ranking order of influences for all members including themselves. Additionally, we observe that in $\sim 74\%$ of the teams the influence assignments converge to a single person as being the most influential unanimously reported by the team, and that $\sim 23\%$ of the teams converge to two individuals as being equally the most influential members.

4.4.1   Origins of interpersonal influence

Qualitatively, we can look at the dynamics of every subject's appraisal of every subject over time. For example, Fig. 4.4 show a team of four subjects and the amount of influence

every team member assigns to everyone over the course of time. It is clear that on aggregate and over time the individuals found member #2 to be the most accurate and therefore they reported member #2 to be the most influential person. Also, we know after answering all questions, member #2 was more accurate than anybody else (correctness rate for member #1= 49%, member #2= 70%, member #3= 36%, and member #4= 58%). This is an example of the emergence of the first hypothesis. This figure illustrates how the interpersonal appraisal reflects the underlying expertise and how teammates were able to uncover that expertise early on in the experiment.

To quantitatively test the two hypotheses, we define two terms based on the influence matrix: confidence and persuasiveness. The individual perception (local) definition of social confidence and persuasiveness for person i take into account column i of the influence matrix. However, the team perception (global) definition uses the stationary probability for person i (index i of the left dominant eigenvector of the influence matrix). The stationary distribution, also known in the literature as the eigenvector centrality [237], takes into account the connectivity level in the network for infinite length paths and hence provides a more general point of view.

Confidence is provided in Eq. [4.11]. The local definition for persuasiveness is Eq. [4.12], and the global definitions for persuasiveness is given in Eq. [4.13]. To compute the persuasiveness we consider the reflective relative appraisal matrix $\mathbf{C}$, which is defined by removing the diagonal elements from matrix $\mathbf{M}$ and re-scaling to be row-stochastic. Another term defined in the following is expertise which is the proportion of questions every member individually answers correctly.

- *Expertise*: Individual correct answer rate (individual accuracy or individual performance) — the proportion of questions one has individually answered correctly until any given time ($\frac{\#\text{correct answers}}{\#\text{answers}}$).
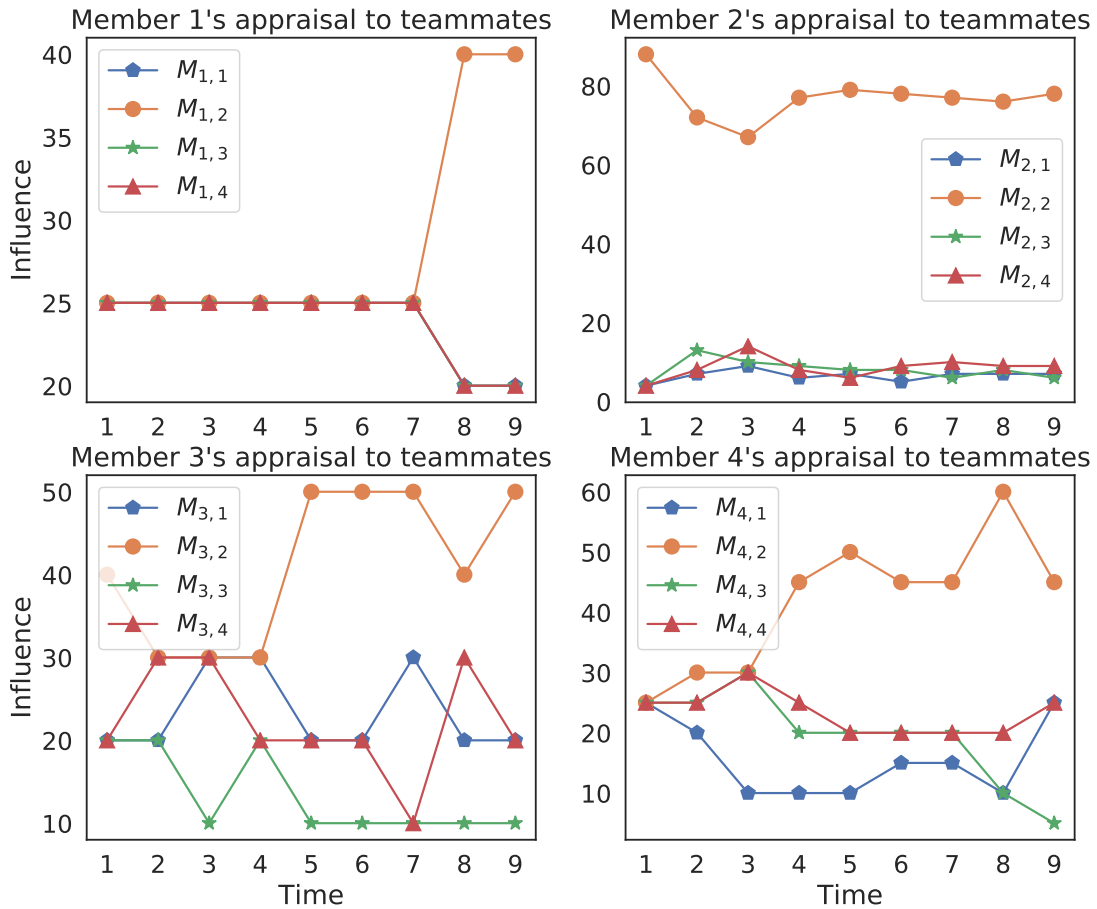
Figure 4.4: Dynamics of the influence matrix in one team. M shows a 4×4 influence matrix for this team. Every panel shows how much every subject reports others influenced them over time. in other words, it shows the amount of appraisal every person assigns to team members including themselves over time. After answering all questions, we observe that member 2 is the most accurate (correctness rate for member #1= 49%, member #2= 70%, member #3= 36%, and member #4= 58%). This figure illustrates the team's interpersonal appraisals reflect the accuracy of the team members, which was ascertained early on in the experiment.

- *Confidence*: Self-appraisal — the amount of influence one assigns to oneself at any given time.

$$\mathbf{M}_{ii}^{(t)}. \tag{4.11}$$

- *Persuasiveness*: Appraisal by others — the amount of influence everybody else is assigning to a particular team member at any given time.

The local perception (accumulative):

$$\frac{1}{n-1} \sum_{j,\, j \neq i} \mathbf{M}_{ji}^{(t)}. \tag{4.12}$$

The global perception (eigenvector):

$$\left(v_{\mathrm{L}}(\mathbf{C}^{(t)}) \right)_i, \tag{4.13}$$

where $\mathbf{C}^{(t)} = \mathrm{diag}\left((\mathbf{M}^{(t)} - \mathbf{D}^{(t)})\mathbb{1}_n \right)^{-1} \left(\mathbf{M}^{(t)} - \mathbf{D}^{(t)} \right)$ is a relative interpersonal influence matrix and $\mathbf{D}^{(t)}$ is a diagonal matrix with the diagonal entries of influence matrix $\mathbf{M}^{(t)}$.

- *Mean reversion*: Reversion to the mean (uniformity) in the appraisals that an individual holds of their teammates:

$$D_i = \sum_{j=1}^{n} ||M_{ij} - \frac{1}{n}||_2^2, \tag{4.14}$$

For the sake of abbreviation, throughout this chapter, we use the aforementioned terms. The empirical distribution of the expertise shows that individuals are more accurate than a random guess (on average individuals have about 50% correct rate when the expected value is 25% for four-choice questions). Also, we found controlling for the
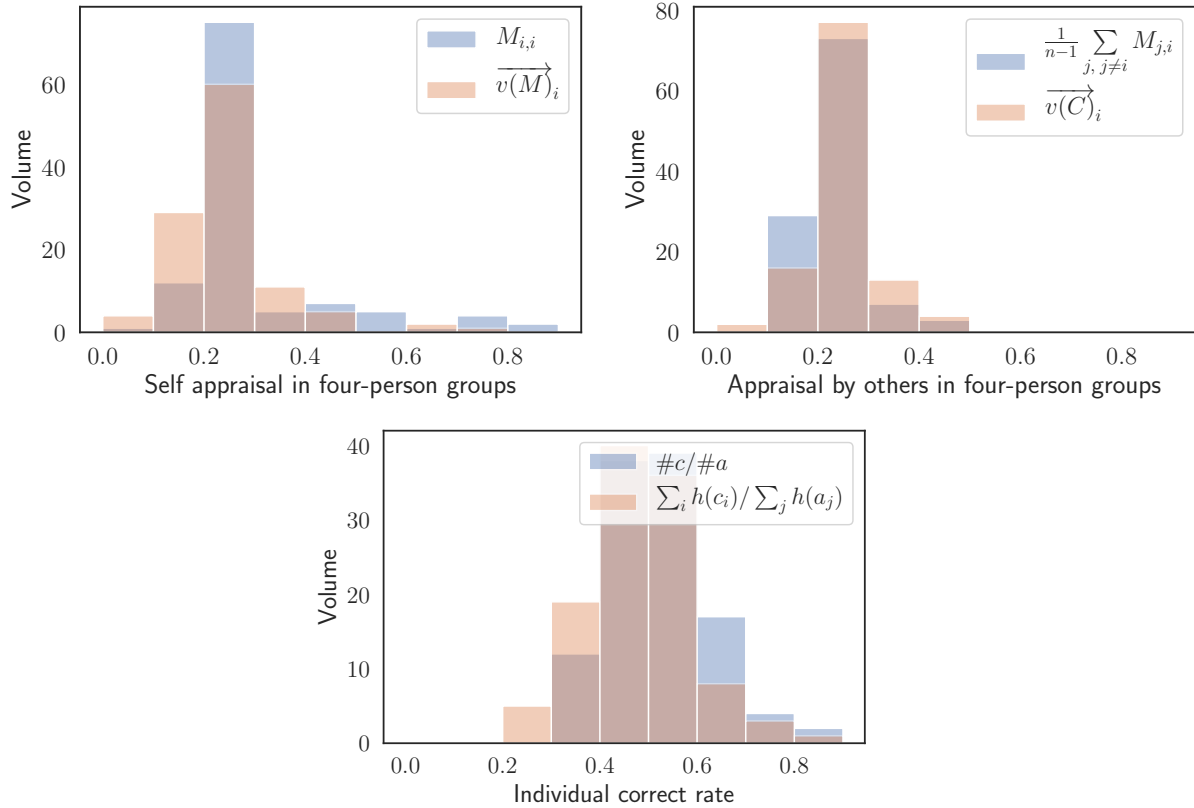
Figure 4.5: Empirical distribution of social confidence and persuasiveness, and expertise for every person at the end of the experiment. Empirical distribution of individuals' expertise at the end of experiment (after answering 45 questions) shows individuals on average answer better than random (25%). It also shows different definitions do not change the distribution of these features.

difficulty of the questions does not change the correctness rate distribution.

Fig. 4.5 shows the distribution of persuasiveness and confidence. The empirical distribution of confidence and persuasiveness shows that *on average* people tend to assign influence uniformly to their teammates, including themselves. This means that for our experiments on groups of four, a matrix with 0.25 in every element can be a competitive baseline for estimating influence matrices. Also, the distributions show that individuals tend to give greater influence to themselves than to others. Moreover, as we observe the empirical distributions for both local and global perceptions are similar in this dataset, we use them interchangeably.

Correlation study of interpersonal influence

To study the relationship between expertise and persuasiveness, we compute the correlation between the amount of persuasiveness with expertise after answering all questions. We use the final influence matrix reported by every team and their expertise at the end of the experiment. Note that, this data satisfies correlation, regression, and causation studies' requirements since the amount of influence one reports for themselves, other teammates report about that person, and their individual correct answer rate are independent and identically distributed.

Here, we report empirical evidence for all the aforementioned hypotheses. Pearson correlation results show that there is a statistically positive correlation between expertise (performance) and average amount of influence one receives (r-value $= 0.35$ and p-value $<$ $2e - 4$). This is the statistical evidence for Hypothesis 1. This finding is an empirical result for the seminal research in the theory of TMS [10, 11, 12]. We provide an empirical evidence for Hypothesis 2 via predicting mean reversion (Eq. [4.14]) using expertise in the following subsection. Finally, we also find that there is a statistical positive correlation between persuasiveness and confidence (r-value $= 0.22$ and p-value $< 2e - 2$). This is the statistical evidence for Hypothesis 3. This is also aligned with past research in confidence heuristics [13, 238, 239, 240, 14]. The result is quite surprising since in this experiment individuals communicate only through chat and nonetheless the expertise and the self-confidence impacted people's judgment stronger than any cognitive biases. Also, our experiments show the type of definition for persuasiveness does not change the sign of this relationship, nor its statistical significance. Thus, due to the large correlation between global and local perceptions of persuasiveness, the similarity of their distributions, and more straightforward local definition, we use its local definition in the rest of the chapter.

Fig. 4.6 demonstrates the Pearson correlations of every pair of metrics defined in

Figure 4.6: Pearson correlation (r-value) of metrics on influence and expertise at the end of the experiment and after answering all questions with statistical significance of p-value < 0.018. All metrics are formally presented in Definitions. The threshold for p-value is chosen using Benjamini-Hochberg (BH) procedure with False Discovery Rate of 5% [9]. For example, persuasiveness for every subject in the final reported influence matrix vs. the expertise by the same subject has r-value $= 0.35$ and p-value ¡ 2e-4. This result shows that expertise is statistically correlated with the amount of appraisal one would receive by others in a team; this phenomenon is consistent with research on Transactive Memory System (TMS) [10, 11, 12]. Surprisingly, this also shows in about two hours with indirect performance exposure, team members are still able to uncover each other's expertise. Moreover, confidence and appraise by others are also statistically correlated which is aligned with the research in confidence heuristics [13, 14].

Definitions. In this figure, all correlations are statistically significant as their corresponding p-values have been corrected using the Benjamini-Hochberg (BH) procedure [9] with False Discovery Rate of 5% has the required p-value < 0.018 as the statistical significance threshold. Note that global persuasiveness is the stationary probability of the influence matrix after removing its main diagonal (defined in Eq. [4.13]).

Predicting Mean reversion	Feature-set 1	Feature-set 2
Intercept	0.10 ***	0.10 ***
Individual performance	**0.07 ****	**0.08 ** (VIF: 1.21)**
Team performance		-0.004 (VIF: 1.21)
	Log-likelihood: 384.4 AIC: -764.8 BIC: -754.4	Log-likelihood: 384.4 AIC: -762.8 BIC: -747.2

Table 4.2: Regression result for predicting mean reversion. The statistical significance demonstrated in regards of p-value: *** $p < 0.01$, ** $p < 0.05$. This result shows the individual performance (expertise) statistically and positively is of predictive of mean reversion.

Regression study of interpersonal influence

Although the correlation between pairs of variables provides a simple view of their relationship, we can utilize a regression model to not only take into account multiple variables but also their interactions. This would incontrovertibly draw a more robust and general picture of the aforementioned metrics. Hence, here we intend to estimate one's average influence reported by their teammates at the end of the experiment. We use the Generalized Linear Model (GLM) method to solve the regression problem. Table 4.3 shows the coefficients and their statistical significance in three least-squares problems (each column shows a separate test).

The empirical evidence for Hypothesis 2 is obtained via regression on expertise and mean reversion. Table 4.2 shows the regression results for predicting mean reversion for every individual. Our results show the more expert one individual is, the more different than equal they appraise their teammates as the expertise is positively and statistically significant of predictive power of the reversion to the mean ($p - value < 0.05$) in all teams. It also shows this is a individual feature as the team average performance is not statistically significant while individual performance stays statistically significant. In fact, this result is the motivation behind using expertise as a weighted average in the cognitive dynamical model described in the next section.

117

	Feature-set 1	Feature-set 2	Feature-set 3	Feature-set 4
Intercept	0.13 ***	0.19 ***	0.12 ***	0.12 ***
Expertise	**0.20 *****		**0.17 ***** (VIF: 1.05)	**0.17 ***** (VIF: 1.11)
Confidence		**0.14 *****	**0.11 ***** (VIF: 1.05)	**0.12 ***** (VIF: 1.06)
Response network out-degree				0.00 (VIF: 2.63)
Sentiment network out-degree				0.00 ** (VIF: 2.54)
	LL: 162.86 AIC: -321.7 BIC: -316.3	LL: 162.90 AIC: -321.8 BIC: -316.4	LL: 168.12 AIC: -330.2 BIC: -322.1	LL: 170.18 AIC: -330.4 BIC: -316.8

Table 4.3: Regression result for predicting persuasiveness. Generalized Linear Model (GLM) regression coefficients and their statistical significance in estimating local persuasiveness at the end of the experiment (after answering 45 questions). Statistical significance is portrayed with *** for $p < 0.01$ for ** and $p < 0.05$. The amount of Variance Inflation Factor (VIF) is provided in parenthesis; this factor estimates how much the variance of a regression coefficient is inflated due to multicollinearity in the model. It is known [17] that statistical results remain significant in models with multicorrelated independent variables when VIF < 5. Evidently, the findings are robust. Taking into account the interactions of all variables, we find that expertise and confidence are consistently statistically predictive of persuasiveness. Networks are extracted from the time and the content of chat messages among individuals and defined in the "Feature-set from logs" part.

Table 4.3 shows that introducing more variables in columns has increased log-likelihood, Bayesian Information Criterion (BIC), and Akaike Information Criterion (AIC). It shows that expertise has a consistently positive and statistical predictive-power on persuasiveness (the empirical evidence for Hypothesis 1). The statistical significance is robust even after adding many more variables shown in the rightmost column. Also, confidence has a positive statistical predictive-power to predict persuasiveness (the empirical evidence for Hypothesis 3). However, its coefficient (importance) is less than the expertise (aligned with research in confidence heuristics [13]). This result is found when the platform provides immediate feedback for every question. If no feedback is provided or there is no right or wrong answer (i.e. judgmental questions), people might use confidence as a more substantial metric in their appraisal distribution.

Causality study of interpersonal influence

To study the order of the effects by confidence, persuasiveness, and expertise and to what extent their effect is supported by data, we propose to use a forecasting causality test. Here, we use Granger causality — a statistical concept of causality that is based on prediction [241, 242, 243]. According to Granger causality, if a signal X_2 "Granger-causes" (or "G-causes") a signal X_1, then past values of X_2 should contain information that helps predict X_1 above and beyond the information contained in past values of X_1 alone. Thus, instead of "Granger-cause" a more appropriate word might be "precedence" [244]. Its mathematical formulation is based on linear regression modeling of stochastic processes [241, 242, 243].

$$X_1(t) = \sum_{j=1}^{q} \alpha_j X_1(t-j) + c_1 + E_1(t)$$

$$X_1(t) = \sum_{j=1}^{q} \alpha_j X_1(t-j) + \sum_{j=1}^{q} \beta_j X_2(t-j) + c_2 + E_2(t)$$

(4.15)

Eq. [4.15] shows the linear regression version of Granger causality which is used in this chapter. The idea behind Eq. [4.15] is that if the variance of the model from E_1 to E_2 is reduced by the inclusion of the X_2 terms in the second equation, then it is said that X_2 G-causes X_1. In other words, X_2 G-causes X_1 if coefficients β are jointly and significantly different from zero. This can be tested by performing an F-test.

To study the causality of the aforementioned variables, we compute expertise, confidence, and persuasiveness in every round. Thus, in this data, for every person, we have three time series with nine data points. For every person, we compute Granger causality of these time series and study what percentage of change in individuals' expertise, confidence, and persuasiveness have statistical causal effects. Note that the exact number of lags, which were statistically significant, could uncover the precedence of these variables. That plausibly opens the door to studying the order of different effects, such as hypotheses 1 and 2, leading to social influence.

Applying statistical tests on three time series per individual is pregnant with false discovery and is absolutely crucial to adjust our results. Ergo, in the following results, obtained p-values are adjusted using Benjamini-Hochberg (BH) [9] controlling procedure with false discovery rate (FDR) of 5%.

Fig. 4.7 depicts empirical evidence for Hypothesis 1 and 3. Fig. 4.7 shows multiple Granger causality tests on the effect of confidence, persuasiveness, and expertise on one another. These results are obtained after applying the BH procedure with FDR=5%
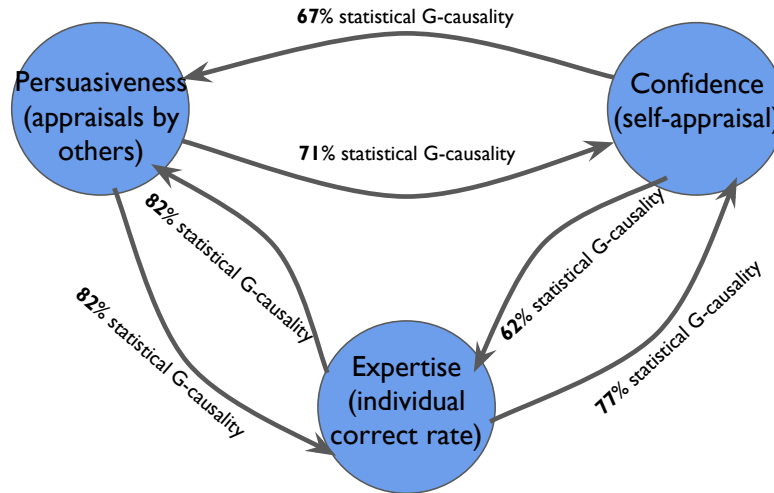
Figure 4.7: Granger causality result. This figure shows the proportion of statistically significant Granger causality of timeseries of confidence, persuasiveness and expertise in all teams. The p-values have been corrected using Benjamini-Hochberg (BH) procedure with False Discovery Rate of 5% has required p-value < 0.03 as statistical significance threshold.

that has required p-value < 0.03 as a statistical significance threshold. Even though the time series are relatively short (only nine data points), this result shows that in most individuals there is statistical causation from confidence to persuasiveness and vice versa over time. The results also show there is a causal relationship from expertise to confidence (aligned with confidence heuristics) and also persuasiveness (TMS [11]). Note that unlike the correlation experiment that was taking into account only the final influence report and expertise, these results are computed from time series of influence and performance for every individual during the course of the experiment.

Next, to study the order of effects given in Fig. 4.7, we use the proportion of statistically significant Granger causality applying different lags. Every lag depicts five questions, as we inquire about their influence matrix every five questions. In this regard, we test the causality once using lag=1 and then by using lag=2. We analyze the proportion of statistical significance only with lag=1 and the rest that needs at least two

previous time data points (lag=2). Thus, we sort the effects based on the descending order of the proportion of lag=1 as an estimate for the underlying order. From the effects in Fig. 4.7, Expertise $\longrightarrow$ Confidence seems to the fastest (as it has the most number of statistical significance effects with lag=1 compared to the rest of the effects). Afterward, Confidence $\longrightarrow$ Persuasiveness and Expertise $\longrightarrow$ Persuasiveness both come very close to each other. And at last, Persuasiveness $\longrightarrow$ Confidence seems the slowest among all. in other words, the order shows that the expertise of individuals quickly impacts their confidence. Both their confidence and their expertise then lead to persuasiveness. However, it seems that confidence has a slightly faster effect. This is perfectly aligned with the past research in confidence heuristic [13] and means that people have an immediate effect by social power and confidence, indeed faster than expertise. However, still, after some time (two lags in this experiment) expertise as a heuristic would be more prominent in the amount of persuasiveness (as 70% of individuals have this causal relationship after maximum two lags). In the end, persuasiveness can also lead to confidence; however, although it happens very often, it happens slower than the aforementioned effects. The delay of the persuasiveness affecting confidences could be because the platform shares individuals' answers with everyone but does not disclose their appraisals of each other. Therefore individuals must learn their confidence from persuasiveness through multiple discussions with their teammates.

4.4.2   Influence matrix estimation

Studying the problem of estimating the influence matrix is novel and challenging. Our data present an unprecedented opportunity to understand team behavior and estimate the interpersonal influence system of teammates. Even though this is a large set of states to estimate, there are a few constraints that make this task feasible. The matrix is

row-stochastic, and all elements fall into $[0, 1]$.

Influence matrix estimation is an applicable problem. Estimating individuals' influence directly from their communication logs and individual performances are useful in any team-based organization. Studying the longitudinal dynamics of a team influence system is rife with information about team behavior. In this experiment, the estimation method is applied for every team in every round using a history of influence matrices, text embeddings, and estimated expertise before that round. Using explainable machine learning and dynamical models, we also attempt toward uncovering the underlying predictive power of different features and mechanisms leading to higher interpersonal influence in teams.

Before studying models to estimate influence matrices, we need a set of measures (metrics) to gauge the accuracy of the estimated influence matrices with the ground truth ones. Here, we use two classical metrics: Mean Square Error (MSE) and the Kullback-Liebler (KL) divergence. Together they portray two different measures of accuracy. MSE pays more attention to the exact estimation of each number in the matrix while KL divergence on each row of the influence matrix focuses on the similarity of the distributions. The MSE and KL divergence of two row-stochastic matrices M and $\hat{M}$ with n rows are defined as follows,

$$\text{MSE}(\mathbf{M}, \hat{\mathbf{M}}) = \tfrac{1}{n}\|\mathbf{M} - \hat{\mathbf{M}}\|_F^2 = \tfrac{1}{n}\sum_{i=1}^{n}\sum_{j=1}^{n}|M_{ij} - \hat{M}_{ij}|^2, \qquad (4.16)$$

$$\text{KL}(\mathbf{M}, \hat{\mathbf{M}}) = \tfrac{1}{n}\sum_{i=1}^{n} D_{\text{KL}}(M_{i,.}\|\hat{M}_{i,.}) = \tfrac{1}{n}\sum_{i=1}^{n}\left(\sum_{j=1}^{n} M_{ij}\log\frac{M_{ij}}{\hat{M}_{ij}}\right). \qquad (4.17)$$

Depending on the application, one may choose any of these metrics. To showcase the generality of our proposed models, we present results on both metrics (Fig. 4.10).

We propose three models with a spectrum of explainability: (i) A black-box deep learning model which is the most accurate, (ii) A white-box linear model using convex optimization that explains substantial features leading to interpersonal influence (Table 4.9), (iii) A cognitive dynamical model which postulates an underlying mechanism. This dynamical model unlike the other two machine learning models does not require much training data as it only has one scalar hyperparameter to choose from. In the following, we introduce the results of estimation using these models.

Influence matrix estimation: cognitive dynamical models

We propose discrete-time dynamical models, of the form $\hat{M}^{(t)} = T(\hat{M}^{(t-1)}, x^{(t-1)})$, that are formulated such that established sociological concepts are baked into their equations. These non-machine learning models only take the history of past local influence weight information and individuals' performance values. These models can be used to provide a single or multi-round forecast of the influence matrices for successive rounds of the experiment.

Our results compare the accuracy of various dynamical models, which are described below in the Materials and Methods section. The models are a baseline model, model based on Hypothesis 1, model based on Hypotheses 1 and 2, and model based on Hypotheses 1, 2 and 3. The models assume that individuals can observe each other's expertise, which they take into account when readjusting the influence weights assigned to one another.

We consider single-round and multi-round forecast, to compare how the models perform when using the previous round's influence matrix versus only the initial round's influence matrix. The *single-round forecast* predicts the influence matrix at rounds $t \geq 2$ using the reported influence matrix from the previous round $M^{(t-1)}$ and the expertise $y^{(t)}$. Note that for the single-round forecast, the prediction comes from the following

124

modification to the dynamics, $\hat{M}^{(t)} = T(M^{(t-1)}, y^{(t-1)})$. Fig. 4.8 (left) illustrates the error of a given model. The *multi-round forecast* predicts $\hat{M}^{(t)}$, for any $t \geq 2$, using the initial reported influence matrix $M^{(1)}$ and the previous round's expertise values $y^{(t-1)}$ as inputs. The following details how the dynamical models are modified to give multi-round forecasts. To estimate $\hat{M}^{(2)}$, the map $T(M^{(1)}, y^{(1)})$ is used. For subsequent rounds $t \geq 3$, the estimate for $\hat{M}^{(t)}$ comes from $T(M^{(t-1)}, y^{(t-1)})$. In summary, the ground truth influence matrix data is propagated over a sequence of rounds to predict the influence matrix at future rounds. Fig. 4.8 (right) illustrates the error of a given model.

Overall for the single and multi-round forecast, we observe increased estimation accuracy for the models that capture more hypotheses. For the single-round forecast, we observe that the accuracy increases for later rounds since individuals adjust influence weights less as the experiment goes on. However, the accuracy for later rounds does not give significant improvements compared to the constant baseline model, since the influence weights remain relatively constant for rounds $t \geq 4$. For the multi-round forecast, as expected, we see that the accuracy decreases for predictions of later rounds; yet consistently provides the most accurate predictions of the influence matrices regardless of whether the model is given the most up-to-date ground truth values. In subsequent sections, we also show that the cognitive dynamical model gives competitive predictions compared to the machine learning models.

Influence matrix estimation: machine learning models

Here, we describe machine learning models to predict the influence matrix at every round. These powerful models are able to take multiple features extracted from the logs of the experiment and learn a mapping to estimate the corresponding influence matrix. In order to learn such mappings, they require training data. Thus, we use a portion of collected logs as the training and apply the trained model on the unseen logs.
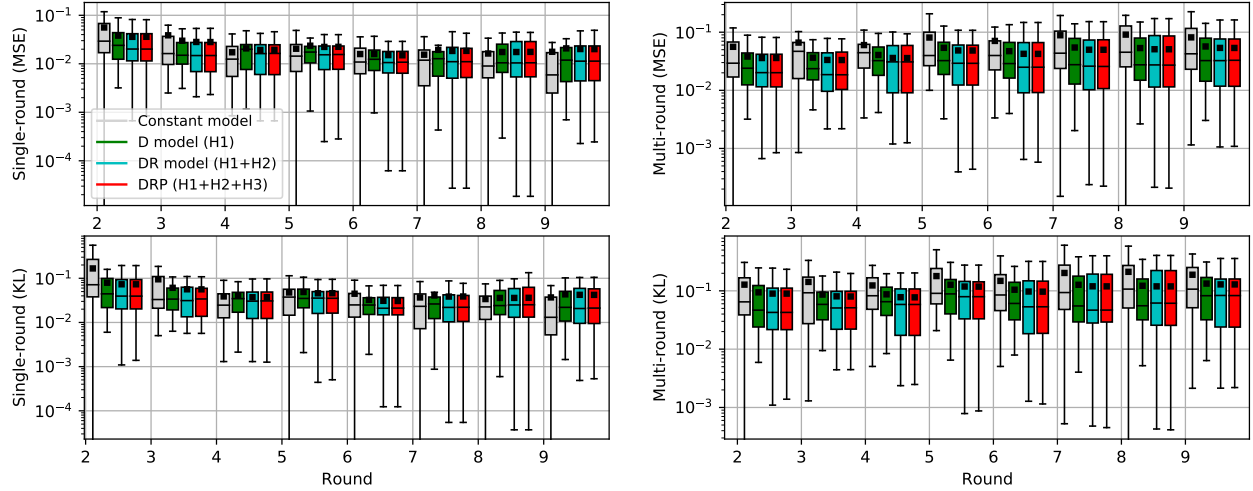
Figure 4.8: Cognitive model evaluation. The mean squared error (MSE) and the Kullback-Leibler (KL) divergence for different dynamical models over nine rounds of influence matrix estimation. Differentiation (D model) takes into account hypothesis 1. Differentiation, Reversion (DR model) is inspired by hypotheses 1 and 2. Differentiation, Reversion, Perceived (DRP model) uses hypotheses 1, 2, and 3. For the models, we use the hyperparameter $\tau = 0.4$. In this figure boxes show the interquartile range of the errors, the whiskers show minimum and maximum of the range of the distribution. In each box, the dot shows the average and the line shows the median of the portrayed distribution. **Left:** Single-round forecast error of various dynamical models for predicting the influence matrix one round ahead. The models estimate $\hat{M}^{(t)}$ using the expertise $\bar{y}^{(t-1)}$ and the reported influence matrix from the previous round $M^{(t-1)}$. **Right:** Multi-round forecast error of various dynamical models for predicting the influence matrix multiple rounds ahead. The models estimate $\hat{M}^{(t)}$ using the expertise $\bar{y}^{(t-1)}$ and the initial ground truth $M^{(1)}$ influence matrix reported by individuals. For rounds $t \geq 2$, the dynamics use the predicted influence matrix from the previous round $\hat{M}^{(t-1)}$, instead of $M^{(t-1)}$. For rounds $t \geq 4$, the influence network remains relatively constant, so the cognitive dynamical model offers incremental improvements to the baseline models for single-round forecast. However, this model gives significant improvements in accuracy from baseline models for all rounds in multi-round prediction.

In order to predict the influence matrix at time t, we use time and content of text messages from the broadcast communication logs until time t, individual correct percent until time t, and reported influence matrices before time t in the following.

• Connectivity networks: In broadcast communication logs, the time between two messages can reveal a directed and weighted evolving network structure among teammates. This approach implies a basic assumption: if a message B appears on a chat log close enough in time to an earlier sent message A, then B is likely a response to A; and, the larger the time gap between two messages is, the less likely the later message is a response to the earlier message. For a message m occurring at time $m.time$ on the log, we define the set of its responses and the connectivity networks as follows

$$R(m) = \{r \mid m.time < r.time \wedge\ t_1 \le r.time - m.time \le t_2$$

$$\wedge\ r.sender \ne m.sender\}$$

$$A_{ij} = \sum_{\substack{p.sender=i \\ q.sender=j \\ q \in R(p)}} \text{weight}(p, q), \qquad (4.18)$$

We define the weights in the connectivity networks (given in   Eq. [4.18]) in three different ways. First is Response network in which the weights in the network, similar to Amelkin *et al.* [92], are calculated based on the duration a response as $\text{weight}(p, q) = e^{-\gamma|p.time - q.time|}$. This networks represents the responsiveness of every individuals toward every other member. The likelihood of a message being a response degrades with the increase of the time gap between the two messages. Second is Sentiment network in which we use Valence Aware Dictionary and sEntiment Reasoner (VADER) as the sentiment analysis toolbox [245] on words in the response message as $\text{weight}(p, q) = \text{sentiment}(q)$. Third is the Emotion network in which Affective norms for English words (ANEW) are

used as the emotion analysis toolbox [246] that examines arousal, valence, and dominance of words in the response message. The weight for emotion network is computed as $\text{weight}(p, q) = \text{emotion}(q)$. In all networks, the summation is performed over all suitable pairs (p, q) of messages p and q in a team's chat log. Thus, these networks are represented as a $n \times n$ matrix with float values and no self-loop.

• Message content embeddings: We use natural language processing to analyze the content of messages. The text embeddings for sentences [28] are generated from a pre-trained sentence embedding model by the last layer of the encoder in the state-of-the-art model, a Robustly Optimized BERT Pretraining Approach (RoBERTa) [18, 27], is generated.

• History of influence matrix: Previous influence matrices.

• Expertise: Individual correctness rate.

We propose a linear maximum likelihood estimation model using convex optimization and a deep neural network model. Fig. 4.2 shows the architecture of the neural network model (see Methods and Materials for details). They both similarly intend to find a linear or nonlinear combination of the aforementioned input features to estimate a row-stochastic influence matrix. We compare the proposed models to the baseline models with a variation of different input features. All models are trained with 80% of the data and tested on the withheld 20%. To compute the statistical significance, we draw 1000 bootstraps with replacement from the hold-out test set.

Due to the application, for every round, we can assume we only have access to the first influence matrix, and we need to predict all influence matrices in future rounds with that. Hence, in Fig. 4.9, we use only the first influence matrix with expertise, text embeddings, and so forth, in every round, to predict a 4×4 influence matrix. It shows the average of Mean Square Error (MSE) for the estimated influence matrix from the ground truth influence matrix (reported by individuals) in every round for every team. MSE is defined on two matrices in Eq. [4.16].

The numbers in parenthesis show the standard error for MSE bootstraps. Fig. 4.9 depicts linear and neural network-based models consistently surpass other baselines with any sets of features. Also, it shows the proposed models are powerful as the more features are introduced, the more accurate they can get. Fig. 4.9 also shows the statistical significance of the proposed models as we can also see by adding more 2.58 times of standard deviation still neural network works better than all other models. All numbers from this figure are shown in Table 4.4.
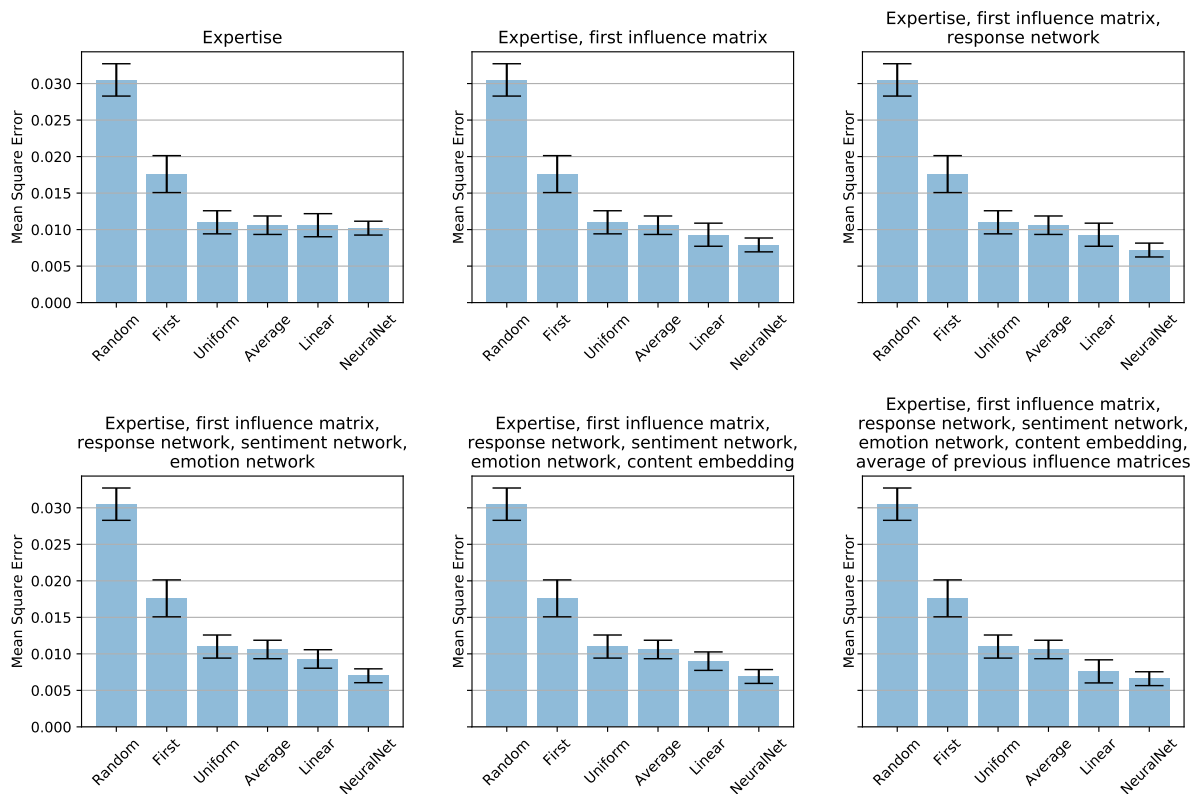
Figure 4.9: Improvement in machine learning models by adding more features. Average of Mean Square Error (MSE) of estimated influence matrix from the ground truth in the test set of influence matrices. Titles show the list of features fed to the models. The error bar shows the standard deviation in 1000 bootstrap on test error. Both machine learning models improve when given more features from the logs.

In another setting, for every round, we assume we have access to the previous influ-

Models / Features	Random baseline	First baseline	Uniform baseline	Average baseline	Linear model	NN model
expertise	0.0305 (0.00007)	0.0176 (0.00008)	0.0110 (0.00005)	0.0106 (0.00004)	0.0106 (0.00005)	**0.0102 (0.00004)**
expertise, first influence matrix	0.0305 (0.00007)	0.0176 (0.00008)	0.0110 (0.00005)	0.0106 (0.00004)	0.0093 (0.00005)	**0.0079 (0.00003)**
expertise, first influence matrix, response network	0.0305 (0.00007)	0.0176 (0.00008)	0.0110 (0.00005)	0.0106 (0.00004)	0.0093 (0.00005)	**0.0072 (0.00003)**
expertise, first influence matrix, response network, sentiment network, emotion network	0.0305 (0.00007)	0.0176 (0.00008)	0.0110 (0.00005)	0.0106 (0.00004)	0.0093 (0.00004)	**0.0070 (0.00003)**
expertise, first influence matrix, response network, sentiment network, emotion network, content embedding	0.0305 (0.00007)	0.0176 (0.00008)	0.0110 (0.00005)	0.0106 (0.00004)	0.0090 (0.0004)	**0.0069 (0.00003)**
expertise, first influence matrix, response network, sentiment network, emotion network, content embedding, average of previous influence matrices	0.0305 (0.00007)	0.0176 (0.00008)	0.0110 (0.00005)	0.0106 (0.00004)	0.0067 (0.00005)	**0.0066 (0.00003)**

Table 4.4: Improvement in machine learning models by adding more features. Average of Mean Square Error (MSE) of estimated influence matrix from the ground truth in the test set of influence matrices reported by individuals. The number in parenthesis shows the standard error in 1000 bootstrap on test error.

ence matrix and expertise to predict the current influence matrix. For this setting, there are more baselines that we can compare our proposed models against. Fig. 4.10 (left) shows MSE divergence error for models using previous influence matrix and expertise. Similarly, the neural network-based model surpasses all baselines and provides statistically significant lower MSE. It is worth mentioning that proposed linear model (Eq. [4.6]) is competitive with the proposed neural network model (Fig. 4.2). Also, interestingly, the proposed cognitive dynamical model (Eq. [4.5]) which does not require any training and is described by a mechanism that postulates past research in social psychology works significantly better than other baselines and competitively close to the proposed machine learning models. Note that both machine learning models use optimization methods for training that requires multiple steps to converge.

Fig. 4.10 shows MSE and KL divergence of the estimated influence matrix from the ground truth reported by individuals. MSE is defined on two matrices in Eq. [4.16] and KL divergence in Eq. [4.17]. MSE and KL divergence provide two different perspectives regarding the efficacy of influence estimation. MSE formulation emphasizes the exact values in matrices. While KL divergence attends to the discrete probability distribution in corresponding rows of two matrices. Fig. 4.10 shows no matter which error measurement we use, two proposed models work efficiently compared to all baselines. It also depicts the neural network-based model surpasses all other models. The problem formulation for MSE of influence matrices is provided in Eq. [4.6], and for probability distribution estimation in every row of influence matrices is given in Eq. [4.7] (see Methods and Materials).

For more details on the results shown in Fig. 4.10, Table 4.5 and Table 4.6 depict MSE of basic baselines and estimation models, respectively. Similarly, Table 4.7 and Table 4.8 show KL divergence of basic baselines and estimation models, respectively. All algorithms use use previous influence matrix and expertise. Note that neural network-
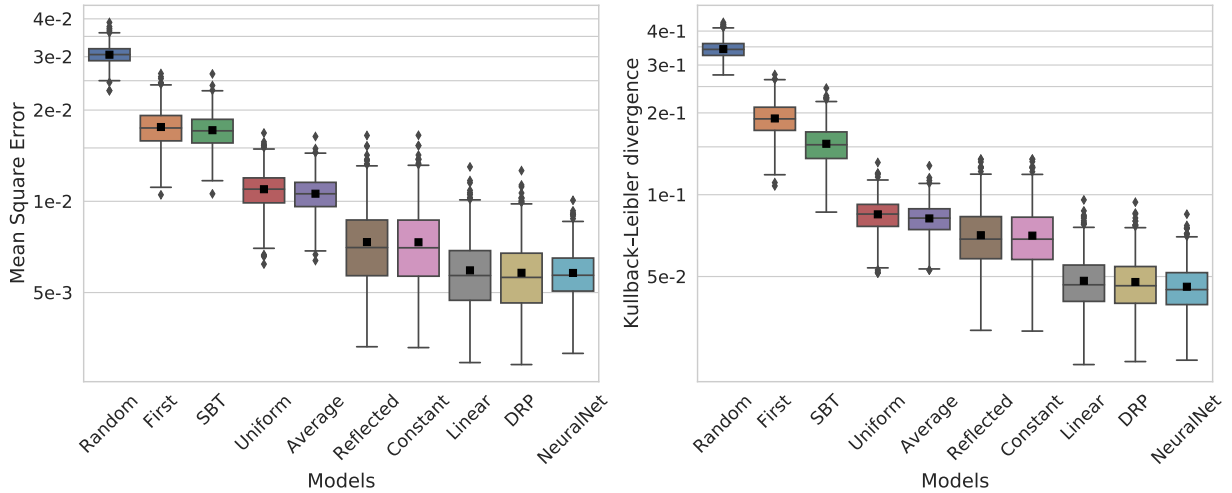
Figure 4.10: Comparison of all models. Mean squared error (MSE) and Kullback–Leibler (KL) divergence of single-round influence matrix prediction for baseline algorithms and the proposed models. Evaluations are applied on 1000 bootstraps of the holdout test dataset (20% of the entire data). All models have access to the expertise and previous influence matrix for every team. The box shows the interquartile range of the errors, the whisker shows minimum and maximum of the range of the distribution, and the dots show the outliers. Baseline models: *Random* baseline is a randomly generated row-stochastic matrix. *First* predicts a team's first influence matrix to be unchanged. *SBT* baseline uses the generalized Structural Balance Theory [15]. *Uniform* predicts a matrix with all elements as $\frac{1}{n}$. *Average* predicts a team's row-stochastic average influence matrix to be the most accurate prediction for any influence matrix. *Reflected* baseline uses reflected appraisal mechanism for prediction [16]. *Constant* predicts the influence matrix to be unchanged from last measured one. Proposed models: Cognitive model based on Differentiation, Reversion, Perceived expertise model *DRP* takes into account the aforementioned hypotheses (1, 2, 3) to predict influence matrices. Moreover, Linear model using convex optimization (*Linear*) and Neural Networks model (*NeuralNet*) are proposed to learn important features from the logs to estimate influence matrices. The figure depicts the proposed models outperform baselines. Surprisingly, this figure shows the reflected appraisal model does not surpass the baseline of considering previous influence matrix to be unchanged (Constant model). Also interestingly, this figure shows that the cognitive dynamical model works competitively with the learning models showing the power behind our empirically proven hypotheses.

Models / Features	Random baseline	First baseline	Uniform baseline	Average baseline	Constant baseline
previous influence matrix	0.0305 (0.00007)	0.0176 (0.00008)	0.0110 (0.00004)	0.0106 (0.00005)	0.0073 (0.00007)
previous influence matrix, expertise	0.0305 (0.00007)	0.0176 (0.00008)	0.0110 (0.00004)	0.0106 (0.00005)	0.0073 (0.00007)

Table 4.5: MSE of estimated influence matrix using basic baselines from the ground truth in the test set of influence matrices reported by individuals. The number in parenthesis shows the standard error in 1000 bootstrap on test set.

Models / Features	SBT model	Reflected appraisal model	Linear model	Cognitive DRP -based model	Neural network -based model
previous influence matrix	0.0172 (0.00007)	N/A	0.0061 (0.00005)	N/A	0.0059 (0.00003)
previous influence matrix, expertise	0.0172 (0.00007)	0.0073 (0.00007)	0.0059 (0.00005)	0.0709 (0.0006)	0.0058 (0.00003)

Table 4.6: MSE of estimated influence matrix using estimation models from the ground truth in the test set of influence matrices reported by individuals. The number in parenthesis shows the standard error in 1000 bootstrap on test set. This table also depicts the proposed learning models (neural network-based, linear, and cognitive DRP-based) outperform baselines.

based model surpasses all baselines and provides statistically and significantly lower error rates.

Table 4.9 sheds light on the importance of every feature set in the linear model optimized using convex optimization which was trained with 80% of the data. This table shows entry-wise l1-norm of estimated parameters in Eq. [4.6]. The values in table 4.9 are sorted from most to least important top to bottom. This result shows the previous influence matrix is the most important feature used to predict the next influence matrix. Interestingly, it also shows expertise is the second most of predictive power and text embedding is third. It shows sentiment, emotion, and quick responsiveness (response network) network are far less substantial in the estimation. It is worth mentioning that

Models / Features	Random baseline	First baseline	Uniform baseline	Average baseline	Constant baseline
previous influence matrix	0.3431 (0.0008)	0.1908 (0.0009)	0.0818 (0.0003)	0.0709 (0.0006)	0.0707 (0.0006)
previous influence matrix, expertise	0.3431 (0.0008)	0.1908 (0.0009)	0.0818 (0.0003)	0.0709 (0.0006)	0.0707 (0.0006)

Table 4.7: KL divergence of estimated influence matrix using basic baselines from the ground truth in the test set of influence matrices reported by individuals. The number in parenthesis shows the standard error in 1000 bootstrap on test set.

Models / Features	SBT model	Reflected appraisal model	Linear model	Cognitive DRP -based model	Neural network -based model
previous influence matrix	0.1540 (0.0008)	N/A	0.0494 (0.0003)	N/A	0.0479 (0.0003)
previous influence matrix, expertise	0.1540 (0.0008)	0.0709 (0.0006)	0.0482 (0.0003)	0.0478 (0.0003)	0.0459 (0.0003)

Table 4.8: KL divergence of estimated influence matrix using estimation models from the ground truth in the test set of influence matrices reported by individuals. The number in parenthesis shows the standard error in 1000 bootstrap on test set. This table also depicts the proposed learning models (neural network-based, linear, and cognitive DRP-based) outperform baselines.

	$l1$-norm of estimated parameters
Previous influence matrix	0.2137 ± 0.0027
Expertise	0.0239 ± 0.0027
Message content embedding	0.0111 ± 0.0003
Message sentiment	0.0078 ± 0.0010
Message emotion	0.0050 ± 0.0007
Message responsiveness	0.0041 ± 0.0004

Table 4.9: Features importance in predicting influence. Entry-wise $l1$-norm of estimated parameter matrix in linear model given in Eq. [4.6] which is trained with 80% of the data. This table shows the importance of each features in the proposed linear model. The embeddings [18], sentiments, and emotions all are computed from the message text content; however, responsiveness is computed from the timestamps of the messages.

due to the origin of memory questions, there is only a brief chat happening for many of the members since they simply do not know the answer. That is probably the reason that text embedding is not as important as the correct answer rate.

4.4.3   Parameter tuning

Here, we provide the results of three different methods used to find an appropriate range for the time window. The first method uses the connectivity network. In order to determine values for λ, γ, and an appropriate time window, we attain values of the average mean square error of a 10-fold cross validation of the network. By plotting the mean square errors in a heatmap for every value of λ and γ, we are able to compare which values of the parameters gave the lowest error. In Fig. 4.11, we find that with $\lambda = 0.2$ and $\gamma = 1$, we achieve an average mean squared error value of 0.8560 at the window $[1, 18]$. This finding is both reasonable and supported by our network, which helps us ensure that our results use parameters that are conducive to our application.

The next method takes the approach of using labeled data and finding the error of different windows. To accomplish this, we labeled 98 messages from team 7 with either

a 0 or a 1, where a 0 indicates that a message was not a response to a previous message and a 1 indicates that the message was a response. We then recorded the predictions of what different time windows would label the data as. For example, if we were looking at a window of $[2, 10]$ and a message was labeled with a 1 and was sent 2 to 10 seconds after any other message, we would classify it as correctly labeled by the window. We did this for each message and calculated precision, recall, F1 score, Receiver Operating Characteristic (ROC) score, and accuracy. To make sense of our findings, we took the best F1 score, shown in Fig. 4.12, out of all of the windows and found that $[1, 21]$ had the best F1 score of 0.75. Other metrics like recall and ROC score had similar results, as the best window for recall was $[1, 21]$ and the best window for the ROC score was $[1, 21]$ with values 0.9783 and 0.7103 respectively.

Our last method took a similar approach for as the previous method, but with the labels of data as time windows themselves rather than binary labels. That is, the new labels told that messages within the time window were direct responses to the message, giving more control over indicating which messages are responses. We recorded which messages were correctly classified over different time windows and found similar results to the second method, where the best F1 score gave an optimal window of $[1, 18]$, as seen in Fig. 4.13.

Eventually, consulting with all tuning experiments, we chose $[1, 18]$ as the time window.

4.5   Conclusion and Future Works

Interpersonal relationships change due to a person's cognitive biases, societal roles, and what their in-group perceptions are, among other factors. These relationships can be modeled as an influence matrix, where weighted edges signify positive or negative
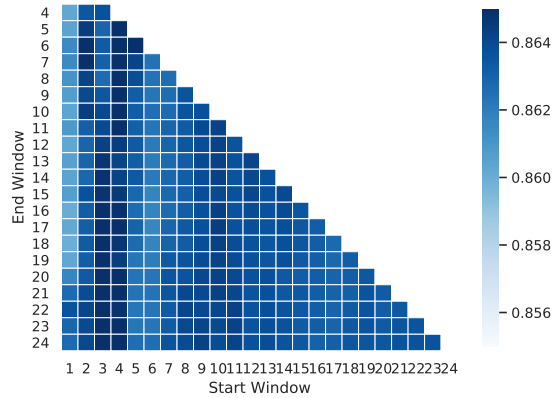
Figure 4.11: Heatmap of MSE of varying time windows attained by applying the linear model using convex optimization model on the response network.
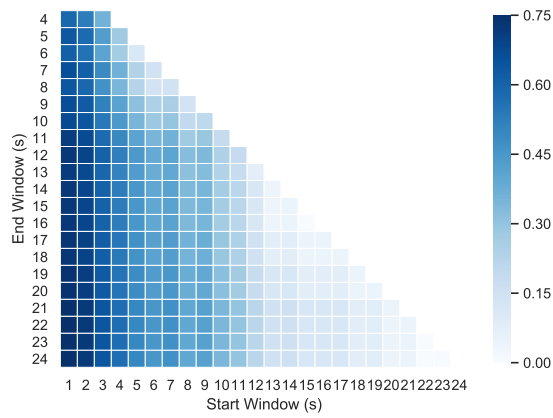
Figure 4.12: Heatmap of the F1 score of varying time windows attained by labeling 98 messages from team 7.
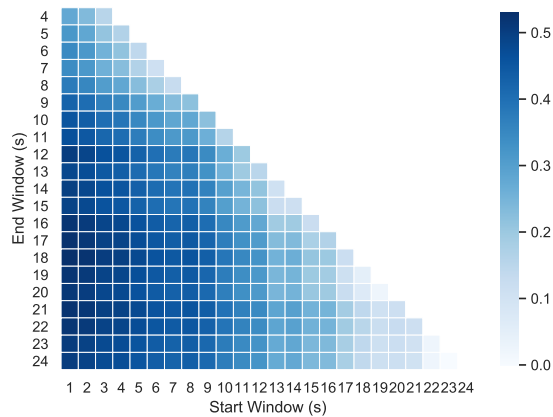
Figure 4.13: Heatmap of the F1 score of varying time windows attained by labeling the same 98 messages from team 7 with window sizes rather than binary labels.

appraisals between people. Being able to estimate these influence matrices has important applications such as marketing advertisements, creating successful political campaigns, and improving the efficiency of communication among team members. This idea of influence matrix estimation has been studied previously but with simulated data or a focus on estimating the total amount of influence from organizations or websites rather than estimating separate values between individuals.

We collected data from human subjects answering trivia questions in teams of four. After individually answering a question, they then collaborated to agree on a final answer through a chat system. The participants were periodically asked to assess their appraisals of each other. We built a machine learning-based model using text content, the time of messages, and individual task performance to estimate the collective influence matrix. In total, we sought to find underlying factors that contribute to the awarded influence. We used convex optimization and neural network models alongside baselines from dynamical models and sociology literature to test our hypothesis. From these findings, we conclude that task performance and higher values of confidence were the two most salient factors in determining the amount of influence one receives in collaborative group settings. We hope this chapter on estimating underlying influence systems in a collaborative environment will spur the establishment of connections with a variety of fields and advance an interdisciplinary understanding of the design of social experiments. We believe the pragmatic implications will be of great use to any individual or organization that manages teams or networks of collaborators.

Chapter 5

Conclusion

In the following, we summarize studies from previous chapters and propose future directions by introducing pertinent open problems in the field.

5.1   Summary of Chapter 2

Chapter 2 addresses a long-standing debate concerning Structural Balance Theory. Structural Balance Theory (SBT) has been applied across disciplines since the 1940s and continues to grow in prominence in fields that study social networks, conflict, and change. This chapter addresses specifically the absence of dynamic, real-world analyses of structural balance and the relationship between a system's balance and performance. This chapter examines a unique dataset that tracks all e-communications (timing and content) between 66 stock traders as they actively traded within a hedge fund over a continuous 2 year period. These data present an unprecedented opportunity to measure how balances of sentiments change over time and how this change in time is related to trading performance. Our models use Markov transition probability matrices, nonparametric regression analyses, and social network null models. We believe the topic of the

chapter will be of great interest across the sciences and reduce errors in the application of SBT. The pragmatic implications will be of great use to any individual or organization that manages teams or networks of collaborators. Our analyses provide the following novel theoretical and empirical findings:

- For the first time, it tests the relationship between balance structures and performance on a longitudinal dataset.

- This chapter shows the emergence of structural balance on the largest longitudinal and field-setting data in the literature.

Contrary to the axioms of SBT, we find that:

- Forbidden relationships exist and persist.

- Stability occurs as much as change.

- Self-correction in teams is limited.

Pragmatic Contributions:

- Decision-makers in balance are 30% likelier to have higher performance than when they are out of balance.

- Forbidden triads persist and can cripple a team or network unless actionable interventions are applied.

5.2 Summary of Chapter 3

In Chapter 3, we propose an extension for structural balance theory to sparse networks and test it on the largest longitudinal dataset yet addressed in empirical research on structural balance. We analyze 23 years of data on public international appraisals of

nations, and we present evidence that this network of appraisals evolves as predicted by a theory of structural balance. With dynamic real-world analyses of structural balance, our research provides empirical findings on long-standing debates in the interdisciplinary field of work on structural balance theory. Interest in this theory has been motivated by its attention to social conflict and social change.

Our findings are listed below:

- We find that disturbances in this evolution are associated with major economic events. Remarkably, the trajectory of the Frobenius norm of sequential transition probabilities that govern the evolution of the network dramatically stabilizes.

- We provide unexpected results regarding this theory, introduce a novel convex optimization method to estimate the dynamics of data, and provide mathematical proof for its optimality and convergence rate.

- we buttress the above findings with an analysis of two additional smaller-scale finance datasets.

- Contrary to the classic axioms of structural balance theory, we find that the main driver of the evolution toward structural balance is the reduction of violations of transitivity (a friend of a friend is a friend).

- An important pragmatic contribution of the chapter is finding that the proposed time-varying Markov model, using sparse structural balance, usefully pinpoints international shocks, and international conflicts.

5.3   Summary of Chapter 4

Chapter 4 uses a unique dataset about 124 human subjects split into groups of four, playing a team-based game of trivia questions for two hours; we collect individual answers before the discussion, team answers after discussion, e-communications (timing and content), and answers to questions and appropriately designed questionnaires. This data presents an unprecedented opportunity to measure how the interpersonal influence system of teammates changes over time and how the dynamics are related to individual performance and communication. Our quantitative models rely upon concepts from cognitive psychology and machine learning to estimate social influence over time.

This chapter addresses long-standing debates on the effects of transactive memory systems (TMS), cognitive heuristics and biases, and influence systems on group decision making. As established in the literature, TMS posits individuals tend to learn over time who is good at what in their team. Key open questions involve understanding how the influence system of a team depends upon the transactive memory system and to what extent higher influence is assigned to experts. Our analyses provide the following novel theoretical and empirical findings.

We find

- Statistically significant empirical support for the theory transactive memory systems, social comparison, and confidence heuristic in teams collaborating on tasks with immediate feedback.

- A novel dynamical model, motivated by the hypotheses from social and psychological science that is validated against the dataset and is used to estimate interpersonal influence matrices using individual performance.

- A set of rigorous analytical results on the asymptotic behavior of the proposed

142

model.

- A novel maximum likelihood estimation model with rigorous loss derivation that outperforms all baselines in estimating the influence matrices in team tasks.

Pragmatic Contributions are:

- Individuals in a communication-based system with feedback can efficiently learn their teammates' skills even without direct access to each others' expertise.

- Our proposed dynamical and neural network model can be used in a chat-based platform with access to individuals' performance to accurately estimate the social influence among group members (who-influence-whom and to what extent).

5.4   Future Directions

This dissertation opens up a number of avenues for future research, particularly, in dealing with signed networks. Similar to the studies in this dissertation, team networks and socio-economic networks would be in focal target of the open problems.

Impact of social life on work performance: An extension to the study in Chapter 2 is to study other aspects of social life on work performance in risky-decision making. One popular aspect is work/life balance. There are multiple studies in this matter; however, there is no study quantifying the impact of work/life balance on longitudinal trading performance. To this end, we can study the social and work communication networks among traders in a company.

Relational ties can often be multidimensional in nature, comprising both social and economic components. Prior research suggests that such 'multiplex' ties can be the conduits of trust and reciprocity, and as a consequence can critically shape organizational

and market outcomes [247, 248, 249]. To test such ideas, extant research has typically emphasized network structure and relied on data collected from affiliation surveys (i.e. self-reported perceptions of ties), or through the use of trace data (e.g. organizational records) to create network snapshots. We can focus on the content of ties to provide a dynamic perspective on multiplexity.

Assume we have a larger finance dataset, similar to the one presented in Chapter 2. We can utilize this data from a real-world organizational social network, comprising of instant messages exchanged by employees of a hedge fund over years to investigate the relationship between sociability (i.e. the ratio of expressive and instrumental communication) and the task performance of organizational experts. Methodologically, depart from past studies in two important ways, we can analyze tie type at the conversation level, and we can utilize emergent machine learning techniques to analyze the content of conversations. Moreover, it would be of high interest to apply Granger causality on the timeseries of work/life ratio and trading profit for individuals. Using this method, we can also estimate the amount of the delay of the aforementioned effect.

Signed networks embedding using structural balance theory: Network embedding models are extremely popular in the network science literature. Particularly, since the inception of Graph Convolutional Network (GCN) [250], a large attention has been devoted to apply well-studied deep neural networks models and convolutional networks to graphs. These models have led to state-of-the-art performance for a variety of applications such as recommender systems [251], semi-supervised classification [250], and traffic prediction [252], to name but a few.

Although many of social networks are signed, the number of network embedding studies on signed networks are far fewer [253, 254, 255, 256] than on unsigned networks. The reason is the two tricks that are used in network embedding studies, meaning combin-

ing the neighborhood and generating random walk, are not easily applicable on signed networks. Thus, there is a need for a well-established theory such as structural balance theory to be used for defining the signed network embedding. There are a few studies that take advantage of balance theory in signed network embedding [255, 233]; however, most of which are not using the correct definition of sparse triads as the building block in the convolutional aggregation unit. One can use the three definitions of balanced sparse triads laid out in Chapter 3 alongside other social theories such as status theory for defining balanced and unbalanced sparse triads. These triads would be useful for encoding these triads as subgraphs in two hop neighborhood of every node in the graph when computing graph convolution function. Sign prediction in static network (similar to [72]) is an application for such models. Additionally, there are many opportunities for studying dynamical signed network embedding in longitudinal setting which have been rarely addressed in the literature. One can use the datasets and sparse triads definitions from Chapter 3 to define embedding method for signed networks in longitudinal setting.

Experimental study on structural balance theory: Despite the rich literature on structural balance theory, there is no specifically designed experimental subject study to quantitatively measure the accuracy of this theory on different task types within different team size. Abimbola *et al.* [257] introduces a card game as a group problem solving task based on Heider's balance theory. It conceptualizes problem solving as a progression towards increasing structural balance and describes an experimental method and stimulus for studying group problem solving based on this conceptual framework. Harari *et al.* [258] uses a series of verbally described interpersonal situations as stories based on Heider's model to be assessed by subjects as a function of certain situational conditions and predispositional interpersonal values. However, none of the aforementioned studies directly take into account people's interpersonal influence. Boss *et al.* [259] applies

Heider's model to a sport-specific situation where two individuals are partner in a two-person game (e.g., doubles in tennis) with the shared task of still winning an almost lost set. In their study, they do not deal with teams of three or larger which is the building block of balance theory. Morrissette *et al.* [145] study the relationship between team performance and structural balance theory in a experimental study with groups of three subjects. They used Cartwright and Harary definition for balance using the normalized number of cycles with even number of negative edges. They found balance has a positive but weak relationship with team performance. Their study only takes into account one time opinion inquiry.

Based on the literature, the open problem would be to execute experimental study and collect longitudinal answers (multi-step inquiries), in teams of size three or more individuals. More precisely, we may give judgemental or intellective tasks to subjects and collect their interpersonal influence, and appraisal toward each others' answers. This is aligned with Heider's POX model [66]; however, unlike studies in the literature, this dataset would shed light on the dynamic of interpersonal influence and opinion appraisals in experimental study in teams. The compendium dataset will be extremely valuable for the literature since the experimental subject study on longitudinal balance theory is rare. Lastly, if collected using POGS, we can take advantage of the unprecedented opportunity of accessing the communication logs as well as opinion change logs, social influence, and teammates' appraisals.

Interpersonal influence estimation: There are many practical open problems to extend the study in Chapter 4. First, we can study the network control problem in which one tries to guide the team to achieve the maximum level of their wisdom of crowd. For this purpose, one needs to design a protocol to collect data via experimental study such that researchers can manipulate the network structure of team communication in

the midst of running an experiment. Second, the type of tasks can be different than intellective. For instance in judgemental tasks, subjects tend to communicate more since everybody has an opinion and usually there is no right or wrong answer. The interpersonal influence accorded by subjects could be drastically different in these types of tasks compared to the ones from intellective tasks. Third, an A/B testing for cognitive biases such as demographic features, social confidence, and over confidence can be further tested on teams if we have groups of exposed and control. One example would be not provide feedback for subjects and study whether social confidence is sufficient for people to find experts in their team or not. Another example is to what extent individuals have negative bias against a stochastic Artificial intelligence agent as part of their team.

Bibliography

[1] S. Wuchty and B. Uzzi, *Human communication dynamics in digital footsteps: A study of the agreement between self-reported ties and email networks*, PLOS ONE **6** (2011), no. 11 e26972.

[2] C. W. Granger, *Causality, cointegration, and control*, Journal of Economic Dynamics and Control **12** (1988), no. 2-3 551–559.

[3] M. O. Jackson and S. Nei, *Networks of military alliances, wars, and international trade*, Proceedings of the National Academy of Sciences **112** (2015), no. 50 15277–15284.

[4] K. Barbieri, O. M. Keshk, and B. M. Pollins, *Trading data: Evaluating our assumptions and coding rules*, Conflict Management and Peace Science **26** (2009), no. 5 471–491.

[5] P. Martin, T. Mayer, and M. Thoenig, *Make trade not war?*, The Review of Economic Studies **75** (2008), no. 3 865–900.

[6] J. R. Oneal and B. Russett, *Assessing the liberal peace with alternative specifications: Trade still reduces conflict*, Journal of Peace Research **36** (1999), no. 4 423–442.

[7] H. Hegre, J. R. Oneal, and B. Russett, *Trade does promote peace: New simultaneous estimates of the reciprocal effects of trade and conflict*, Journal of Peace Research **47** (2010), no. 6 763–774.

[8] X. He, L. Liao, H. Zhang, L. Nie, X. Hu, and T.-S. Chua, *Neural collaborative filtering*, in *Proceedings of the 26th International Conference on World Wide Web*, pp. 173–182, International World Wide Web Conferences Steering Committee, 2017.

[9] Y. Benjamini and Y. Hochberg, *Controlling the false discovery rate: a practical and powerful approach to multiple testing*, Journal of the Royal Statistical Society: Series B (Methodological) **57** (1995), no. 1 289–300.

[10] K. Lewis, D. Lange, and L. Gillis, *Transactive memory systems, learning, and learning transfer*, Organization Science **16** (2005), no. 6 581–598.

[11] K. Lewis, *Measuring transactive memory systems in the field: scale development and validation*, Journal of Applied Psychology **88** (2003), no. 4 587.

[12] K. Lewis, *Knowledge and performance in knowledge-worker teams: A longitudinal study of transactive memory systems*, Management Science **50** (2004), no. 11 1519–1533.

[13] J. P. Thomas and R. G. McFadyen, *The confidence heuristic: A game-theoretic analysis*, Journal of Economic Psychology **16** (1995), no. 1 97–113.

[14] P. C. Price and E. R. Stone, *Intuitive evaluation of likelihood judgment producers: Evidence for a confidence heuristic*, Journal of Behavioral Decision Making **17** (2004), no. 1 39–57.

[15] K. Kułakowski, P. Gawroński, and P. Gronek, *The heider balance: A continuous approach*, International Journal of Modern Physics C **16** (2005), no. 05 707–716.

[16] W. Mei, N. E. Friedkin, K. Lewis, and F. Bullo, *Dynamic models of appraisal networks explaining collective learning*, IEEE Transactions on Automatic Control **63** (2017), no. 9 2898–2912.

[17] B. Everitt and A. Skrondal, *The Cambridge dictionary of statistics*, vol. 106. Cambridge University Press Cambridge, 2002.

[18] Y. Liu, M. Ott, N. Goyal, J. Du, M. Joshi, D. Chen, O. Levy, M. Lewis, L. Zettlemoyer, and V. Stoyanov, *Roberta: A robustly optimized bert pretraining approach*, arXiv preprint arXiv:1907.11692 [**cs**] (2019).

[19] L. A. DeChurch and J. R. Mesmer-Magnus, *The cognitive underpinnings of effective teamwork: a meta-analysis.*, Journal of applied psychology **95** (2010), no. 1 32.

[20] M. Greene, *The demise of the lone author*, Nature **450** (2007), no. 7173 1165–1165.

[21] B. Uzzi, S. Mukherjee, M. Stringer, and B. Jones, *Atypical combinations and scientific impact*, Science **342** (2013), no. 6157 468–472.

[22] S. Wuchty, B. F. Jones, and B. Uzzi, *The increasing dominance of teams in production of knowledge*, Science **316** (2007), no. 5827 1036–1039.

[23] Templafy. https://info.templafy.com/blog/how-many-emails-are-sent-every-day-top-email-statistics-your-business-needs-to- August, 2020.

[24] K. Burke. https://www.textrequest.com/blog/texting-statistics-answer-questions/, May, 2016.

[25] T. Mikolov, I. Sutskever, K. Chen, G. S. Corrado, and J. Dean, *Distributed representations of words and phrases and their compositionality*, in *Advances in neural information processing systems*, pp. 3111–3119, 2013.

[26] J. Pennington, R. Socher, and C. D. Manning, *Glove: Global vectors for word representation*, in *Proceedings of the 2014 conference on empirical methods in natural language processing (EMNLP)*, pp. 1532–1543, 2014.

[27] J. Devlin, M.-W. Chang, K. Lee, and K. Toutanova, *Bert: Pre-training of deep bidirectional transformers for language understanding*, arXiv preprint arXiv:1810.04805 [**cs**] (2018).

[28] D. Cer, Y. Yang, S.-y. Kong, N. Hua, N. Limtiaco, R. S. John, N. Constant, M. Guajardo-Cespedes, S. Yuan, C. Tar, *et. al.*, *Universal sentence encoder*, ArXiv preprint arXiv:1803.11175 [**cs**] (2018).

[29] L. Euler, *Leonhard euler and the königsberg bridges*, Scientific American **189** (1953), no. 1 66–72.

[30] M. E. Newman, *The structure and function of complex networks*, SIAM review **45** (2003), no. 2 167–256.

[31] M. E. Newman, A.-L. E. Barabási, and D. J. Watts, *The structure and dynamics of networks*. Princeton university press, 2006.

[32] M. E. Newman, *The mathematics of networks*, The new palgrave encyclopedia of economics **2** (2008), no. 2008 1–12.

[33] M. Newman, *Networks*. Oxford university press, 2018.

[34] L. Page, S. Brin, R. Motwani, and T. Winograd, *The pagerank citation ranking: Bringing order to the web.*, tech. rep., Stanford InfoLab, 1999.

[35] X. Yan, P. S. Yu, and J. Han, *Substructure similarity search in graph databases*, in *Proceedings of the 2005 ACM SIGMOD international conference on Management of data*, pp. 766–777, 2005.

[36] X. Yan and J. Han, *gspan: Graph-based substructure pattern mining*, in *2002 IEEE International Conference on Data Mining, 2002. Proceedings.*, pp. 721–724, IEEE, 2002.

[37] C. C. Aggarwal, M. A. Bhuiyan, and M. Al Hasan, *Frequent pattern mining algorithms: A survey*, in *Frequent pattern mining*, pp. 19–64. Springer, 2014.

[38] R. Milo, S. Shen-Orr, S. Itzkovitz, N. Kashtan, D. Chklovskii, and U. Alon, *Network motifs: Simple building blocks of complex networks*, Science **298** (2002), no. 5594 824–827.

[39] W. Ye, O. Askarisichani, A. Jones, and A. Singh, *Deepmap: Learning deep representations for graph classification*, arXiv preprint arXiv:2004.02131 (2020).

[40] P. Erdős and A. Rényi, *On the evolution of random graphs*, Publ. Math. Inst. Hung. Acad. Sci **5** (1960), no. 1 17–60.

[41] D. J. Watts and S. H. Strogatz, *Collective dynamics of 'small-world' networks*, nature **393** (1998), no. 6684 440–442.

[42] R. Albert and A.-L. Barabási, *Statistical mechanics of complex networks*, Reviews of modern physics **74** (2002), no. 1 47.

[43] J. Leskovec, J. Kleinberg, and C. Faloutsos, *Graph evolution: Densification and shrinking diameters*, ACM transactions on Knowledge Discovery from Data (TKDD) **1** (2007), no. 1 2–es.

[44] L. Festinger, *A Theory of Cognitive Dissonance*, vol. 2. Stanford University Press, 1962.

[45] T. Y. Chang, D. H. Solomon, and M. M. Westerfield, *Looking for someone to blame: Delegation, cognitive dissonance, and the disposition effect*, The Journal of Finance **71** (2016), no. 1 267–302.

[46] W. N. Goetzmann and N. Peles, *Cognitive dissonance and mutual fund investors*, Journal of Financial Research **20** (1997), no. 2 145–158.

[47] T. Casciaro and M. S. Lobo, *Competent jerks, lovable fools, and the formation of social networks*, Harvard Business Review **83** (2005), no. 6 92–99.

[48] T. Casciaro and M. S. Lobo, *When competence is irrelevant: The role of interpersonal affect in task-related ties*, Administrative Science Quarterly **53** (2008), no. 4 655–684.

[49] R. Guimera, B. Uzzi, J. Spiro, and L. A. N. Amaral, *Team assembly mechanisms determine collaboration network structure and team performance*, Science **308** (2005), no. 5722 697–702.

[50] F. Heider, *Social perception and phenomenal causality.*, Psychological review **51** (1944), no. 6 358.

[51] X. Zheng, D. Zeng, and F.-Y. Wang, *Social balance in signed networks*, Information Systems Frontiers **17** (2015), no. 5 1077–1095.

[52] F. Heider, *Attitudes and cognitive organization*, The Journal of Psychology **21** (1946), no. 1 107–112.

[53] D. Cartwright and F. Harary, *Structural balance: a generalization of Heider's theory.*, Psychological review **63** (1956), no. 5 277.

[54] J. Kunegis, S. Schmidt, A. Lommatzsch, J. Lerner, E. W. De Luca, and S. Albayrak, *Spectral analysis of signed graphs for clustering, prediction and visualization*, in Proceedings of the 2010 SIAM International Conference on Data Mining, pp. 559–570, 2010.

[55] G. Facchetti, G. Iacono, and C. Altafini, *Computing global structural balance in large-scale signed social networks*, Proceedings of the National Academy of Sciences **108** (2011), no. 52 20953–20958.

[56] P. Doreian and A. Mrvar, *Partitioning signed social networks*, Social Networks **31** (2009), no. 1 1–11.

[57] G. Simmel, *Conflict and the web of group affiliations*, Trans. K. Wolff and R. Bendix. New York: Free Press (1955).

[58] D. Z. Basil and P. M. Herr, *Attitudinal balance and cause-related marketing: An empirical application of balance theory*, Journal of Consumer Psychology **16** (2006), no. 4 391–403.

[59] A. G. Woodside, *Advancing means–end chains by incorporating heider's balance theory and fournier's consumer–brand relationship typology*, Psychology & Marketing **21** (2004), no. 4 279–294.

[60] J. S. Fink, H. M. Parker, M. Brett, and J. Higgins, *Off-field behavior of athletes and team identification: Using social identity theory and balance theory to explain fan reactions*, Journal of Sport Management **23** (2009), no. 2 142–155.

[61] H. B. McDonald and R. Rosecrance, *Alliance and structural balance in the international system: A reinterpretation*, Journal of Conflict Resolution **29** (1985), no. 1 57–82.

[62] D. Easley and J. Kleinberg, *Networks, Crowds, and Markets: Reasoning About a Highly Connected World*. Cambridge University Press, 2010.

[63] M. Szell, R. Lambiotte, and S. Thurner, *Multirelational organization of large-scale social networks in an online world*, Proceedings of the National Academy of Sciences **107** (2010), no. 31 13636–13641.

[64] A. Ilany, A. Barocas, L. Koren, M. Kam, and E. Geffen, *Structural balance in the social networks of a wild mammal*, Animal Behaviour **85** (2013), no. 6 1397–1405.

[65] E. C. Johnsen, *Network macrostructure models for the Davis-Leinhardt set of empirical sociomatrices*, *Social Networks* **7** (1985), no. 3 203–224.

[66] F. Heider, *The Psychology of Interpersonal Relations*. Psychology Press, 2013.

[67] J. A. Davis, *Clustering and structural balance in graphs*, *Human Relations* **20** (1967), no. 2 181–187.

[68] J. A. Davis and S. Leinhardt, *The structure of positive interpersonal relations in small groups.*, .

[69] P. W. Holland and S. Leinhardt, *Transitivity in structural models of small groups*, *Comparative Group Studies* **2** (1971), no. 2 107–124.

[70] S. A. Marvel, J. Kleinberg, R. D. Kleinberg, and S. H. Strogatz, *Continuous-time model of structural balance*, *Proceedings of the National Academy of Sciences* **108** (2011), no. 5 1771–1776.

[71] C. Altafini, *Dynamics of opinion forming in structurally balanced social networks*, *PloS one* **7** (2012), no. 6 e38135.

[72] J. Leskovec, D. Huttenlocher, and J. Kleinberg, *Signed networks in social media*, in *Proceedings of the SIGCHI conference on human factors in computing systems*, pp. 1361–1370, ACM, 2010.

[73] N. P. Hummon and P. Doreian, *Some dynamics of social balance processes: bringing Heider back into balance theory*, *Social Networks* **25** (2003), no. 1 17–49.

[74] A. Srinivasan, *Local balancing influences global structure in social networks*, *Proceedings of the National Academy of Sciences* **108** (2011), no. 5 1751–1752.

[75] A. B. Sørensen and M. T. Hallinan, *A stochastic model for change in group structure*, *Social Science Research* **5** (1976), no. 1 43–61.

[76] A. Papoulis and S. U. Pillai, *Probability, random variables, and stochastic processes*. Tata McGraw-Hill Education, 2002.

[77] D. Aldous and J. Fill, *Reversible markov chains and random walks on graphs*, 1995.

[78] J. E. McGrath, *Social Psychology: A Brief Introduction*. Holt, Rinehart and Winston, 1964.

[79] D. R. Ilgen, J. R. Hollenbeck, M. Johnson, and D. Jundt, *Teams in organizations: From input-process-output models to imoi models*, *Annual Review of Psychology* **56** (2005) 517–543.

[80] A. Anagnostopoulos, L. Becchetti, C. Castillo, A. Gionis, and S. Leonardi, *Online team formation in social networks*, in *Proc. of WWW*, pp. 839–848, ACM, 2012.

[81] T. Lappas, K. Liu, and E. Terzi, *Finding a team of experts in social networks*, in *Proc. of ACM SIGKDD*, pp. 467–476, ACM, 2009.

[82] A. Bhowmik, V. S. Borkar, D. Garg, and M. Pallan, *Submodularity in team formation problem.*, in *Proc. of SDM*, pp. 893–901, SIAM, 2014.

[83] A. Saxena and J. Burmann, *Factors affecting team performance in globally distributed setting*, in *Proc. of Conference on Computers and People Research*, pp. 25–33, ACM, 2014.

[84] S. W. Kozlowski and D. R. Ilgen, *Enhancing the effectiveness of work groups and teams*, *Psychological Science in the Public Interest* **7** (2006), no. 3 77–124.

[85] G. L. Stewart, *A meta-analytic review of relationships between team design features and team performance*, *Journal of Management* **32** (2006), no. 1 29–55.

[86] M. Deutsch, *An experimental study of the effects of cooperation and competition upon group process*, *Human Relations* **2** (1949), no. 3 199–231.

[87] B. Barron, *When smart groups fail*, *The Journal of the Learning Sciences* **12** (2003), no. 3 307–359.

[88] D. J. Devine and J. L. Philips, *Do smarter teams do better a meta-analysis of cognitive ability and team performance*, *Small Group Research* **32** (2001), no. 5 507–532.

[89] K. J. Shim and J. Srivastava, *Team performance prediction in massively multiplayer online role-playing games (mmorpgs)*, in *Proc. of International Conference on Social Computing and Networking*, pp. 128–136, IEEE, 2010.

[90] K. Lewis and B. Herndon, *Transactive memory systems: Current issues and future research directions*, *Organization Science* **22** (2011), no. 5 1254–1265.

[91] J. A. Grand, M. T. Braun, G. Kuljanin, S. W. Kozlowski, and G. T. Chao, *The dynamics of team cognition: A process-oriented theory of knowledge emergence in teams*, *Journal of Applied Psychology* **101** (2016), no. 10 1353.

[92] V. Amelkin, O. Askarisichani, Y. J. Kim, T. W. Malone, and A. K. Singh, *Dynamics of collective performance in collaboration networks*, *PloS One* **13** (2018), no. 10 e0204547.

[93] X.-H. Dang, O. Askarisichani, and A. K. Singh, *Learning multiclassifiers with predictive features that vary with data distribution*, in *2018 IEEE International Conference on Big Data (Big Data)*, pp. 673–682, IEEE, 2018.

[94] L. A. Coser, *The functions of social conflict*, vol. 9. Routledge, 1956.

[95] B. Uzzi, *Social structure and competition in interfirm networks: The paradox of embeddedness*, Administrative science quarterly (1997) 35–67.

[96] S. Mukherjee, Y. Huang, J. Neidhardt, B. Uzzi, and N. Contractor, *Prior shared success predicts victory in team competitions*, Nature Human Behaviour **3** (2019), no. 1 74.

[97] C. A. Klofstad, A. E. Sokhey, and S. D. McClurg, *Disagreeing about disagreement: How conflict in social networks affects political behavior*, American Journal of Political Science **57** (2013), no. 1 120–134.

[98] T. Casciaro and M. S. Lobo, *When competence is irrelevant: The role of interpersonal affect in task-related ties*, Administrative Science Quarterly **53** (2008), no. 4 655–684.

[99] A. M. Petruzzelli, *The impact of technological relatedness, prior ties, and geographical distance on university–industry collaborations: A joint-patent analysis*, Technovation **31** (2011), no. 7 309–319.

[100] J. Wang, *Knowledge creation in collaboration networks: Effects of tie configuration*, Research Policy **45** (2016), no. 1 68–80.

[101] M. De Choudhury, W. A. Mason, J. M. Hofman, and D. J. Watts, *Inferring relevant social networks from interpersonal communication*, in *Proceedings of the 19th international conference on World wide web*, pp. 301–310, ACM, 2010.

[102] M. E. Newman, S. Forrest, and J. Balthrop, *Email networks and the spread of computer viruses*, Physical Review E **66** (2002), no. 3 035101.

[103] N. E. Friedkin, *A formal theory of reflected appraisals in the evolution of power*, Administrative Science Quarterly **56** (2011), no. 4 501–529.

[104] C. M. Rawlings and N. E. Friedkin, *The structural balance theory of sentiment networks: Elaboration and test*, American Journal of Sociology **123** (2017), no. 2 510–548, [https://doi.org/10.1086/692757].

[105] S. Aral and C. Nicolaides, *Exercise contagion in a global social network*, Nature communications **8** (2017) 14753.

[106] K. P. Smith and N. A. Christakis, *Social networks and health*, Annu. Rev. Sociol **34** (2008) 405–429.

[107] M. S. Granovetter, *The strength of weak ties*, in *Social networks*, pp. 347–367. Elsevier, 1977.

[108] S. Holes, *The social structure of competition*, 1992.

[109] P. M. Blau, *The dynamics of bureaucracy*, vol. 196. University of Chicago Press, Chicago, 1955.

[110] M. Crozier, *The bureaucratic phenomenon, Chicago, IL: University of Chicago* (1964).

[111] S. Luo, F. Morone, C. Sarraute, M. Travizano, and H. A. Makse, *Inferring personal economic status from social network location, Nature communications* **8** (2017) 15227.

[112] D. Barkoczi and M. Galesic, *Social learning strategies modify the effect of network structure on group performance, Nature communications* **7** (2016) 13109.

[113] J. A. Davis, *The Davis/Holland/Leinhardt studies: An overview, Perspectives on Social Network Research* (1979).

[114] T. Antal, P. L. Krapivsky, and S. Redner, *Dynamics of social balance on networks, Physical Review E* **72** (2005), no. 3 036121.

[115] P. Jia, N. E. Friedkin, and F. Bullo, *The coevolution of appraisal and influence networks leads to structural balance, IEEE Transactions on Network Science and Engineering* **3** (2016), no. 4 286–298.

[116] Y. Yang, N. V. Chawla, and B. Uzzi, *A network's gender composition and communication pattern predict women's leadership success, Proceedings of the National Academy of Sciences* **116** (2019), no. 6 2033–2038.

[117] J. A. Bargh and E. L. Williams, *The automaticity of social life, Current directions in psychological science* **15** (2006), no. 1 1–4.

[118] J. A. Bargh and M. J. Ferguson, *Beyond behaviorism: On the automaticity of higher mental processes, Psychological Bulletin* **126** (2000), no. 6 925.

[119] J. A. Bargh, S. Chaiken, R. Govender, and F. Pratto, *The generality of the automatic attitude activation effect, Journal of Personality and Social Psychology* **62** (1992), no. 6 893.

[120] J. A. Bargh, K. L. Schwader, S. E. Hailey, R. L. Dyer, and E. J. Boothby, *Automaticity in social-cognitive processes, Trends in Cognitive Sciences* **16** (2012), no. 12 593–605.

[121] J. Willis and A. Todorov, *First impressions: Making up your mind after a 100-ms exposure to a face, Psychological science* **17** (2006), no. 7 592–598.

[122] N. K. Baym, Y. B. Zhang, and M.-C. Lin, *Social interactions across media: Interpersonal communication on the internet, telephone and face-to-face*, *New Media & Society* **6** (2004), no. 3 299–318.

[123] V. J. Dubrovsky, S. Kiesler, and B. N. Sethna, *The equalization phenomenon: Status effects in computer-mediated and face-to-face decision-making groups*, *Human-computer interaction* **6** (1991), no. 2 119–146.

[124] G. Labianca, D. J. Brass, and B. Gray, *Social networks and perceptions of intergroup conflict: The role of negative relationships and third parties*, *Academy of Management journal* **41** (1998), no. 1 55–67.

[125] G. Labianca, *Negative ties in organizational networks*, in *Contemporary perspectives on organizational social networks*, pp. 239–259. Emerald Group Publishing Limited, 2014.

[126] W. R. Gilks, S. Richardson, and D. Spiegelhalter, *Markov chain Monte Carlo in practice*. Chapman and Hall/CRC, 1995.

[127] S. Saavedra, K. Hagerty, and B. Uzzi, *Synchronicity, instant messaging, and performance among financial traders*, *Proceedings of the National Academy of Sciences* **108** (2011), no. 13 5296–5301.

[128] W. Antweiler and M. Z. Frank, *Is all that talk just noise? The information content of internet stock message boards*, *The Journal of Finance* **59** (2004), no. 3 1259–1294.

[129] G. Liu, Y. Xu, and K. Tomsovic, *Bidding strategy for microgrid in day-ahead market based on hybrid stochastic/robust optimization*, *IEEE Transactions on Smart Grid* **7** (2016), no. 1 227–237.

[130] W. Brock, J. Lakonishok, and B. LeBaron, *Simple technical trading rules and the stochastic properties of stock returns*, *The Journal of Finance* **47** (1992), no. 5 1731–1764.

[131] P. C. Tetlock, *Giving content to investor sentiment: The role of media in the stock market*, *The Journal of Finance* **62** (2007), no. 3 1139–1168.

[132] R. E. Whaley, *The investor fear gauge*, *The Journal of Portfolio Management* **26** (2000), no. 3 12–17.

[133] S. Saavedra, R. D. Malmgren, N. Switanek, and B. Uzzi, *Foraging under conditions of short-term exploitative competition: the case of stock traders*, *Proceedings of the Royal Society of London B: Biological Sciences* **280** (2013), no. 1755 [http://rspb.royalsocietypublishing.org/content/280/1755/20122901.full.pdf].

[134] B. Uzzi and S. Dunlap, *How to build your network*, *Harvard Business Review* **83** (2005), no. 12 53 – 60.

[135] K. K. Cetina and U. Bruegger, *Traders' engagement with markets*, *Theory, Culture & Society* **19** (2002), no. 5-6 161–185.

[136] D. M. Romero, B. Uzzi, and J. Kleinberg, *Social networks under stress*, in *Proceedings of the 25th International Conference on World Wide Web*, (Geneva, Switzerland), pp. 9–20, International World Wide Web Conferences Steering Committee, 2016.

[137] J. O. Morrissette, *An experimental study of the theory of structural balance*, *Human Relations* **11** (1958), no. 3 239–254.

[138] S. I. Donaldson and E. J. Grant-Vallone, *Understanding self-report bias in organizational behavior research*, *Journal of Business and Psychology* **17** (2002), no. 2 245–260.

[139] F. Heider, *The psychology of interpersonal relations*, *New York: Wiley.* (1958) 206.

[140] M. Boss and J. Kleinert, *Explaining social contagion in sport applying Heider's balance theory: First experimental results*, *Psychology of Sport and Exercise* **16** (2015), no. Part 3 160 – 169.

[141] T. Gilovich, R. Vallone, and A. Tversky, *The hot hand in basketball: On the misperception of random sequences*, *Cognitive Psychology* **17** (1985), no. 3 295–314.

[142] Q. Li and J. Racine, *Cross-validated local linear nonparametric regression*, *Statistica Sinica* (2004) 485–512.

[143] Q. Li and J. S. Racine, *Nonparametric Econometrics: Theory and Practice.* Princeton University Press, 2007.

[144] R. B. Cattell, *New concepts for measuring leadership, in terms of group syntality*, *Human Relations* **4** (1951), no. 2 161–184.

[145] J. O. Morrissette, J. C. Jahnke, K. Baker, and N. Rohrman, *Degree of structural balance and group effectiveness*, *Organizational Behavior and Human Performance* **2** (1967), no. 4 383 – 393.

[146] K. K. Cetina and U. Bruegger, *Global microstructures: The virtual societies of financial markets*, *American Journal of Sociology* **107** (2002), no. 4 905–950, [https://doi.org/10.1086/341045].

[147] B. Liu, R. Govindan, and B. Uzzi, *Do emotions expressed online correlate with actual changes in decision-making?: The case of stock day traders*, *PLOS ONE* **11** (01, 2016) 1–11.

[148] B. Uzzi and J. Spiro, *Collaboration and creativity: The small world problem*, *American Journal of Sociology* **111** (2005), no. 2 447–504.

[149] O. Askarisichani, J. N. Lane, F. Bullo, N. E. Friedkin, A. K. Singh, and B. Uzzi, *Structural balance emerges and explains performance in risky decision-making*, *Nature Communications* **10** (June, 2019) 2648.

[150] F. Harary, *A structural analysis of the situation in the Middle East in 1956*, *Journal of Conflict Resolution* **5** (1961), no. 2 167–178.

[151] M. Moore, *An international application of Heider's balance theory*, *European Journal of Social Psychology* **8** (1978), no. 3 401–405.

[152] P. Gellman, *The elusive explanation: balance of power 'theory' and the origins of World War I*, *Review of International Studies* **15** (1989), no. 2 155–182.

[153] T. Antal, P. L. Krapivsky, and S. Redner, *Social balance on networks: The dynamics of friendship and enmity*, *Physica D: Nonlinear Phenomena* **224** (2006), no. 1-2 130–136.

[154] P. Doreian and A. Mrvar, *Structural balance and signed international relations*, *Journal of Social Structure* **16** (2015) 1.

[155] A. M. Belaza, K. Hoefman, J. Ryckebusch, A. Bramson, M. van den Heuvel, and K. Schoors, *Statistical physics of balance theory*, *PLOS One* **12** (2017), no. 8 e0183696.

[156] M. Szell, R. Lambiotte, and S. Thurner, *Multirelational organization of large-scale social networks in an online world*, *Proceedings of the National Academy of Sciences* **107** (2010), no. 31 13636–13641, [https://www.pnas.org/content/107/31/13636.full.pdf].

[157] J. Leskovec, D. Huttenlocher, and J. Kleinberg, *Predicting positive and negative links in online social networks*, in *Proceedings of the 19th International Conference on World Wide Web*, pp. 641–650, ACM, 2010.

[158] T. M. Newcomb, *The prediction of interpersonal attraction.*, *American Psychologist* **11** (1956), no. 11 575.

[159] M. Shahriari, O. Askarisichani, J. Gharibshah, and M. Jalili, *Sign prediction in social networks based on users reputation and optimism*, *Social Network Analysis and Mining* **6** (2016), no. 1 91.

[160] D. Lazer, A. Pentland, L. Adamic, S. Aral, A.-L. Barabási, D. Brewer, N. Christakis, N. Contractor, J. Fowler, M. Gutmann, *et. al.*, *Computational social science*, *Science* **323** (2009), no. 5915 721–723.

[161] A. Shilliday and J. Lautenschlager, *Data for a worldwide ICEWS and ongoing research*, *Advances in Design for Cross-Cultural Activities* (2012) 455.

[162] N. E. Friedkin, A. V. Proskurnikov, and F. Bullo, *Positive contagion and the macrostructures of generalized balance*, *Network Science* (2019) 1–14.

[163] F. Harary, *On the measurement of structural balance*, *Behavioral Science* **4** (1959), no. 4 316–323.

[164] P. Abell, *Structural balance in dynamic structures*, *Sociology* **2** (1968), no. 3 333–352.

[165] W. de Nooy, *The sign of affection: Balance-theoretic models and incomplete signed digraphs*, *Social Networks* **21** (1999), no. 3 269–286.

[166] E. Terzi and M. Winkler, *A spectral algorithm for computing social balance*, in *International Workshop on Algorithms and Models for the Web-Graph*, pp. 1–13, Springer, 2011.

[167] J. D. Montgomery, *Balance theory with incomplete awareness*, *Journal of Mathematical Sociology* **33** (2009), no. 2 69–96.

[168] T. Chiba, H. Hino, S. Akaho, and N. Murata, *Time-varying transition probability matrix estimation and its application to brand share analysis*, *PLOS One* **12** (2017), no. 1 e0169981.

[169] J. Friedman, T. Hastie, and R. Tibshirani, *A note on the group lasso and a sparse group lasso*, *arXiv preprint arXiv:1001.0736* (2010).

[170] S. Boyd and L. Vandenberghe, *Convex Optimization*. Cambridge University Press, 2004.

[171] S. Diamond and S. Boyd, *CVXPY: A Python-embedded modeling language for convex optimization*, *Journal of Machine Learning Research* **17** (2016), no. 83 1–5.

[172] E. Mammen, S. van de Geer, *et. al.*, *Locally adaptive regression splines*, *The Annals of Statistics* **25** (1997), no. 1 387–413.

[173] R. J. Tibshirani *et. al.*, *Adaptive piecewise polynomial estimation via trend filtering*, *The Annals of Statistics* **42** (2014), no. 1 285–323.

[174] S.-J. Kim, K. Koh, S. Boyd, and D. Gorinevsky, ℓ_1 *trend filtering*, *SIAM review* **51** (2009), no. 2 339–360.

[175] G. Hardy, J. Littlewood, and G. Polya, *Inequalities. cambridge: Cambridge university press.[1952]*, .

[176] Y.-X. Wang, J. Sharpnack, A. J. Smola, and R. J. Tibshirani, *Trend filtering on graphs*, The Journal of Machine Learning Research **17** (2016), no. 1 3651–3691.

[177] E. Shils *et. al.*, *Center and periphery.* Chicago: University of Chicago Press, 1975.

[178] M. Bourgeois and N. E. Friedkin, *The distant core: social solidarity, social distance and interpersonal ties in core–periphery structures*, Social networks **23** (2001), no. 4 245–260.

[179] K. Juszczyszyn, K. Musial, and M. Budka, *Link prediction based on subgraph evolution in dynamic social networks*, in *2011 IEEE Third International Conference on Privacy, Security, Risk and Trust and 2011 IEEE Third International Conference on Social Computing*, pp. 27–34, IEEE, 2011.

[180] A. M. Belaza, J. Ryckebusch, A. Bramson, C. Casert, K. Hoefman, K. Schoors, M. van den Heuvel, and B. Vandermarliere, *Social stability and extended social balance—quantifying the role of inactive links in social networks*, Physica A: Statistical Mechanics and its Applications **518** (2019) 270–284.

[181] E. Estrada and M. Benzi, *Walk-based measure of balance in signed networks: Detecting lack of balance in social networks*, Physical Review E **90** (2014), no. 4 042802.

[182] S. Kumar, F. Spezzano, V. Subrahmanian, and C. Faloutsos, *Edge weight prediction in weighted signed networks*, in *IEEE International Conference on Data Mining*, pp. 221–230, 2016.

[183] S. Kumar, B. Hooi, D. Makhija, M. Kumar, C. Faloutsos, and V. Subrahmanian, *Rev2: Fraudulent user prediction in rating platforms*, in *Proceedings of the ACM International Conference on Web Search and Data Mining*, pp. 333–341, ACM, 2018.

[184] S. Hochreiter and J. Schmidhuber, *Long short-term memory*, Neural computation **9** (1997), no. 8 1735–1780.

[185] M. H. DeGroot, *Reaching a consensus*, Journal of the American Statistical Association **69** (1974), no. 345 118–121.

[186] N. E. Friedkin and E. C. Johnsen, *Social influence and opinions*, Journal of Mathematical Sociology **15** (1990), no. 3-4 193–206.

[187] A. Das, S. Gollapudi, and K. Munagala, *Modeling opinion dynamics in social networks*, in *Proceedings of the 7th ACM International Conference on Web Search and Data Mining*, pp. 403–412, 2014.

[188] N. E. Friedkin and F. Bullo, *How truth wins in opinion dynamics along issue sequences*, Proceedings of the National Academy of Sciences **114** (2017), no. 43 11380–11385.

[189] P. Jia, A. MirTabatabaei, N. E. Friedkin, and F. Bullo, *Opinion dynamics and the evolution of social power in influence networks*, SIAM Review **57** (2015), no. 3 367–397.

[190] C. Ravazzi, R. Tempo, and F. Dabbene, *Learning influence structure in sparse social networks*, IEEE Transactions on Control of Network Systems **5** (2017), no. 4 1976–1986.

[191] M. H. DeGroot, *Reaching a consensus*, Journal of the American Statistical Association **69** (1974), no. 345 118–121.

[192] C. Altafini, *Consensus problems on networks with antagonistic interactions*, IEEE Transactions on Automatic Control **58** (2012), no. 4 935–946.

[193] A. V. Proskurnikov and R. Tempo, *A tutorial on modeling and analysis of dynamic social networks. Part I*, Annual Reviews in Control **43** (2017) 65–79.

[194] W. Chen, Y. Wang, and S. Yang, *Efficient influence maximization in social networks*, in *Proceedings of the 15th ACM SIGKDD International Conference on Knowledge Discovery and Data Mining*, pp. 199–208, 2009.

[195] O. AskariSichani and M. Jalili, *Influence maximization of informed agents in social networks*, Applied Mathematics and Computation **254** (2015) 229–239.

[196] J. Leskovec, L. A. Adamic, and B. A. Huberman, *The dynamics of viral marketing*, ACM Transactions on the Web **1** (2007), no. 1 5.

[197] W. Chen, C. Wang, and Y. Wang, *Scalable influence maximization for prevalent viral marketing in large-scale social networks*, in *Proceedings of the 16th ACM SIGKDD International Conference on Knowledge Discovery and Data Mining*, pp. 1029–1038, ACM, 2010.

[198] X. Song, B. L. Tseng, C.-Y. Lin, and M.-T. Sun, *Personalized recommendation driven by information flow*, in *Proceedings of the 29th Annual International ACM SIGIR Conference on Research and development in information retrieval*, pp. 509–516, 2006.

[199] D. Ienco, F. Bonchi, and C. Castillo, *The meme ranking problem: Maximizing microblogging virality*, in *IEEE International Conference on Data Mining Workshops*, pp. 328–335, 2010.

[200] Y. Li, D. Zhang, and K.-L. Tan, *Real-time targeted influence maximization for online advertisements*, *Proceedings of the VLDB Endowment* **8** (2015), no. 10 1070–1081.

[201] J. Weng, E.-P. Lim, J. Jiang, and Q. He, *Twitterrank: finding topic-sensitive influential twitterers*, in *Proceedings of the third ACM International Conference on Web Search and Data Mining*, pp. 261–270, 2010.

[202] E. Bakshy, J. M. Hofman, W. A. Mason, and D. J. Watts, *Everyone's an influencer: quantifying influence on twitter*, in *Proceedings of the fourth ACM International Conference on Web Search and Data Mining*, pp. 65–74, 2011.

[203] J. Leskovec, A. Krause, C. Guestrin, C. Faloutsos, C. Faloutsos, J. VanBriesen, and N. Glance, *Cost-effective outbreak detection in networks*, in *Proceedings of the 13th ACM SIGKDD International Conference on Knowledge Discovery and Data Mining*, pp. 420–429, ACM, 2007.

[204] J. R. P. French Jr. and B. Raven, *The bases of social power*, in *Studies in Social Power* (D. Cartwright, ed.), pp. 150–167. Institute for Social Research, University of Michigan, 1959.

[205] E. B. Goldsmith, *Social influence history and theories*, in *Social Influence and Sustainable Consumption*, pp. 23–39. Springer, 2015.

[206] N. E. Friedkin, *A formal theory of reflected appraisals in the evolution of power*, *Administrative Science Quarterly* **56** (2011), no. 4 501–529.

[207] P. Jia, N. E. Friedkin, and F. Bullo, *The coevolution of appraisal and influence networks leads to structural balance*, *IEEE Transactions on Network Science and Engineering* **3** (2016), no. 4 286–298.

[208] A. Srinivasan, *Local balancing influences global structure in social networks*, *Proceedings of the National Academy of Sciences* **108** (2011), no. 5 1751–1752.

[209] J. R. Austin, *Transactive memory in organizational groups: the effects of content, consensus, specialization, and accuracy on group performance*, *Journal of Applied Psychology* **88** (2003), no. 5 866.

[210] Y. C. Yuan, I. Carboni, and K. Ehrlich, *The impact of awareness and accessibility on expertise retrieval: A multilevel network perspective*, *Journal of the American Society for Information Science and Technology* **61** (2010), no. 4 700–714.

[211] D. W. Liang, R. Moreland, and L. Argote, *Group versus individual training and group performance: The mediating role of transactive memory*, *Personality and Social Psychology Bulletin* **21** (1995), no. 4 384–393.

[212] P. R. Laughlin and A. L. Ellis, *Demonstrability and social combination processes on mathematical intellective tasks*, Journal of Experimental Social Psychology **22** (1986), no. 3 177–189.

[213] P. R. Laughlin, *Social combination processes of cooperative problem-solving groups on verbal intellective tasks*, Progress in Social Psychology **1** (1980) 127–155.

[214] J. V. Wood, *Theory and research concerning social comparisons of personal attributes*, Psychological Bulletin **106** (1989), no. 2 231.

[215] J. A. Shepperd, *Productivity loss in performance groups: A motivation analysis.*, Psychological bulletin **113** (1993), no. 1 67.

[216] J. A. Shepperd and R. A. Wright, *Individual contributions to a collective effort: An incentive analysis*, Personality and social psychology bulletin **15** (1989), no. 2 141–149.

[217] J. R. Beatty, R. W. Haas, and D. Sciglimpaglia, *Using peer evaluations to assess individual performances in group class projects*, Journal of Marketing Education **18** (1996), no. 2 17–27.

[218] H. K. Davison, V. Mishra, M. N. Bing, and D. D. Frink, *How individual performance affects variability of peer evaluations in classroom teams: A distributive justice perspective*, Journal of Management Education **38** (2014), no. 1 43–85.

[219] J. A. Drexler Jr, T. A. Beehr, and T. A. Stetz, *Peer appraisals: Differentiation of individual performance on group tasks*, Human Resource Management: Published in Cooperation with the School of Business Administration, The University of Michigan and in alliance with the Society of Human Resources Management **40** (2001), no. 4 333–345.

[220] J. S. Miller and R. L. Cardy, *Self-monitoring and performance appraisal: rating outcomes in project teams*, Journal of Organizational Behavior: The International Journal of Industrial, Occupational and Organizational Psychology and Behavior **21** (2000), no. 6 609–626.

[221] H. London, P. J. Meldman, and A. VAN C. LANCKTON, *The jury method: How the persuader persuades*, Public Opinion Quarterly **34** (1970), no. 2 171–183.

[222] O. Askarisichani and M. Jalili, *Inference of hidden social power through opinion formation in complex networks*, IEEE Transactions on Network Science and Engineering **4** (2017), no. 3 154–164.

[223] L. E. Castro and N. I. Shaikh, *A particle-learning-based approach to estimate the influence matrix of online social networks*, Computational Statistics & Data Analysis **126** (2018) 1–18.

[224] L. E. Castro and N. I. Shaikh, *Influence estimation and opinion-tracking over online social networks*, *International Journal of Business Analytics* **5** (2018), no. 4 24–42.

[225] S. T. Smith, E. K. Kao, D. C. Shah, O. Simek, and D. B. Rubin, *Influence estimation on social media networks using causal inference*, in *IEEE Statistical Signal Processing Workshop (SSP)*, pp. 328–332, 2018.

[226] M. Gomez-Rodriguez, L. Song, N. Du, H. Zha, and B. Schölkopf, *Influence estimation and maximization in continuous-time diffusion networks*, *ACM Transactions on Information Systems* **34** (2016), no. 2 1–33.

[227] N. Du, L. Song, M. G. Rodriguez, and H. Zha, *Scalable influence estimation in continuous-time diffusion networks*, in *Advances in Neural Information Processing Systems*, pp. 3147–3155, 2013.

[228] Q. Deng and Y. Dai, *How your friends influence you: Quantifying pairwise influences on twitter*, in *International Conference on Cloud and Service Computing*, pp. 185–192, IEEE, 2012.

[229] S. Ye and S. F. Wu, *Measuring message propagation and social influence on twitter.com*, in *International Conference on Social Informatics*, pp. 216–231, Springer, 2010.

[230] F. Riquelme and P. González-Cantergiani, *Measuring user influence on twitter: A survey*, *Information Processing & Management* **52** (2016), no. 5 949–975.

[231] A. Almaatouq, A. Noriega-Campero, A. Alotaibi, P. Krafft, M. Moussaid, and A. Pentland, *Adaptive social networks promote the wisdom of crowds*, *Proceedings of the National Academy of Sciences* **117** (2020), no. 21 11379–11386.

[232] C. Manteli, B. Van Den Hooff, and H. Van Vliet, *The effect of governance on global software development: An empirical research in transactive memory systems*, *Information and Software Technology* **56** (2014), no. 10 1309–1321.

[233] C.-C. Huang and P.-K. Chen, *Exploring the antecedents and consequences of the transactive memory system: An empirical analysis*, *Journal of Knowledge Management* **22** (2018) 92–118.

[234] D.-A. Clevert, T. Unterthiner, and S. Hochreiter, *Fast and accurate deep network learning by exponential linear units (elus)*, *arXiv preprint arXiv:1511.07289* [**cs**] (2015).

[235] K. He, X. Zhang, S. Ren, and J. Sun, *Delving deep into rectifiers: Surpassing human-level performance on imagenet classification*, in *Proceedings of the IEEE International Conference on Computer Vision*, pp. 1026–1034, 2015.

[236] N. Srivastava, G. Hinton, A. Krizhevsky, I. Sutskever, and R. Salakhutdinov, *Dropout: a simple way to prevent neural networks from overfitting*, Journal of Machine Learning Research **15** (2014), no. 1 1929–1958.

[237] P. Bonacich, *Power and centrality: A family of measures*, American Journal of Sociology **92** (1987), no. 5 1170–1182.

[238] B. D. Pulford, A. M. Colman, E. K. Buabang, and E. M. Krockow, *The persuasive power of knowledge: Testing the confidence heuristic*, Journal of Experimental Psychology: General **147** (2018), no. 10 1431.

[239] H. Mercier and D. Sperber, *"two heads are better" stands to reason*, Science **336** (2012), no. 6084 979–979.

[240] R. Hertwig, *Tapping into the wisdom of the crowd—with confidence*, Science **336** (2012), no. 6079 303–304.

[241] C. W. Granger, *Investigating causal relations by econometric models and cross-spectral methods*, Econometrica: Journal of the Econometric Society **37** (1969) 424–438.

[242] C. W. Granger, *Testing for causality: a personal viewpoint*, Journal of Economic Dynamics and Control **2** (1980) 329–352.

[243] C. W. Granger, *Essays in econometrics: collected papers of Clive WJ Granger*, vol. 32. Cambridge University Press, 2001.

[244] E. E. Leamer, *Vector autoregressions for causal inference?*, in *Carnegie-Rochester Conference series on Public Policy*, vol. 22, pp. 255–304, North-Holland, 1985.

[245] C. J. Hutto and E. Gilbert, *Vader: A parsimonious rule-based model for sentiment analysis of social media text*, in *Eighth International AAAI Conference on weblogs and social media*, 2014.

[246] M. M. Bradley and P. J. Lang, *Affective norms for english words (anew): Instruction manual and affective ratings*, tech. rep., Technical report C-1, the center for research in Psychophysiology, 1999.

[247] B. Uzzi, *Embeddedness in the making of financial capital: How social relations and networks benefit firms seeking financing*, American sociological review (1999) 481–505.

[248] L. M. Verbrugge, *Multiplexity in adult friendships*, Social Forces **57** (1979), no. 4 1286–1309.

[249] D. Krackhardt and J. R. Hanson, *Informal networks*, Harvard business review **71** (1993), no. 4 104–111.

[250] T. N. Kipf and M. Welling, *Semi-supervised classification with graph convolutional networks*, *arXiv preprint arXiv:1609.02907* (2016).

[251] R. Ying, R. He, K. Chen, P. Eksombatchai, W. L. Hamilton, and J. Leskovec, *Graph convolutional neural networks for web-scale recommender systems*, in *Proceedings of the 24th ACM SIGKDD International Conference on Knowledge Discovery & Data Mining*, pp. 974–983, 2018.

[252] L. Zhao, Y. Song, C. Zhang, Y. Liu, P. Wang, T. Lin, M. Deng, and H. Li, *T-gcn: A temporal graph convolutional network for traffic prediction*, *IEEE Transactions on Intelligent Transportation Systems* (2019).

[253] S. Yuan, X. Wu, and Y. Xiang, *Sne: signed network embedding*, in *Pacific-Asia conference on knowledge discovery and data mining*, pp. 183–195, Springer, 2017.

[254] J. Huang, H. Shen, L. Hou, and X. Cheng, *Signed graph attention networks*, in *International Conference on Artificial Neural Networks*, pp. 566–577, Springer, 2019.

[255] T. Derr, Y. Ma, and J. Tang, *Signed graph convolutional networks*, in *2018 IEEE International Conference on Data Mining (ICDM)*, pp. 929–934, IEEE, 2018.

[256] J. Kim, H. Park, J.-E. Lee, and U. Kang, *Side: representation learning in signed directed networks*, in *Proceedings of the 2018 World Wide Web Conference*, pp. 509–518, 2018.

[257] G. A. Abimbola, P. R. Duimering, and Z. Zhong, *A balance theory approach to group problem solving*, .

[258] H. Harari, *An experimental evaluation of heider's balance theory with respect to situational and predispositional variables*, *The Journal of social psychology* **73** (1967), no. 2 177–189.

[259] M. Boss and J. Kleinert, *Explaining social contagion in sport applying heider's balance theory: First experimental results*, *Psychology of Sport and Exercise* **16** (2015) 160–169.